NOTICE

The quality of this microform is heavily dependent upon the quality of the original thesis submitted for microfilming. Every effort has been made to ensure the highest quality of reproduction possible.

If pages are missing, contact the university which granted the degree.

Some pages may have indistinct print especially if the original pages were typed with a poor typewriter ribbon or if the university sent us an inferior photocopy.

Reproduction in full or in part of this microform is governed by the Canadian Copyright Act, R.S.C. 1970, c. C-30, and subsequent amendments.

AVIS

La qualité de cette microforme dépend grandement de la qualité de la thèse soumise au microfilmage. Nous avons tout fait pour assurer une qualité supérieure de reproduction.

S'il manque des pages, veuillez communiquer avec l'université qui a conféré le grade.

La qualité d'impression de certaines pages peut laisser à désirer, surtout si les pages originales ont été dactylographiées à l'aide d'un ruban usé ou si l'université nous a fait parvenir une photocopie de qualité inférieure.

La reproduction, même partielle, de cette microforme est soumise à la Loi canadienne sur le droit d'auteur, SRC 1970, c. C-30, et ses amendements subséquents.

STUDY ON FRICTION

BASE ISOLATORS

A Thesis

in

The Centre

for

Building Studies

Presented in Partial Fulfillment of the Requirements
for the degree of Master of Engineering at
Concordia University
Montreal, Quebec, Canada

March 1991

ISBN 0-315-64760-4

Abstract

Study on Friction Base Isolators

Xi Wang

This paper deals with friction base isolators with and without resilient restraint. The frictional properties of various sheet materials between the interfaces and the elastic properties of a rubber restraint were determined. Using the computer program DRAIN-2D, various intensities and frequencies of the excitation were employed in computer simulation. The peak relative displacements and the maximum accelerations of the mass were determined, for different coefficient of friction and elastic restraint. A decision on the optimum friction coefficient for a pure-friction system and the most appropriate values for the friction and the spring constants for resilient-friction base isolator was made. A series of laboratory experiments on a shaking table was conducted.

ACKNOWLEDGEMENTS

The author would like to express my sincere thanks to Professor Cedric Marsh and Dr. Avtar Pall, my supervisors, for their guidance, criticism, corrections throughout this study. Their keen interest in my work and knowledge in the subject field has directed me to the final completion of this research.

The author also wishes to thank Dr. Oscar A. Pekau, Dr. D. Feldman and Dr.H.K.Ha for their valuable advice in this study.

Additional thanks are due to Mr.J.Zilka, lab technician, who aided me on laboratory tests, to Dr. H.Nadeau and Mr. S. Belanger for their help in the use of computer.

Last, the financial support provided by the Natural Science and Engineering Research Council of Canada is gratefully acknowledged.

TABLE OF CONTENTS

LIST OF FIGURES

LIST OF TABLES

LIST OF SYMBOLS

μ	Friction Coefficient
μ_s	Static Friction Coefficient
μ_d	Dynamic Friction Coefficient
g	Acceleration due to Gravity
W	Weight of Structure
L	Depth of Structure
ω	Angular Frequency of the Block
p	Wind Pressure
u	Displacement of the Block Relative to the Ground
x	Absolute Displacement of the Block
x_g	Horizontal Ground Displacement
M	Mass of the Block
k	Spring Constant
E'	Elastic Modulus
E''	Loss Modulus
E^*	Complex Modulus
σ'	In-phase Stress
σ''	Out-of-phase Stress
δ	Loss Angle
t	Time

Chapter I

Introduction

1.1 General

The classical method of protecting buildings against earthquakes is to dissipate energy by nonlinear deformation of structural elements. Energy absorbed through inelastic deformations inevitably gives rise to structural and non-structural damage.

Another method to limit the dynamic forces that act on the structure makes use of isolators between the foundation of the building and the ground, causing the building to be partially decoupled from the ground motion.

The idea of base isolation was proposed over one hundred years ago. Recent developments include the multilayer rubber bearing of J.M. Kelly[45], and the resilient friction base isolator developed by Mostaghel[46] which incorporates multiple sliding surface of Teflon restrained by a rubber core.

In conventional building systems, the ground motion creates a horizontal force on the base of the structure. Base isolators limit the ability to transmit this force; If no

force is exerted on the structure during a seismic event, it is theoretically not necessary to design the structure to resist earthquake action. This ideal is not practical and a compromise is sought.

There are two important types of isolator. In the first, the building rests on laminated rubber supports, similar to bridge expansion supports, which permit horizontal motion without slipping, and have high hysteretic damping. In the second, which is the subject of this study, the building is supported on surfaces which can slide. In this, the simplest form of base isolator, the sliding surface acts as a "fuse" to limit the base shear force. Resilient restraint can be added to control the displacement of the structure relative to the ground.

1.2 Research objective

A comprehensive comparative study is difficult since there is no agreed definition of performance criteria. In fact there is not one single performance criterion but several, and some of these are at cross purposes to each other. Hadian and Tseng have suggested eleven desired performance criteria related to the safety and reliability of base isolated structures.[1] A generally well understood objective is to minimize the force (acceleration) transmitted by the base

isolator. Another is to minimize the displacement of the structure relative to the ground. Either goal can only be achieved at the expense of the other. In all cases the stability of the structure must be maintained in the presence of strong gusts of wind.

In practical terms, acceptable systems will:

(1) have a single sliding surface in each isolator,

(2) remain stable at the maximum design displacements,

(2) provide increasing resistance with increasing displacements,

(4) not degrade under repeated cyclic load,

(5) have quantifiable engineering parameters, (e.g. sliding force, and force-deflection characteristics).

A pure-friction base isolation system(P-F)[33][48][49], using a sliding friction, was proposed by A. Pall. This system appears to be the simplest among all isolation systems and can be effective in reducing accelerations without a large relative displacement.

For this system there is a desirable coefficient of friction, to balance acceleration and displacement, for which a suitable material is to be found. This optimum may be a structural property, independent of the earthquake type or intensity, or it may be specific for a particular earthquake

and building form.

By introducing a resilient restraint, the intention is to permit the use of a lower coefficient of friction to reduce the acceleration without increasing the displacement. The preferred combination of coefficient of friction and spring constant is then to be determined.

Therefore, the purposes of this study were:

(1) to demonstrate the most suitable friction coefficient for the pure-friction system.

(2) to find a desirable combination of coefficient of friction and spring constant for the resilient-friction base isolation system.

(3) to demonstrate the relative performance of these two systems.

1.3 Thesis Organization

Chapter II is devoted to the pure-friction base isolator. The various aspects discussed are:

The influence of the friction coefficient.

The equations of motion.

Computer simulation of the response to ground motion.

Measurement of coefficient of friction.

Shaking table tests.

Chapter III is devoted to the resilient-friction base isolator and the following subjects are discussed:

Equations of motion.

Computer simulation.

Shaking table tests.

In the chapter IV is a discussion on the design of R-FBI system, with suggestions for future work.

Chapter II

Pure-Friction Base Isolator

2.1 General

The basic model of friction originated from Coulomb [38] [39] [40], however the picture of friction, based on his consideration of the sliding surfaces, can be considered as a framework at best. The asperities are certainly not rigid , but will undergo elastic deformations, both along and normal to the surface. In practical cases, the surface of contact between two bodies is often curved, and the actual area of contact in such cases increases with the total weight. Lubricants can reduce the friction by filling the hollows and reducing the effective roughness.

For the materials with a nominally constant Coulomb friction coefficient, observations show that the coefficient, μ, for low relative speeds is approximately independent of the speed[4], the result of this is that for earthquakes with low velocity content an isolator exhibits little sensitivity to variations in frequency content. For higher speeds, μ decreases with increasing velocity, and for this reason a base isolated structure is sensitive to variations in the frequency of seismic excitations with high velocity content.

It appears that under ideal conditions (perfectly dry, hard surfaces) the static coefficient coincides with the dynamic coefficient for low speeds, but in most practical cases, an drop in the value of μ takes place as soon as motion starts. This fact can be explained by assuming that the asperities on one surface can jump part of the way over the gap between asperities on the other. In the friction-type base isolator there may be some benefit in such behaviour: the static friction coefficient is for withstanding wind load, while the dynamic friction coefficient reduces the acceleration transmitted during continuous sliding.

2.2 Properties of Teflon

Teflon, as a friction material, has many special properties which are quite different from most friction materials[18] [19] [20]. Because of the exposed fluorine atoms on the outside of the polymer chain, there is poor adhesion to itself and to other solids.

Well fabricated samples show no brittleness under impact, even at temperatures as low as -200°C. The maximum working temperature is about 250°C [5].

Experimental work[20][21]indicates that the coefficient of sliding friction between virgin PTFE and any other material

is influenced by a number of factors, including the roughness of material, the contact stress, the speed of motion, the amount of previous wear, the temperature and even the relative humidity of the air. In general terms, lower coefficients of friction are obtained with smoother contact surfaces, high contact stresses, lower speeds, previous use, higher temperature, and increased relative humidity. The different factors influence the behaviour to differing extents. The initial static coefficient of friction between PTFE and stainless steel falls with increasing contact stress, but rises with increasing steel surface roughness. It is demonstrated that the surface finish of the PTFE has no practical effect on the friction, presumably because the surface is soft enough to adapt itself by deforming.

To achieve satisfactory friction values, the contact stress should exceed about 3 N/mm^2, but the maximum stress is limited by the material backing the PTFE. For the higher values of the stress, special attention is needed to attaching, and possibly restraining the PTFE.

To achieve the lowest friction characteristics, the contact surface should be harder than the PTFE and should have a smooth finish, better than 0.4 μm CLA. Where appropriate, sliding movements should occur parallel with, and not across the direction of machining of the contact surface, for the

lowest values of μ. The contact surface must be larger than the PTFE, and edges must never be permitted to pass on to the PTFE in service, otherwise marking, and even rippling, can result[6].

2.3 Friction sliding element

The idea of a sliding joint as an isolation system is an attractive one for low-cost housing since it can be constructed using no complicated technology.

The friction sliding element has two functions: supporting the weight of the structure and providing the "fuse" to limit the horizontal base shear.

Considerable work has been done to show the effectiveness of friction sliding elements as a base isolator [6][21][33], especially in protecting the structure from high amplitude oscillations that fall in the same frequency range as the natural frequencies of the structure[22][23][33][37][43]. With proper design, friction sliding elements can reduce the peak acceleration transmitted to the structure and significantly reduce the deflection of the structure while keeping the peak relative displacement of the base to a manageable limit.

The friction sliding element in a base isolator is

very rigid in the vertical direction. Hence, the isolator does not provide isolation against vertical ground motion. The response of structures to vertical ground motion may cause non-uniform distribution of vertical load on the isolators leading to variations in frictional resistance affecting the horizontal sliding displacements.

There is a factor which tends to limit this potential effect. The variation of the vertical load is at a much higher frequencies than that of the horizontal load. This leads to a high degree of decoupling between horizontal and vertical responses.

For a rigid body, pure-friction isolators provide a bound, μg, on the peak acceleration transmitted to the body, in which μ is the friction coefficient and g is the acceleration due to gravity.

In the P-F system the relative displacement decreases with increasing friction coefficients,but higher friction coefficients lead to greater accelerations transmitted to the base of the structure. Ideally the sliding interfaces should have the tendency to slide continuously, for the design earthquake, in order to minimise the energy input and to prevent higher frequency input to the structure caused by stick-slip behaviour. This requires that the friction

coefficient between sliding interfaces should be relatively low. A low coefficient prevents high ground acceleration from being transmitted to the structure, but the coefficient must be high enough to limit the relative displacement to a small fraction of the maximum ground motion. A coefficient of friction of 0.2 has been proposed as a good compromise[49]. This is well in excess of that required to resist wind load.

2.4 Behaviour of Teflon in base isolation system

Teflon with a low friction coefficient has been used for the past several years to accommodate thermal movement, creep, and shrinkage of concrete arising in bridge applications. More recently, Kelly[6] proposed it as part of aseismic isolation systems, with a sliding plane of Teflon and highly polished stainless steel. The condition at the interface (type of Teflon, roughness of stainless steel, bearing pressure, velocity and acceleration of sliding, etc.) dictates the transmission of force to the structure, and the design of the element requires a knowledge of the frictional properties.

Coulomb's constant friction coefficient has been used to model the friction characteristic of Teflon elements, and it is agreed that under certain conditions the Coulomb's model

can result in a useful estimation of the peak response, provided that an appropriate value of the coefficient of friction is used.

Other studies have been made to find appropriate mathematical model for a Teflon-steel interface under the conditions of interest. Some of them are based on the principles of the theory of viscoplasticity. Based on previous tests[6], the mathematical model proposed by Bouc (1971)[47] and subsequently extended by [7] gave better approximations. In this study, however, the simple model has been used.

A breakaway friction coefficient higher than the dynamic value is another attractive feature. Before sliding, the coefficient can attain to 0.14 or more, and is large enough to withstand the wind force, but low enough to slide under strong earthquake action which can overcome the static friction force, while the reduced coefficient after sliding limits the acceleration.

The theory given in section 2.6.1, based on a constant value of Coulomb friction, predicts stick-slip behaviour for a certain range of acceleration. For a Teflon-steel interface[6] with varying friction coefficient, it was observed in earlier tests[6] that for cases even in which the acceleration of the excitation was below the critical value,

continuous sliding still occurred. This was attributed to the high ratio of static and dynamic friction coefficients, which will be explained in section 2.6.3.

2.5 Wind and seismic loads

The coefficient of friction must ensure the stability of the building under wind loads. Many researchers have been interested in the topic of wind effects on base isolated structures[8][9].

Assuming a wind pressure = 1.5 kPa, and a gravity force for the building d = 2800 N/m^3 (this value is based on a typical concrete building), the relationship between wind force and coefficient of friction is obtained as follows:

$$\text{Wind load} = pA \tag{2.1}$$

Friction force due to vertical load of building

$$= W\mu = (dAL)\mu \tag{2.2}$$

For stability: $pA < (dAL)\mu$

$$\therefore \quad \mu > p/(dL) = 1500/(2800L) = 0.54/L \tag{2.3}$$

where:

μ = static coefficient of friction

p = wind pressure = 1.5 kPa

A = windward area of structure

W = weight of structure (N)

L = depth of building (Fig.1).

The required coefficient of friction, μ, decreases as L increases, and if L is greater than 10 meters, μ is less than 0.054, showing that the friction required to provide the stability of low to medium rise concrete buildings against wind load is small.

To avoid uplift due to rocking of the structure during an earthquake, the overturning moment due to seismic load should not exceed the stabilizing moment due to gravity. Treating the structure as a rigid block, on a pure-friction base, the maximum overturning moment is $\mu Wh/2$, while the gravity moment is $WL/2$, where h is height of the structure. Thus at the critical condition

$$\therefore \mu = L/h \qquad (2.4)$$

If μ were 0.2, then $h = 5L$ would provide the height limit. Since the earthquake forces are dynamic in nature, conservatively 'h' shall be not more that 2L.

2.6 Governing equations

2.6.1 Conditions for sliding

Figure (2) represent a rigid body supported on the pure-friction system. The effect of any flexibility of the

building is neglected. The system is subjected to horizontal ground motion. As long as the intensity of ground motion is small, the friction force prevents any relative lateral displacement. When the ground acceleration exceeds μg, the base starts to slide. The friction force is assumed to keep the same value as sliding continues. In some cases, there is separation and then reattachment, called stick-slip behaviour. The conditions for this to occur are described by the following equations:

Using Coulomb friction, for harmonic excitation, sliding of a rigid body occurs[36] when

$$\frac{\mu g}{A} < 1 \qquad (2.5)$$

stick-slip behaviour occurs when (equation 2.30)

$$0.537 < \frac{\mu g}{A} < 1 \qquad (2.6)$$

and continuous sliding occurs when

$$\frac{\mu g}{A} < 0.537 \qquad (2.7)$$

in which:

μ = the coefficient of friction

A = the maximum harmonic acceleration

Practice shows that the stick-slip behaviour is not good for

base isolation since it can lead to high frequency input to the structure, and the continuous sliding behaviour is preferred.

During sliding(the "slip" condition), the equation of motion is[25]:

$$\ddot{u}[t] = \mu g - \ddot{x}_g[t] \qquad (2.8)$$

where,

μ = the dynamic friction coefficient

g = the acceleration due to gravity

u = the displacement of the base relative to the ground

x_g = the horizontal ground motion

Whenever the base moves with to the ground, the relative non-sliding condition is:

$$\dot{u} = 0 \qquad (2.9)$$

which holds as long as:

$$\mu g - |\ddot{x}_g| > 0 \qquad (2.10)$$

This is the "stick" condition.

It should be pointed out that the dynamic coefficient of friction μ varies with the relative velocity and pressure in some cases. However, such changes of friction coefficient are not considered in this analysis.

2.6.2 General solution of SDOF system with Coulomb friction force

Consider the case of continuous sliding described by equation (2.8), and assuming the equation of motion, in the first time interval in which $\dot{u}_b$ does not change sign, becomes

$$\ddot{u} = \mu g - \ddot{x}_g \qquad (2.8)'$$

where $0 < t < t_1$

If the body starts at rest and the ground acceleration exceeds μg, the initial conditions at $t = 0$ are

$$u[0] = -x_g[0] \qquad \dot{u}[0] = -\dot{x}_g[0] \qquad (2.11)$$

$$\dot{x}[0] = \mu g \qquad (2.12)$$

where x is the absolute displacement of the body.

Denoting the solution to this problem by u_1, then

$$u_1[t] = \tfrac{1}{2}\mu g t^2 - x_g[t] \qquad (2.13)$$

The time t_1 is now defined by $\dot{u}_1[t_1] = 0$, or

$$\mu g t_1 - \dot{x}_g[t_1] = 0 \qquad (2.14)$$

Since the condition of continuous sliding was assumed, for subsequent time intervals $t_{n-1} < t < t_n$, $n = 2,3,4\ldots$, in which $\dot{u}$ consecutively changes sign, then:

$t_{n-1} < t < t_n$, $n = 2,3,4,..,$

$$\ddot{u}[t] = (-1)^{n+1}\mu g - \ddot{x}_g[t] \qquad (2.15)$$

and initial conditions

$$\dot{u}_n(t_{n-1}) = 0 \qquad (2.16)$$

$$u_n(t_{n-1}) = u_{n-1}(t_{n-1}) \qquad (2.17)$$

The first integral of equation (2.15) yields

$$\dot{u}_n = (-1)^{n+1}\mu g(t-t_{n-1}) - \dot{x}_g + \dot{x}_g[t_{n-1}] \qquad (2.18)$$

$t_{n-1} < t < t_n$; $n = 2, 3, 4, \ldots$.

The time t_n for $n = 1,2,3,\ldots$ is now defined generally $\dot{u}_n[t] = 0$, i.e.

$$\mu g t_1 - \dot{x}_g[t_1] = 0 \qquad (2.19)$$

$$(-1)^{n+1}\mu g(t_n-t_{n-1}) - \dot{x}_g[t_n] + \dot{x}_g[t_{n-1}] = 0 \qquad (2.20)$$

$n = 2, 3, 4, \ldots$

Solving equation (2.20) for $x_g(t_n)$, writing the resulting equation for n, n-1, n-2,... 1, gives:

$$\dot{x}_g[t_n] = \dot{x}_g[t_{n-1}] + (-1)^{n+1}\mu g(t_n-t_{n-1})$$

$$\dot{x}_g[t_{n-1}] = \dot{x}_g[t_{n-2}] + (-1)^{n}\mu g(t_{n-1}-t_{n-2})$$

.....

$$\dot{x}_g[t_2] = \dot{x}_g[t_1] + (-1)^{3}\mu g(t_2-t_1)$$

$$\dot{x}_g[t_1] = \mu g t_1 \qquad (2.21)$$

Adding these together:

$$\dot{x}_g[t_n] = \mu g \sum_{k=1}^{n} (-1)^{k+1}(t_k - t_{k-1}); \quad n = 2,3,4,... \qquad (2.22)$$

Insertion of equation (2.22) into equation (2.18) and setting $u_n + x_g = x$, leads to the result

$$\dot{x} = \mu g[2\sum_{k=1}^{n-1} (-1)^{k+1} t_k + (-1)^{n+1} t]$$

for $t_{n-1} < t < t_n$; $n = 2,3,4,$ (2.23)

where x is the absolute displacement of the body

A second integration and utilization of equation (2.17) leads to the evaluation of the displacement x

$$x = \frac{(-1)^{n+1}}{2}\mu g t^2 + \mu g[(-1)^n \cdot t_{n-1} + \sum_{k=1}^{n-1} (-1)^{k+1} \cdot (t_k - t_{k-1})]\, t - \dot{x}_g(t_1)$$

$$+ \mu g \sum_{k=2}^{n-1} (-1)^k \cdot t_k^2; \quad for \quad t_{n-1} < t < t_n; \quad n = 2,3,\ldots, \qquad (2.24)$$

The preceding derivations have simple graphical representations. Equation (2.20) can be written as

$$\frac{\dot{x}_g[t_n] - \dot{x}_g[t_{n-1}]}{t_n - t_{n-1}} = (-1)^{n+1}\mu g \qquad (2.25)$$

This represents a series of straight lines alternately having slopes μg and $-\mu g$ between time t_{n-1} and t_n, and the values of t_n are the abscissas of intersections of the graph of $x_g[t]$

with the straight lines. This is shown in Fig.3(a). Corresponding to the points of the intersection $\dot{u} = 0$, equation (2.18) shows that the sequence of connected broken lines represents the graph of velocity of the block. Also the displacement x at any time t is the algebraic sum of the areas of the triangles A_1, A_2, A_3,... formed by the sequence of broken lines and the t-axis, from the origin to the position t, In particular, for $t = t_n$,

$$x[t_n] = \sum_{k=1}^{n} A_k - \frac{1}{2}A_n \qquad (2.26)$$

$$A_k = \frac{(-1)^{k+1}\dot{x}[t_k]^2}{\mu g} \qquad (2.27)$$

in which $n = 1,2,3,4,...$

Now the stick-slip behaviour described by Eq.(2.6) is considered. Graphical interpretation affords a simple means of determining time intervals of separated and joined motions. The rigid body can stick to the ground only at time t_n when it has the same velocity as the ground.

The remaining requirement for attachment is:

$$|\ddot{x}_g[t_n]| < \mu g$$

This is shown in detail in Fig.3(b). For $t_n < t < t'_n$ the tangent to the path of the body is less than μg, therefore, motion will be in the joined mode along the path SS′, and t'_n is tne first instant of time at which

$$|\ddot{x}_g| \geq \mu g$$

At t'_n the body separates from the ground and proceeds along a straight line with slope of

$$|\ddot{x}| = \mu g$$

As long as the tangent to the path of the body is less than the slope $\pm\mu g$, the sliding will terminate.

To include stick-slip behaviour, an additional term is required and the final expression becomes:

$x[t_n]$ = part I + part II

= x due to separated motion + x due to joined motion

$$= -\frac{(-1)^{n+1}}{2}\mu g t^2 + \mu g[(-1)^n t_{n-1} + \sum_{k-1}^{n-1}(-1)^{k+1}(t_k - t_{k-1})]\,t - \dot{x}_g[t_1]\,t_1$$

$$+ \mu g \sum_{k-2}^{n-1}(-1)^k t_k^2 + \sum_{s-1}^{m}\int_{t_s}^{t'_s}\dot{x}_g[t]\,dt \qquad (2.28)$$

in which m is the number of reattachments that have taken place, t_{n-1} is the time when stick starts in each cycle, and s and s′ are points at the beginning and end of the stick interval respectively.

2.6.3 Response for harmonic excitation

The preceding development will be applied to certain special types of ground motion. For the important case of harmonic ground motion,

$$\dot{x}_g = V_0 \cos\omega t$$

there exists a critical coefficient of friction, μ_{cr}, which ensures that for $\mu < \mu_{cr}$ there will be no reattachments or periods of joined motion except possibly at the start of the motion. To observe this, refer to Fig.4(a), which shows the geometrical construction. Point M is the point whose tangent intersects the curve at a point C with a tangent of equal but opposite slope. Equating the ordinate of C, i.e.,

$$\dot{x}[t^*+\pi/\omega] = -V_0\cos\omega t$$

with the ordinate of C on tangent line to the curve at M, one obtains

$$t^* = (1/\omega)\cdot\arctan 2/\pi \qquad (2.29)$$

Substitution of this result into the equation of motion

$$\ddot{x} = -\mu g$$

at $t = t^*$ leads to the determination of μ_{cr} as given by

$$\mu_{cr} = \frac{2V_0\omega}{g\sqrt{4+\pi^2}} = 0.537\frac{V_0\omega}{g} \qquad (2.30)$$

Considering the zigzag strip bounded by lines of types I and II as shown in Fig.4(b). the points D, E are determined such that the slope of the tangent lines I at these points are alternately $-\mu g$ and μg. Subsequently, lines II are drawn from these points having a slope opposite to that of the tangent. Except for a possible sticking or joined motion at the beginning, the body will acquire linearly varying velocity with alternately $\pm\mu g$ accelerations falling entirely in the strip for all succeeding periods.

For example, if the initial velocity is to the left of D, there will be joined motion until D, separation at D, velocity decrease along line I and subsequent linear velocity variations lying in the strip. If the starting velocity is between D and D′, separation takes place immediately and thereafter as in the previous case. Thirdly, if initial velocity lies between D′ and D", separation starts immediately followed by a sticking-together period up to E. Subsequently, there will be no reattachment. Finally, for initial velocity between D" and E, the situation will be the same as the first case when the initial velocity was to the left of D.

Further consideration is given for the case of $\mu_s \neq \mu_d$, where μ_s and μ_d are static and dynamic friction coefficients respectively. It is found from Fig.4(c) that the response of the block will follow the curve of ground motion as long as

the tangent to the curve is less than $\mu_s g$, otherwise, it will follow the straight line with the slope of $\mu_d g$. Thus:

$2V_0\cos\omega t = (\pi/\omega)\mu_d g$; $\quad V_0\omega\sin\omega t = \mu_s g$ (neglecting negative)

$\therefore \tan\omega t = (2/\pi)(\mu_s/\mu_d)$ and $t = (1/\omega)\tan^{-1}[(2/\pi)(\mu_s/\mu_d)]$

The critical friction coefficient μ_{cr} derived in Eq.(2.30) is the special case when $\mu_s=\mu_d$. Different ratios of μ_s and μ_d give different values of μ_{cr}, and a ratio of μ_s and μ_d greater than 1 extends the range of the continuous sliding.

2.7 Computer simulation

2.7.1 Introduction

The computer program DRAIN2D[10] was employed to study the dynamic behaviour of the structure supported on a pure-friction system. Ground excitation is defined by time histories of ground acceleration, in this study, a sine-wave, the EL-CENTRO earthquake record, and their modified forms were used for the horizontal ground motions. The dynamic analysis process is based on constant Coulomb friction. All support points are assumed to move identically, thus, a single mass constrained against rotation and vertical translation can be used in the computer simulation. The pure friction device is modelled as a bar which may yield in tension or in compression with an ideal rigid-plastic behaviour(Fig.5).

The variable input includes:

(1) Friction coefficient

(2) Factor to change the intensity of the EL-CENTRO record

To study the behaviour under different intensity of excitation, the intensity of the EL-CENTRO record was multiplied by the factors of 1.5 and 0.5.

(3) Factor to change the frequency content of the EL-CENTRO record

In many respects the EL-CENTRO 1940 earthquake may be referred to as a standard earthquake. The Fourier spectrum of its amplitude shows that the energy is distributed in the frequency range of about 1 to 4 Hz with its peak at abouc 1.5 Hz[24][27]. This is the distribution of energy for most of the available major earthquake records.

The normal duration of the excitation is 7 seconds. The frequency content was changed by mutiplying the duration by factors of 0.5 and 2.0. As the intensity was maintained, the amplitudes of the ground displacement changed by the factors of 0.25 and 4.

The dynamic response is determined by step-by-step integration, with a constant acceleration assumed within any time step. For earthquake motion, in a finite time step, the calculation followed is[26]

$$[M]\{\Delta\ddot{u}_b\} + [C_T]\{\Delta\dot{u}_b\} + [K_T]\{\Delta u_b\} = -[M]\{\Delta\ddot{u}_g\} \qquad (2.31)$$

where $\{\Delta\ddot{u}_b\}$, $\{\Delta\dot{u}_b\}$, $\{\Delta u_b\}$ are the increments of acceleration, velocity and displacement, respectively, relative to the ground; $\{\Delta\ddot{u}_g\}$ is the increment of ground acceleration; [M] is the mass matrix; and $[C_T]$ and $[K_T]$ are tangent values of the damping and stiffness matrices for the structure. In our calculation for pure-friction system, $[C_T]$ and $[K_T]$ are zero since they do not enter into the analysis.

The advantage of the constant acceleration method is that it is more stable for the longer period of vibration[29] [30] [32] [41], compared with a linear variation of acceleration with respect to time, but for vibration modes with longer periods, the response computed by the constant acceleration method may be slightly less accurate than by the linear acceleration method.

The basic equations for the constant acceleration method are as follows:
in each digitized interval, $\Delta t = t_i - t_{i+1}$, the horizontal component of ground acceleration can be represented by

$$\ddot{u} = \frac{1}{2}(\ddot{u}_i + \ddot{u}_{i+1}) \tag{2.32}$$

$$\dot{u} = \dot{u}_i + \int_{t_i}^{t} \ddot{u}\, dt \tag{2.33}$$

$$u = u_i + \int_{t_i}^{t} \dot{u}\, dt \tag{2.34}$$

where u, $\dot{u}$, $\ddot{u}$ are the displacement, velocity and acceleration respectively in Δt.

The resulting displacements, velocities and accelerations are obtained by solving

$$\begin{aligned}[\frac{4}{\Delta t^2}[M] + \frac{2}{\Delta t}[C] + [K]]\{\Delta u\} &= -[M]\{\Delta \ddot{u}_g\} \\ &+ [M]\{2\ddot{u}_i + \dot{u}_i\frac{4}{\Delta t}) + [C]\{2\dot{u}_i\}\end{aligned} \tag{2.35}$$

Using dynamic time-history analysis, as variable output, peak relative displacement and maximum acceleration of the mass were evaluated for different coefficients of friction and spring constants.

2.7.2 Results

The uppermost curve in Fig.6 is the relationship between peak relative displacement and friction coefficient. It shows that the increase of the friction coefficient has a significant effect in reducing the peak relative displacement in the range of low friction coefficients, ($\mu < 0.12$), but there is little further change for higher friction coefficients. The relative displacement is zero when μg is

equal to the peak ground acceleration.

The lowest curve in Fig.7 represents the maximum acceleration of the mass as the friction coefficient changes. As the maximum acceleration is caused by the friction coefficient, the relationship between them is linear. If no slipping occurs, the acceleration is that of the fixed-base case. To minimise the acceleration of the superstructure, the friction coefficient should be as small as possible.

To study the sensitivity of a pure-friction system to various types of excitation, different intensities and frequency contents of the excitation were used as input.

1) It is shown in Fig.8 that the peak relative displacement is quite sensitive to variation in the intensity for the pure friction system, especially for lower friction coefficients, becoming less sensitive as the friction coefficient increases.
2) Fig.9 gives the response for different frequency contents, showing that the relative displacement is sensitive to variations in frequency content, and such sensitivity gets less as the friction coefficient increases.

2.7.3 Conclusions from the parametric studies

For EL-CENTRO record, the maximum displacement is seen

in Fig.6 to be very strongly infleunced by the friction coefficient up to a value around μ=0.12, for which case the relative displacement was 0.1 of the maximum ground motion. Higher values of the friction coefficient increase the acceleration(Fig.7), but with only a small reduction in relative displacement.

Using the relationship developed for continuous sliding, and the maximum acceleraiton for EL-CENTRO of 0.32g gives a desirable coefficient of 0.537x0.32 = 0.17. This suggests that the condition of continuous sliding at peak acceleration is given a resonable initial estimate. Doubling the intensity of earthquake(Fig.8), shows that the desirable coefficient of friction lies in the same range, thus the optimum is not sensitive to variations in intensity.

2.8 Laboratory tests

2.8.1 Introduction

The potential of friction base isolators to reduce the acceleration without a large relative displacement has been demonstrated by the computer analysis. To implement these ideas, suitable materials must be selected for the sliding surfaces and their efficacy in controlling seismic response must be demonstrated.

The experimental program was designed to obtain information on:

1) The coefficient of friction of different materials, including both static and dynamic.
2) The behaviour of a base isolated mass when resting on these materials for the sliding surfaces.

2.8.2 Previous work on friction materials

1) Brass and steel

The damping behaviour of brass alloy has been reported by A.L.Kimball[11]. However, some of the literature suffers from a lack of systematic investigation. There are two papers[12][13] that cover a wide range of alloys, however, neither of these includes a sufficiently wide range of frequencies. There is still a need to study the damping behaviour of brass.

Leaded bronze brass against a stainless steel surface is known to be the most suitable combination for a stable behaviour.

2) Teflon and stainless steel

Teflon has been used in building structures only in recent years[42]. Many researchers[14][15][16] devoted their effort not so much to its physical properties for base isolation, but more

to the establishment of a proper mathematical model for the physical process. As we have shown, Teflon, as a friction material, is quite different from other common friction materials, especially when sliding on the stainless steel plate, and has many desirable properties for base isolation.

However, at present, data on its friction properties provided by the literature are inconsistent. The reason is due to the difference of the test conditions. In addition, the mathematical model describing the friction process is still approximate. Therefore, some further study was necessary.

2.8.3 Experimental procedure

A series of tests were conducted using the shaking table in the structural laboratory of Concordia University.

[1] Support arrangement (Fig.11(a))

Four sliding supports were installed between the block and the shaking table. The support was formed by pairs of steel disks, 180 mm in diameter and 25.4 mm in height. The bottom disk was welded to the shaking table. To avoid non-uniform distribution of vertical load on the supports, a 25ϕ steel ball rested in central pockets, one in the steel plate bolted to the concrete block and the other in the top disk. The friction material was placed between each pair of steel disks.

[2] Materials and specimen preparation (Fig.11(b))

(1) The materials forming the sliding interface included :

a) A leaded brass (henceforth called brass) plate of 30 x 30 x 1/16 inch in thickness. The plate was cut into square shapes of 7 x 7 inches, and the four corners bent down to retain it in position. Both surfaces were kept clean and smooth before the tests.

b) An unfilled virgin sheet type teflon of 24 x 24 x 1/16 inch in thickness. The sheet was cut into square shapes of 7x7 inches and circular shapes of 1.6 and 2.4 inches in diameter. Both sides were kept dry and clean.

c) Stainless steel sheet has dimensions of 20 x 30 inches and 1/16 inches in thickness. The sheet was cut into square shapes of 7 x 7 inches. The specified requirements of the sheet were: ASME SA-240; type 304; Rockwell B; Hardness 88; Roughness of surface < 0.05 μm CLA. The stainless steel sheets were kept clean and smooth before each test.

(2) The material forming the sliding mass

A block of 1.5 x 1.5 x 0.4 metres, weighing 2025kg (4525lb), was assembled from four concrete blocks, each is 0.75 x 1.5 x 0.2 metres, connected together by long bolts.

[3] Testing apparatus

The testing apparatus is shown schematically in Fig.10 and Fig.12.

(a) Shaking table

The shaking table measuring 4mx6m, and the movement is nominally one dimensional. The motion of the table is controlled by the sweep generator (112 wavetek), which is a voltage controlled oscillator. The range of frequency can be varied continuously from 0 Hz to 10 Hz.

The driving force is provided by a hydraulic actuator controlled by a Moog valve The signals to control the actuator are simultaneously sent to the oscilloscope for display.

(b) Control of the block

To limit the horizontal displacement of the concrete block, a hydraulic jack was installed at each side of the block, in the direction of motion, reacting against brackets welded to the surface of the table (Fig.12(b)). These hydraulic jacks were also used to move the block when measuring static friction coefficients. Between the jacks and the concrete block, rubber pads were inserted to avoid damage to the block due to impact force. These rubber pads also provided the resilient restraints in R-FBI system. A load cell measured the force between the jack and the concrete block.

To provide lateral restraint, rollers with vertical axis were placed on both sides of the block.

(c) Measuring and analyzing devices

(1) An accelerometer, type 511, was used to detect the acceleration of the block or the table. The range of measurement is from 0 to 1g.

(2) A linear transducer, which incorporated a strain indicator, type P350, read by a HP3466A Digital Voltment, gave the displacements of the table relative to the mass, and sent the signals of the displacements to the oscilloscope.

(3) The Storage Oscilloscope, type PM3310Philips, has two functions:
it receives the signals from the strain indicators and the sweep generator for display on the screen of the oscilloscope, and sends these signals to the X-Y plotter(7035HP).

All instrumentation was calibrated prior to each test.

[4] Test method

The tests were of two types: static and dynamic.

(1) Static tests

The purpose of static tests was to determine the static friction coefficients between the materials.

Because the block had four supports, a possible difference of friction coefficients due to non-uniform support reactions had to be considered. The readings for the friction coefficient were obtained for three conditions: (1) with the bolts that hold the blocks together in the loose condition, (2) just snug, and (3) fully tightened, to check the difference due to warping of the block.

The hydraulic jack was used to provide the horizontal force, which was measured by a load cell, required to slide the block. The force at the start of motion gave the static friction coefficient.

The block was pushed forward and then backward to get two forces, which were averaged. The readings for the three conditions of bolt tightening were averaged to get the final friction coefficient of the material.

The first combination tested was the steel disk and the brass sheet. The top steel disk was polished, and the brass sheet was held on the bottom disk by a soldered ring. Thus slip could only occur between the top disk and the brass

sheet.

The second combination was between the polished steel disk and the stainless steel sheet. The stainless steel sheet was fixed on the brass sheet by bolts, and the brass sheet was held on the bottom disk by a soldered ring. Slip occurred between the top disk and the stainless steel sheet. The stainless steel sheet was polished and kept clean before each test.

The third combination was the unfilled Teflon and the polished stainless steel sheet. The breakaway coefficients of friction were measured under different pressures. To produce the different pressures on the interface, Teflon specimens of different areas were used: a square 180x180mm and three circles: 60mm, 40mm and 30mm in diameter. The pressures on the interface were, respectively, $0.2N/mm^2$, $1.8N/mm^2$, $4N/mm^2$, $7.1N/mm^2$. The square Teflon sheet was bolted on a metal plate(180x180x0.8mm) with a soldered ring to hold on the top disk. A metal plate of 180x180x0.8mm, with a central hole to match the Teflon circles, and a soldered ring to hold on the top disk, was used for the Teflon specimens.

(2) Dynamic tests

The purpose of the dynamic tests was to establish the dynamic response for each type of interface under various

conditions.

To obtain dynamic response for different frequencies of the shaking table, the frequency was held constant or changed continuously from 1 Hz to 10 Hz in different time intervals, between 2 and 16 seconds. The amplitude of the motion is changed with the frequency. The accelerations of the table and of the concrete block were measured, and the displacement time-histories were recorded for the different frequencies. The check on the dynamic friction coefficient was obtained by measuring the acceleration at the start of motion.

The sliding surface was cleaned at the conclusion of each test to maintain the original condition.

2.8.4 Results

(a) Static test

Static friction coefficients of different materials are listed in Table 1. The interface between brass and steel gives the highest friction coefficient, 0.318. The interface between Teflon and polished stainless steel sheet exhibits the smallest static friction coefficient, 0.064. The stability of buildings under wind load has been discussed before, and these coefficients of friction are sufficient for medium or low buildings.

As is known, the breakaway coefficient between Teflon and stainless steel sheet is pressure dependent, approaching a constant for high pressures, as shown in Fig.13.

These results are somewhat different from those of previous researchers, some higher some lower, since many factors in our test are different from others, such as roughness of the interface, hardness of materials, methods of test, and test surroundings.

(b) Dynamic test

The dynamic tests were conducted:

(1) to study the behaviour at different rates of change of the frequency as the frequency sweeps from 1 to 10 Hz in different time intervals.

(2) to obtain the time-history responses for constant frequency.

For stainless steel and steel:

The static friction coefficient was 0.122. The dynamic friction coefficient of 0.1 was obtained by measuring the acceleration of the block during vibration.

Frequency sweep:

The mean relative displacement of the block varied with the rate of change of the frequency (see Fig.14), as did the

residual displacements. The residual displacement was also different for different directions of frequency change.
Under the action of a frequency sweep the block wandered at random. The maximum relative displacements occurred between 7 and 8 Hz when contact was made with the rubber bumpers.
When the frequency changed very quickly, as from 1 to 10 Hz in 2 seconds, a relative displacement was still observed, illustrating that when continuous sliding occurs, any minor bias in the loading can cause the block to wander.
Constant frequency:
After about 7 Hz(acceleration of the table = 0.12g), continuous sliding occurred, and continued to 9 Hz(Fig.15). This range is approximately consistent with results derived theoretically.

For brass and steel

Frequency sweep:
The relative and residual displacement again appeared in general to be random, once sliding had started(Fig.16).
Constant frequency:
Fig.17 shows that the relative displacement time-history of the block for each frequency. After 7 Hz, sliding occurred. The peak relative displacement was smaller than for the interface of steel and stainless steel.

2.9 Conclusion

In a pure-friction system, the aim is to reduce the acceleration of the structure, and to limit the relative displacement. To avoid stick-slip behaviour the coefficient of friction should be as low as is practical.

Study of Fig.6 and Fig.7 indicates that a coefficient of 0.12-0.22 is the most desirable range when considering both displacement and acceleration.

Fig.6 shows that this coefficient lies in the range where any increase will have little effect on relative displacement, and this provides a reasonable target value for the design.

Relative displacement, however, may be large due to wandering as there is no positive restoring force.

Chapter III

Resilient-friction Base Isolator (R-FBI)

R-FBI is a system which has evolved from a sliding type isolator. This system incorporates the characteristic of a friction material with the resilience of rubber[46]. Fig.18 shows a schematic diagram of this system. Since the energy dissipated due to viscous damping of rubber is small (represented by a dashpot in Fig.18) it was not considered in this study. The rubber element provides a horizontal restoring force and carries no gravity load. The interfacial friction force acts as the structural fuse.

In such a system, the vertical load of the building is carried on a sliding surface, which is rigid in the vertical direction. The resilient element is independent of the sliding device and can be installed anywhere in the base plane. This is distinct from isolators with multiple layers of rubber which must carry the vertical load while displacing horizontally, which may lead to instability due to the resulting eccentricity of the vertical load, and from the R-FBI system developed by Mostaghel which may lead to shear strain concentration due to non-uniform slip of the sliding surfaces.

With a sliding surface restrained elastically, the

natural frequency changes with amplitude, thus resonance does not occur, as can happen with the multiple rubber bearings.

As long as the intensity of ground motion is small, the friction force prevents any lateral relative motion. When the lateral acceleration exceeds the friction force μg, the base starts to slide, causing the rubber element to deform and build resistance, which increases as the relative displacement increases. Although it is difficult to achieve resonance in a spring-friction system, the natural frequency of the system should be lower than the frequency range of the ground motion.

In order to show the isolation characteristics of the R-FBI, the horizontal response of a rigid structure supported on an R-FBI is considered. This ignores any other interaction of the superstructure and the isolation system.

In this study, the rubber element is modelled by a linear relationship between the resistance and the relative displacement.

3.1 Governing Equations

3.1.1 Derivation of Equations

The following symbols are used in the derivations to follow:

u = displacement of the body relative to the ground = $x - x_g$

x_g = horizontal ground displacement

x = absolute displacement of the body

k = spring constant for the resilient restraint

ω = angular frequency of the body controlled by the resilient restraint: = $(k/M)^{1/2}$, (natural frequency = $2\pi/\omega$)

M = mass of body

μ_d = sliding friction coefficient

g = acceleration due to gravity

3.1.1.1 The sliding condition of the body

When a rigid body supported on the R-FBI system is subjected to the horizontal ground excitation, the body is acted on by a force made up of the spring force, $ku = M\omega^2 u$, and the friction force, $M\mu g$, which determine the motion of the body.

In a non-sliding phase ($\dot{u} = \ddot{u} = 0$),

$$\mu g - | \ddot{x}_g + \omega^2 u | > 0 \qquad (3.1)$$

At the start of a sliding phase the inequality (3.1) changes to

$$\mu g - | \ddot{x}_g + \omega^2 u | = 0 \qquad (3.2)$$

In a sliding phase ($\dot{u} \neq 0$)

$$\mu g - x_g \varnothing \omega u \tag{3.3}$$

The equations (3.1) to (3.3) are used to check if the system is in a non-sliding or sliding phase.

3.1.1.2 The equations of motion

Based on the Fig.18, neglecting the damping represented by the dashpot, the behaviour of the isolator is governed by the following equations:

Assume:

(1) the system is in a sliding phase.

(2) the sliding friction coefficient μ_d is constant.

(3) $\dot{u}$ does not change sign in each time interval(from t_{n-1} to t_n).

(4) the structure is a rigid body with a SDOF.

(5) the body is subjected to the horizontal ground motion.

The equation of motion becomes[25] [31]

$$\ddot{u} + \omega^2 u = (-1)^{n+1} \cdot \mu_d \cdot g - \ddot{x}_g(t) \tag{3.4}$$

Using the initial conditions leads to the expressions of u_1 and u_n:

$$u_1(t) = \int_0^t \omega^{-1}\sin\omega(t-\tau)\,[\mu_d g - \ddot{x}_g(\tau)]\,d\tau - x_g(0)\cos\omega t - \dot{x}_g(0)\frac{\sin\omega t}{\omega} \tag{3.5}$$

where $0 \le t \le t_1$; $0 \le \tau \le t$, and $\dot{u}_1(t_1) = 0$:

$$u_n(t) = \int_{\tau=t_{n-1}}^{t} \omega^{-1}\sin\omega(t-\tau)\,[(-1)^{n+1}\mu_d g - \ddot{x}_g(\tau)]\,d\tau + u_{n-1}(t_{n-1})\cos\omega(t-t_{n-1}) \tag{3.6}$$

where $t_{n-1} \le t \le t_n$; $t_{n-1} \le \tau \le t$; $n=2,3,4,.....$

The end of each time interval can be found by

$$\dot{u}_n(t_n) = 0$$

For the derivation of the solutions to the equation of motion refer to the appendix.

3.1.2 Discussion of the equations

From the above results, it is seen that:

(1) the response of the body supported on R-FBI system is related to the earthquake input, the friction coefficient between the sliding interface, and the natural frequency of the body controlled by the resilient restraint.

(2) in a sliding phase, for a specified ground excitation input, the relative displacement becomes smaller and the

acceleration of the mass gets greater as the natural frequency of the body increases (i.e. as the spring constant k increases), and as the coefficient of friction increases.

3.1.3 Discussion on optimum values of parameters for R-FBI system

For an R-FBI system, the two parameters that control the behaviour of the system are the sliding friction coefficient between the interfaces, μ_d and the rigidity of the spring, k.

The same evaluation criteria for the most suitable values of the parameters are used, namely:

(1) a reduced acceleration transmitted into the superstructure

(2) a low relative displacement of the superstructure

Using the different ground excitation inputs may lead to different values of μ and k, or there may be a set of values that is the best for all types and intensities of earthquake. Since the future earthquake can not be predicted, this would be the preferred case.

3.2 Computer simulation

3.2.1 Introduction

The time-history dynamic analysis computer program, DRAIN2D, was used to find the dynamic response of the R-FBI. A truss element with rigid/strain hardening characteristics was used to model the resilient-friction system, which has a hysteresis loop shown in Fig.19.

It is to be noted that the spring constant, k, used models an ideal spring element, and the friction coefficient is assumed to be constant during the time-history analysis.

The EL-CENTRO N-S 1940 earthquake record and their factored forms were used as the horizontal ground excitation. A harmonic frequency sweep was also used. The friction coefficient, μ, and the lateral stiffness, k, were varied, and the behaviour determined in each case.

3.2.2 Results

Using the EL-CENTRO record, the peak relative displacement and maximum acceleration of the body obtained are shown in Fig.6 and Fig.7 respectively.

The relation between the peak relative displacement and the friction coefficient for different spring constants is

illustrated in Fig.6, which shows that only in the low range of friction coefficients, does a addition of a spring effectively decrease the peak relative displacement. This means that the variations of the peak relative displacement become more sensitive to the change of spring constant as the friction coefficient become smaller. In the range of higher friction coefficients, a change of spring constant has little effect on the peak relative displacement.

Fig.7 represents the relationship between the maximum acceleration of the body and the friction coefficient. The results show that increases in the spring constant lead to increases in the acceleration of the body. The greater the friction coefficient, the less sensitive is the acceleration of the body to the changes of the spring constant.

Changes in intensity

To obtain the behaviour of the isolator under variations in the intensity of excitation, the accelerogram of the EL-CENTRO 1940 earthquake was multiplied by factors of 1.5 and 0.5, thereby changing the intensity, while its frequency content remained unchanged. The amplitude changed by factors of the same magnitude.

Fig.20 shows the relative displacement of the body when subjected to 1.5 EL-CENTRO earthquake:

(1) When $\mu < 0.14$

For the same friction coefficient, the peak relative displacement is much greater than that for 1.0 EL-CENTRO, and the peak relative displacement changes more as the spring constant changes.

(2) When $\mu > 0.14$

For the same friction coefficient, comparing the results for 1.0 EL-CENTRO, the increases in peak relative displacement become less than that when $\mu < 0.14$.

Fig.21 shows the relative displacement for 0.5 EL-CENTRO earthquake:

(1) the change of spring constant has some effect on the peak relative displacement for friction coefficients below 0.11.

(2) for the same friction coefficient, the peak relative displacement becomes smaller than that for 1.0 EL-CENTRO.

The maximum accelerations for 1.5 and 0.5 EL-CENTRO are shown in Fig.22 and 23. For the same friction coefficient, the presence of the spring can cause a higher acceleration of the body. However, the acceleration response is almost insensitive to variations in the intensity of the excitation, especially when the restoring force is weak. By doubling the intensity of ground excitation, the acceleration transmitted to the body by the isolator increases only a

little.

Changes in frequency content

To study the dynamic behaviour of the isolator with a different frequency content, the accelerogram of the EL-CENTRO 1940 earthquake was modified by multiplying the time scale by factors of 0.5 and 2.0 while maintaining the same acceleration. As a consequence the amplitudes were factored by 0.25 and 4 respectively. Fig.24 and 25 show that the relative displacement is relatively insensitive to the frequency content, when the isolator provides a weak restoring force, but very sensitive when it provides a strong restoring force for the EL-CENTRO record.

Table 2 shows the time-history response of the R-FBI system with a weak restoring force. It is seen that the spring force is smaller than the friction force in almost the whole time history. This means that the R-FBI system is still a friction-type isolator, with the resilient restraint acting mainly to control the displacement.

Response to a frequency sweep

When the frequency of a harmonic signal sweeps from 1 Hz to 10 Hz in 2 seconds (Fig.26), R-FBI system exhibits very good behaviour in the reduction of acceleration after slip, especially in the higher frequency range, which can be

seen in Fig.27.

3.3 Laboratory test

3.3.1 Introduction

A resilient restraint to the pure friction system, permits the use of a lower friction coefficient, and the results obtained from the numerical analyses show that the restoring force controls the relative displacement while the lower friction coefficient, reduces the peak acceleration of the structure. Tests were conducted to examine this behaviour.

3.3.2 Experimental procedure

No change was made in the arrangement used to test P-F system, other than the use of the rubber pads attached to the rams of the hydraulic jacks, which were brought into contact with the block. The pads had a spring constant of 2.6×10^5 N/m, giving a natural frequency of 1.8 Hz. The sliding surfaces were between Teflon and polished stainless steel sheet. The Teflon specimen was 60mm in diameter. The friction coefficients of the materials are: $\mu_s = 0.081$, $\mu_d = 0.048$. Constant frequency excitation for 1 Hz to 9 Hz and a frequency sweep, from 1 Hz to 10 Hz, of different durations were again used. The responses of the table and the block were recorded, in particular the relative displacement and the peak

accelerations.

3.3.3 Results

Constant frequency

In Fig.28 is shown the peak relative displacement of the block at constant frequencies. Starting at 7 Hz (acceleration =0.08g), the displacement increases continuously up to 9 Hz, and then approximately remains constant. It is always smaller than the response for stainless steel and steel without restraint.

Frequency sweep

Fig.29 shows how, for frequency sweeps from 1 Hz to 10 Hz in 2 seconds, the relative displacement of the block was controlled by the resilient restraint.

Once started, sliding was continuous, even when the peak acceleration was relatively low. This is attributed to the low value of μ_d and the high ratio of μ_s/μ_d, which extends the range of the continuous sliding.

3.4 Discussion of the results

The benefit of introducing a resilient element is to reduce the base shear by reducing the friction coefficient, while the resilient element acts as a controlling device to reduce the

peak displacement. This has been demonstrated in the tests. However, there is no claim that the optimum values were used, as the natural frequency of the system was somewhat high.

For the same friction coefficient, the presence of a resilient element increases the acceleration transmitted, although it is small if the restoring force is weak. However, since by its presence it can permit a reduction in the friction coefficient from that required in a pure-friction system, the final effect of R-FBI is to decrease the acceleration transmitted, without increasing the peak relative displacement.

The smaller friction coefficient improves the horizontal isolation, and the weak resilient action reduces the natural frequency of the structure below the dominant frequency of the ground motion. These two properties also make an R-FBI system less sensitive to variations in intensity and frequency content of the ground motion.

From the results of computer analysis, it is found that a desirable combination for the friction coefficient and natural frequency, where EL-CENTRO 1940 N-S record was used as the ground excitation, was given when $\mu = 0.14$ and $f = 0.4$ Hz. This combination gives the same peak relative displacement of the block, as for $\mu = 0.2$ in the P-F system(Fig.6), but with acceleration reduced by 25%(Fig.7). However, this combination

is only a suggested one, since the actual friction coefficient is not a single value.

The results also show that, in this case, the friction force is large relative to the spring force(Table 2), and thus the R-FBI system functions mainly as a structural fuse.

Since an R-FBI system is a friction type isolator, the horizontal stiffness changes with the displacement, and therefore cannot become resonant.

Should the static coefficient of friction be higher than the dynamic one, the resilient restraint will act in conjunction with the lower value and thereby reduce the total force.

Chapter IV

Discussion for Design of R-FBI system and Recommendations

Base-isolation is a design concept based on the premise that a structure can be substantially decoupled from potentially damaging earthquake motions, and thereby reduce the probability of significant inelastic distortion, structural and nonstructural damage, and the loss of building function. Base isolators respond to horizontal ground motion only. In this paper no proposals are advanced to accommodate vertical motion.

In choosing the appropriate values for the parameters in R-FBI system, the following design requirements are to be considered:

(1) Wind loads

Base-isolated structures must resist wind loads in accordance with the general wind design provisions. This gives the minimum required static friction coefficient. As the buildings considered are usually concrete and masonry, the vertical loads are high, and only a small coefficient is required, usually less than 0.1.

(2) Maximum base shear force

The maximum shear force exerted at the base of building,

or at any level in the building should be such that the structural and nonstructural elements remain fully elastic during the design earthquake with minimum secondary damage. This force depends directly on the friction coefficient and the stiffness of the resilient restraint, and should be such that the base shear is less than that which would occur for the design earthquake in the absence of a base isolator. The value of the base shear for the EL-CENTRO record according to the National Building Code of Canada would be typically 0.17 W.

(3) Resilient restraint

The purpose of the resilient restraint is to control the relative displacement, and thereby permit the use of a lower coefficient of friction for a specified limiting displacement under the action of the design earthquake. For the EL-CENTRO record with a peak ground motion of 0.21 m and the maximum acceleration 0.32g, analysis shows that the relative displacement can be reduced to 0.02 m when the acceleration is reduced to 0.15g(see Fig.6 and Fig.7).

(4) Size of the isolator

The isolation system should be designed to be stable under the full design vertical loads at the maximum horizontal displacement. This determines the dimensions of the sliding surfaces.

(5) Rigidity of the base and foundation

The analytical model of the building has assumed that all base isolators participate equally in the response, without regard to their plan location. This requires that the building has a rigid diaphragm at the upper plane of the base isolators. In addition, the structure at the lower plane of the base isolators should have the necessary stiffness to limit the translation of the anchorage of the isolators relative to the ground in the horizontal plane.

(6) Irregular motion

The analytical model does not include the effects of torsional ground motions and plan irregularity. The spring constant in a base isolator should match the mass above the base isolator, but specific analysis for a particular building and design earthquake is required. Because of the unknown or changing direction of ground motion, the isolator must accommodate both translation and rotation of the building.

(7) Uplift

Friction base isolators are not, in general, used where there is an uplift due to overturning. Special design may be possible.

(8) Durability

As the design of an R-FBI system is based on certain values of the coefficient of friction and the spring constant, it is important that these values do not change significantly with time.

A simple design of R-FBI is proposed in Fig.30, which is proportioned to satisfy the anticipated requirements. Its features are:

(1) it has a single sliding surface.

(2) the rubber acts in compression instead of in shear.

(3) it accommodates all directions of motion in the horizontal plane.

(4) it is stable at large horizontal displacements.

Recommendations for further studies

The study of the R-FBI system has been confined to a single degree of freedom structure. Further studies might consider the interaction between the isolator and an elastic structure.

Because the isolator proposed accepts any direction of horizontal motion, it is expected to behave equally well for torsional models of the building or ground motion, but this could be a subject for further consideration.

At present, a number of researchers [35] are devoting their efforts to 3-D isolation systems, to include vertical motion, as there is some evidence that it may become a critical factor for building damage. Therefore, some attention should be given to this vertical motion.

Since sway will occur in a building during an earthquake, present base isolators are applied only in low and medium rise buildings to avoid uplift. Consideration can be given to added means of anchorage to improve the behaviour of base isolators in high-rise buildings.

List of References

[1] A.H. Hadjian and W.S. Tseng, 'A Comparative Evaluation of Passive Seismic Isolation Schemes', Journal of Base isolation and Passive Energy Dissipation (Ed. C. Rojahn), ATC-17, National Bureau of Standards, 1986.

[2] R.P. Bron, 'Physical Testing of Rubbers', Applied Science Publishers Ltd, London, 1979.

[3] R. Chen, X. Wang, and C. Wang, 'Behaviours and Application of Rubber Bearing', Beijing Institute of Archtectural Design, Beijing, China. 1987.

[4] David Tabor, 'Friction-The Present State of Our Understanding', Journal of Lubrication Technology, April, 1980.

[5] J.E. Long 'Bearings in Structural Engineering', John Wiley and Sons, Inc. New York. 1974.

[6] R. Chen, X. Wang, and C. Wang, 'Tests of Teflon Bearing', Beijing Institute of Architectural Design, Beijing, China. 1987.

[7] Wen, Y.K. 'Method of Random Vibration of

Hysteretic Systems,' J. Engrg. Mech. Div. ASCE, 102(2). 1976.

[8] Paul Henderson and Milos Novak, 'Response of Base-isolated Buildings to Wind Loading', Journal of Earthquake Engineering and Structural Dynamics, VOL. 18, 1989.

[9] M. Novak and L. El Hifnawy, 'Effect of Base Isolation on Structural Response to Earthquake and Wind', Proc. 8th Eur. Conf. Earthquake Eng. Lisbon, 1986.

[10] Kannan, A.E. and Powell, G.H., 'Drain-2D, A General Purpose Computer Program for Dynamic Analysis of Inelastic Plane Structures', College of Engineering, Uni. of California, Berkeley, 1973.

[11] A.L. Kimball, 'Physical behaviour of Alloys', Trans. of the North East Coast Institution of Engineers and Shipbuilders, 1963.

[12] W.H. Hatfied, G. Stanfield and L. Rotherham, 'Further Work on Alloy,' Trans. of the North East Coast Institution of Engineers and Shipbuilders. 1965

[13] C. Schabtach and R.O. Fehr, 'Alloys Behaviours', Trans.

of the North East Coast Institution of Engineers and Shipbuilders. 1966

[14] Uetz, H. and Hakenjos, V., 'Friction Experiments in Teflon Subjected to Reciprocal Motion', Journal of Structural Engineering, April, 1967

[15] J.E. Long, 'The Performance of PTFE in Bridge Bearings', Civil Engineering and Public Works Review, 64 No. 754. 1974.

[16] E.I. du Pont de Nemours and Co., 'Selecting the Right Teflon PTFE Compound', Reprint No.47 from J. Teflon. 1982.

[17] Milind Pimprikar, 'Elastomeric Bearing Pad Performance Under High Stress', Master's thesis, Department of Civil Engineering, Concordia University 1983.

[18] E.I. du Pont de Nemours and Co., 'The how's and why's of friction for Teflon Resins' Reprint No.19 from J. Teflon. 1978

[19] E.I. du Pont de Nemours and Co., 'Teflon: Mechanical Design Data', Report No.43, Wilmington, DE, 1981.

[20] D.G. Flom and N.T. Porile, 'Friction of Teflon Sliding on Teflon', J. Appl. Physics, No.26 1955.

[21] R.G. Tyler, 'Dynamic Tests on PTFE Sliding Layers Under Earthquake Conditions', Bull. New Zealand Natl. Soc. Earthquake Engineering, No.10, 1977.

[22] Avtar S. Pall, 'Limit Slip Bolted Joints - A Device to Control the Seismic Response of Large Panel Structures', PhD thesis, Centre for Building Studies, Concordia University. 1979.

[23] Parvaneh Baktash, 'Friction Damped Braced Frames', PhD thesis, Centre for Building Studies, Concordia University, 1989.

[24] Steven L. MoCabe and Willam J.Hall 'Evaluation of Structural Response and Damage Resulting from Earthquake Ground Motion', Report No. UILU-ENG-87-2009, Uni. of Illinois, Urbana, Illinois, Sept. 1987.

[25] Ray W. Clough and Joseph Penzien 'Dynamics of Structures', McGraw-Hill, Inc. 1975.

[26] Roy R. Craig, Jr. 'Structural Dynamics - An Introduction to Computer Methods', John Wiley and Sons, Inc. 1981.

[27] N.M. Newmark and Emilio Rosenblueth, 'Fundamentals of Earthquake Engineering', Prentice-Hall, Inc. Englewood Cliffs, N.J. 1971.

[28] C. Hepburn and R.J.W. Reynolds, 'Elastomers: Criteria for Engineering Design', Applied Science Publishers Ltd. London, 1979.

[29] N.M. Newmark, 'A Method of Computation for Structural Dynamics', Journal of the Engineering Mechanics Division, ASCE, July, 1959.

[30] S. Levy and W.D. Kroll, 'Errors Introduced by Step-by-Step Integration of Dynamic Response' National Bureau of Standards Report, USA, February, 1951.

[31] 'An Introduction to Earthquake Engineering', 2nd ed. Science Publishers, Beijing, China. 1985.

[32] E.L. Wilson, I. Farhoomand and K.J. Bathe, 'Nonlinear Dynamic Analysis of Complex Structures', Journal of Earthquake Engineering and Structural Dynamics, Vol.1, 1973.

[33] Avtar S. Pall and C.Marsh, 'Response of Friction Damped Braced Frames', Journal of the Structural Division,

ASCE, Vol.108, No. ST6 June, 1982.

[34] T.C. Liauw, Q.L. Tian and Y.K. Cheung, 'Structures on Sliding Base Subject to Horizontal and Vertical Motions', Journal of Structural Engineering Division, ASCE, Vol. 114, No.9, September, 1988.

[35] N. Tokuda, A.Kashiwazaki and M. Akimoto, 'Shaking Test of 3-D Isolator by Using Air Spring and Rubber Bearing', Journal of Earthquake Engineering and Structural Dynamics, Tokyo, Japan. May, 1987

[36] B. Westermo and F. Udwadia, 'Periodic Response of a Sliding Oscillator System to Harmonic Excitation', Journal of Earthquake Engineering and Structural Dynamics, Vol.11, 1983.

[37] Ahmadi, G. and Mostaghel, N., 'On Dynamics of a Structure with a Frictional Foundation', Journal De Mechanique. April, 1982.

[38] Bernard, J.E., 'The Simulation of Coulomb Friction in Mechanical Systems', Simulation, Vol 34 No.1 Jan., 1980.

[39] Tkachenko, V.Ya., 'Simulation of Dry Friction',

Automation and Remote Control, Vol. 35 1974.

[40] Villagio, P., 'An Elastic Theory of Coulomb Friction', Arch. Ratl. Mech. Anal., Vol 70 1979.

[41] Clen V. Berg and Donald A. DaDeppo, 'Dynamic Analysis of Elasto-plastic Structures', Journal of the Engineering Mechanics Division, ASCE, Vol. 86 No. EM2, April, 1960.

[42] C. Terry Dooley and Rita Robison, 'Seismic Surgery', Journal of Civil Engineering, ASCE, Vol.60 No.9 September, 1990.

[43] A. Filiatrault and S. Cherry, 'Comparative Performance of Friction Damped Systems and Base Isolation Systems for Earthquake Retrofit and Aseismic Design', Journal of Earthquake Engineering and Structural Dynamics, Vol.16, 1988.

[44] A.G. Buswell, E.Gee and E.R. Thornley, 'Dynamic testing and interpretation of results', J.Institute of Rubbeer Industry, Report No.43, 1967.

[45] J.M. Kelly and S.B. Hodder, 'Experimental study of lead and elastomeric dampers for base isolation systems in

laminated neoprene bearings', Bulletin of the New Zealand and National Society for Earthquake Engineering, Vol.15, No.2, June 1982.

[46] N. Mostaghel and M. Khodaverdian, 'Seismic Response of Structures Supported on R-FBI System', Report No. UTEC 87- 035, Department of Civil Engineering, University of Utah, September 1987.

[47] Bouc, R. 'Modele mathematique d'hysteresis.' Acustica, No. 24(1), 1971

[48] Marsh, C., Pall, A.S., 'Friction-devices to Control Seismic Response' Second ASCE/EMD Specialty Conference on Dynamic Response of Structures, Atlanta U.S.A., Jan. 1981

[49] Pall, A.S., Pall, R., 'Friction Base Isolated House in Montreal', Proceedings Sixth Canadian Conference on Earthquake Engineering, Toronto 1991

Appendix A

1 Engineering Properties of Rubber

To provide the resilient element it is proposed to introduce a rubber cushion to restrain the circular sliding disks, as shown in Fig.30, thus a study of the behaviour of rubber was made. Rubber material is viscoelastic and hence its response to dynamic stressing is a combination of an elastic response and a viscous response and energy is lost in each cycle. A simple model to represent this behaviour is a spring and dashpot in parallel.

For sinusoidal strain the motion is described by:

$$\varepsilon = \varepsilon_{\circ} \sin \omega t \qquad (1)$$

where:

ε = strain

$\varepsilon_{\circ}$ = maximum strain amplitude

ω = angular frequency

t = time

If the rubber were a perfect spring the stress would be similarly sinusoidal and in phase with the strain. However, because the rubber is viscoelastic the stress will not be in phase with the strain but can be considered to precede it by the phase angle δ.

Usually, the stress is considered as a vector having two components, one in phase with the displacement and one 90° out of phase, and to define corresponding in-phase, out-of-phase and the resultant (complex) moduli. The vector moduli in tension or compression can be defined by :

$$E^* = E' + iE'' \qquad (2)$$

where:

E^* = complex modulus,

E' = in-phase or elastic modulus,

E'' = out-phase or loss modulus.

It can be also shown that:

$$E' = \sigma'/\varepsilon_o = (\sigma_o / \varepsilon_o)\cos\delta = |E^*|\cos\delta \qquad (3)$$

$$E'' = \sigma'' /\varepsilon_o = (\sigma_o / \varepsilon_o)\sin\delta = |E^*|\sin\delta \qquad (4)$$

$$|E^*| = (E'^2 + E''^2)^{1/2} \qquad (5)$$

$$\text{Loss tangent, } \tan\delta = E''/E' = \sigma''/\sigma' \qquad (6)$$

where:

σ''= amplitude of out-of-phase stress

σ'= amplitude of in-phase stress

Elastic modulus E' of rubber represents the behaviour of an equivalently ideal spring, that means it is independent of frequency and temperature and has nothing to do with damping effect of rubber. The behaviour of loss modulus E'' is more complex, which is related to loss angle of rubber. Loss modulus and loss angle arise from the viscous damping. Their values directly reflect the energy loss due to deformation of the rubber.

Hysteresis loss can be used to described the energy loss due to damping, which is dependent on the loss modulus and strain. The energy loss per unit volume of material during one sinusoidal cycle is given by[44]:

$$H = \pi \varepsilon^2 E'' \qquad (7)$$

where:

H = hysteresis loss

ε = one half peak-to-peak dynamic strain

E"= viscous modulus

Therefore, greater values of E" should be taken for damping purpose, and greater values of E′ for deflecting energy. This should be considered as rubber is used in different isolators for different purposes.

A rubber element, like a spring, provides a restoring force in the R-FBI system. When a building is analyzed on rubber type bearings for earthquake action, it is usual to treat the combined system by a linear viscously damped model. In fact, the viscoelastic behaviour of rubbers is not linear; stress is not proportional to strain, particularly at high strains. Therefore, it is necessary to limit it to small strains.

The result in practice is that dynamic stiffness and moduli are strain dependent and the hysteresis loop will be a ellipse. Dynamic properties for rubber are also dependent on frequency and temperature. The general form of the effect of

temperature on complex modulus and tgα shows that the viscous behaviour of rubber becomes weaker as temperature increases, and attention should be given to this when rubber is used for damping purpose. The effect of increasing or decreasing frequency is to shift the curves to the right or left respectively along the temperature axis. Tests have shown that, at room temperature, the order of magnitude of the effect of temperature on modulus for a typical rubber is 1% per °C and the effect of frequency of the order of 10% per decade.[2]

Another feature worth mentioning is that a difference in chemical structure of the elastomer can change the location of a dynamic response curve on the frequency scale but it will not change the overall shape of the frequency dependency appreciably.

Thus the behaviour of an elastomeric element differs in two important respects from the simple spring:

(1) the modulus of the elastomer varies with the applied frequency, which means that the stiffness of the element varies similarly;

(2) energy is dissipated internally by viscous damping of the rubber (even though it is not the main part of the energy dissipated in the isolator).

In practice, a rubber is required to be soft at low

frequencies but with the stiffness (proportional to the dynamic modulus) increasing with frequency. This rule arises because large amplitude motion is normally only required at low frequencies.

If the fundamental frequency of the fixed-base building is much higher than that of the isolated system, say 3 Hz as compared to 0.5 Hz for the isolated case, the first mode of the isolated building is mainly a rigid body mode with all deformation in the rubber. The second mode of the isolated building has a frequency about 50% to 100% above the first fixed-base frequency. The seismic input (acceleration) to the isolated structure can be treated as an equivalent lateral load which is proportional to the first mode(rigid body mode) in the isolated case. Since it is a characteristic of a linear vibrating system that all modes are mutually orthogonal, all modes higher than the first will be orthogonal to the input motion, so that if there are high energies in the earthquake ground movement at the frequencies of these higher modes, this energy cannot be transmitted into the isolated building. This is the principle of rubber, as a isolator, to prevent high frequency input. Furthermore, the damping capability of the rubber is relatively small in R-FBI system. Thus, the rubber element works mainly not by absorbing these energies but by shifting the fundamental frequency of the building out of the exciting frequencies.

Rubber is resilient, and the rebound resilience is the main attractive feature of the simple rubber element. The resilience R is approximately related to the loss tangent, which can be obtained by the special test as follows:

$$R=\frac{E_R}{E_T}=\exp(-\pi tg\alpha) \tag{8}$$

where E_R = reflected energy

E_T = incident energy

α = loss angle

The relationship is not particularly accurate because $tg\alpha$ is strain dependent and the strain cannot be controlled under dynamic conditions.

2 Engineering Experience on Rubber Application

There are many types of base isolator which use rubber. One uses a laminated rubber bearing(LRB), of the type in expansion joint for bridges. Considerable work has been done to show its effectiveness as a base isolation system, and especially has it filters the high frequency energy content of ground acceleration.

However, studies show that the rubber bearing type base isolators are sensitive to severe variations in the frequency content of earthquakes, and if the predominant

frequency of excitation is low (as in the case of a soft site), the rubber bearing type base isolator can act as an amplifier and impose large displacement demands on the base.[3]

Since rubber isolator element is subjected to the horizontal and vertical loads at the same time, its stiffness and damping characteristics are affected by changes in the vertical load during rocking[28] [34].

Another type use multiple sliding surfaces with central rubber core. In practice, this type, at higher loads, can suffer from a shear blocking phenomenon, where the plates moved in groups instead of sliding individually. This is due to different friction forces at the sliding interfaces, caused by the fact that the friction coefficients are not exactly the same, and thus cause shear strain concentrations at the levels of sliding interfaces.

For an improved R-FBI isolator which is to use rubber, it is suggested that:

(1) the rubber element should act to resist lateral motion only, not to combine the vertical loads.

(2) friction surface should provide the essential base isolation the number of sliding interfaces should be reduced to the minimum.

The proposed base isolator with a single sliding

surface and the circular rubber cushion acts as these purposes(Fig.30).

Appendix B

Derivation of Equations of Motion for R-FBI System

[1] symbol note:

u = displacement of the body relative to the ground = $x - x_g$

k = spring constant

ω = natural frequency of the body controlled by the resilient restraint: $M\omega^2 = k$

μ_d = sliding friction coefficient

g = acceleration of gravity

x_g = horizontal ground displacement

x = absolute displacement of the body

a_n, b_n = constants determined by the initial conditions, $n=1,2,3,...$

[2] Assumption:

(1) the system is in a sliding phase.

(2) the sliding friction coefficient μ_d does not change with the sliding velocity and the pressure of bearing.

(3) $\dot{u}$ does not change sign in each time interval (from t_{n-1} to t_n).

(4) the superstructure is a rigid body with a SDOF.

(5) the body is subjected to the horizontal ground motion.

(6) the viscous damping of rubber (represented by dashpot in Fig.21) was not considered.

[3] Derivation of the Equation

The equation of motion becomes:

$$\ddot{u} + \omega^2 u = (-1)^{n+1}\cdot\mu_d\cdot g - \ddot{x}_g(t) \tag{1}$$

Associated homogeneous equation:

$$\ddot{u} + \omega^2 u = 0$$

has integral bases {cosωt, sinωt}.

Using Green's function method, if the solution to Eq.(1) is denoted by $u_1(t)$ in the first time interval ($0 \le t \le t_1$, $0 \le \tau \le t$), then

$$u_1(t) = -\int_0^t G(t,\tau)\,[\mu_d\cdot g - \ddot{x}_g(\tau)]\,d\tau + a_1\cos\omega t + b_1\frac{\sin\omega t}{\omega} \tag{2}$$

where

$$G(t,\tau) = \frac{\det\begin{vmatrix}\cos\omega\tau & \cos\omega t\\ \sin\omega\tau & \sin\omega t\end{vmatrix}}{\omega} = \frac{\sin\omega t\cos\omega\tau - \cos\omega t\sin\omega\tau}{\omega} = \frac{1}{\omega}\sin\omega(t-\tau) \tag{3}$$

The first differentiation with respect to t of Eq.(2) yields

$$\dot{u}_1(t) = \int_0^t \cos\omega(t-\tau)\,[\mu_d g - \ddot{x}_g(\tau)]\,d\tau - \omega a_1 \sin\omega t + b_1 \cos\omega t \tag{4}$$

where $0 \le t \le t_1$; $0 \le \tau \le t$

If the body starts at rest, the initial conditions at $t_0 = 0$ are

$$u(0) = -x_g(0) \tag{5}$$

$$\dot{u}(0) = -\dot{x}_g(0) \tag{6}$$

Incorporating the initial conditions, the solution of Eq.(1) gives($0 \le t \le t_1$, $0 \le \tau \le t$)

$$u_1(t) = \int_0^t \omega^{-1}\sin\omega(t-\tau)\,[\mu_d g - \ddot{x}_g(\tau)]\,d\tau - x_g(0)\cos\omega t - \dot{x}_g(0)\frac{\sin\omega t}{\omega} \tag{7}$$

Where t_1 is defined by: $\dot{u}_1(t_1) = 0$ (8)

$$\dot{u}_1(t_1) = \int_0^{t_1} \cos\omega(t_1-\tau)\,[\mu_d g - \ddot{x}_g(\tau)]\,d\tau + \omega x_g(0)\sin\omega t_1 - \dot{x}_g(0)\cos\omega t_1 = 0$$

For the second time interval, the solution to Eq.(1) is denoted by $u_2(t)$

$$u_2(t) = \int_{\tau-t_1}^{t} \omega^{-1}\sin\omega(t-\tau)\,[-\mu_d g - \ddot{x}_g(\tau)]\,d\tau + a_2\cos\omega(t-t_1) + b_2\frac{\sin\omega(t-t_1)}{\omega} \tag{9}$$

where $t_1 \le t \le t_2$; $t_1 \le \tau \le t$

The first differentiation with respect to t of Eq.(9) becomes

$$\dot{u}_2(t) = \int_{\tau-t_1}^{t} \cos\omega(t-\tau)\,[-\mu_d g - \ddot{x}_g(\tau)]\,d\tau - a_2\omega\sin\omega(t-t_1) + b_2\cos\omega(t-t_1) \tag{10}$$

where $t_1 \le t \le t_2$, $t_1 \le \tau \le t$

The initial conditions in the second time interval are

$$u_1(t_1) = u_2(t_1) \tag{11}$$

$$\dot{u}_2(t_1) = 0 \tag{12}$$

Utilization of Eq.(11) and Eq.(12) leads to evaluation of a_2 and b_2

$$a_2 = \int_0^{t_1} \omega^{-1}\sin\omega(t_1-\tau)\,[\mu_d g - \ddot{x}_g(\tau)]\,d\tau - x_g(0)\cos\omega t_1 - \dot{x}_g(0)\frac{\sin\omega t_1}{\omega}$$

$b_2 = 0$

thus $a_2 = u_1\ (t_1)$

Substituting expressions of a_2 and b_2 into Eq.(9):

$$u_2(t) = \int_{\tau=t_1}^{t} \omega^{-1}\sin\omega(t-\tau)\,[-\mu_d g-\ddot{x}_g(\tau)]\,d\tau + u_1(t_1)\cos\omega(t-t_1) \tag{13}$$

where $t_1 \le t \le t_2$; $t_1 \le \tau \le t$

and t_2 is defined by $\dot{u}_2(t_2) = 0$ (14)

$$\dot{u}_2(t_2) = \int_{\tau=t_1}^{t_2} \cos\omega(t_2-\tau)\,[-\mu_d g-\ddot{x}_g(\tau)]\,d\tau - u_1(t_1)\,\omega\sin\omega(t_2-t_1) = 0$$

For subsequent time intervals $t_{n-1} \le t \le t_n$, $t_{n-1} \le \tau \le t$, $n=3,4,5,\ldots$, the solution to the Eq.(1) is represented by $u_n(t)$, then:

$$u_n(t) = \int_{\tau=t_{n-1}}^{t} \omega^{-1}\sin\omega(t-\tau)\,[(-1)^{n+1}\mu_d g-\ddot{x}_g(\tau)]\,d\tau + a_n\cos\omega(t-t_{n-1}) + b_n\frac{\sin\omega(t-t_{n-1})}{\omega} \tag{15}$$

The first differentiation about t of Eq.(15) yields

$$\dot{u}_n(t) = \int_{\tau=t_{n-1}}^{t} \cos\omega(t-\tau)\,[(-1)^{n+1}\mu_d g-\ddot{x}_g(\tau)]\,d\tau - a_n\omega\sin\omega(t-t_{n-1}) + b_n\cos\omega(t-t_{n-1}) \tag{16}$$

Similarly, the initial conditions in these time intervals:

$$u_{n-1}(t_{n-1}) = u_n(t_{n-1}) \tag{17}$$

$$\dot{u}_n(t_{n-1}) = 0 \tag{18}$$

Using initial conditions leads to expressions of a_n and b_n:

$a_n = u_{n-1}(t_{n-1})$, $\qquad b_n = 0$

and t_n is defined by $\dot{u}_n(t_n) = 0$ (19)

$$\dot{u}_n(t_n) = \int_{\tau=t_{n-1}}^{t_n} \cos\omega(t_n-\tau)\,[(-1)^{n+1}\mu_d g - \ddot{x}_g(\tau)]\,d\tau$$
$$- u_{n-1}(t_{n-1})\,\omega\sin\omega(t_n-t_{n-1}) = 0$$

Final expression for $t_{n-1} \le t \le t_n$, $t_{n-1} \le \tau \le t$, $n=3,4,5,\ldots$:

$$u_n(t) = \int_{\tau=t_{n-1}}^{t} \omega^{-1}\sin\omega(t-\tau)\,[(-1)^{n+1}\mu_d g - \ddot{x}_g(\tau)]\,d\tau \tag{20}$$
$$+ u_{n-1}(t_{n-1})\cos\omega(t-t_{n-1})$$

FIGURES

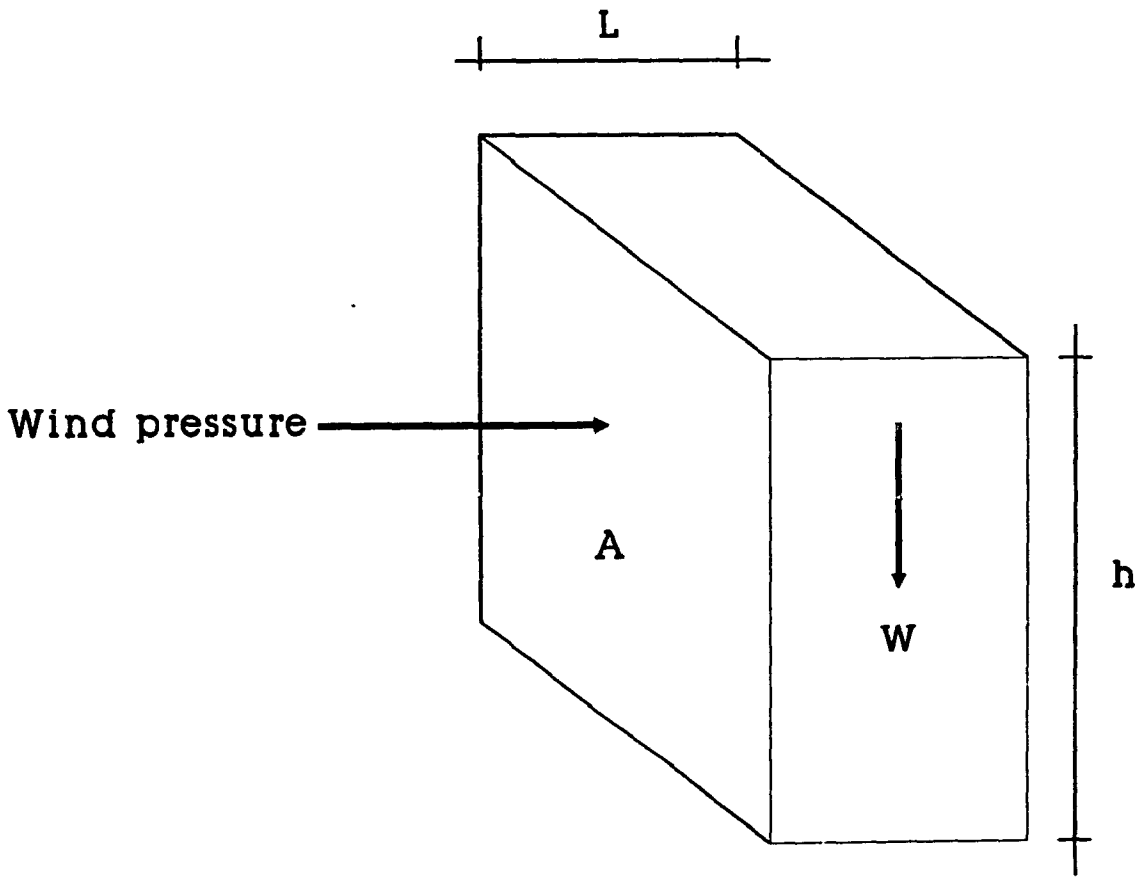

Fig.1 Example for a Typical Office Building

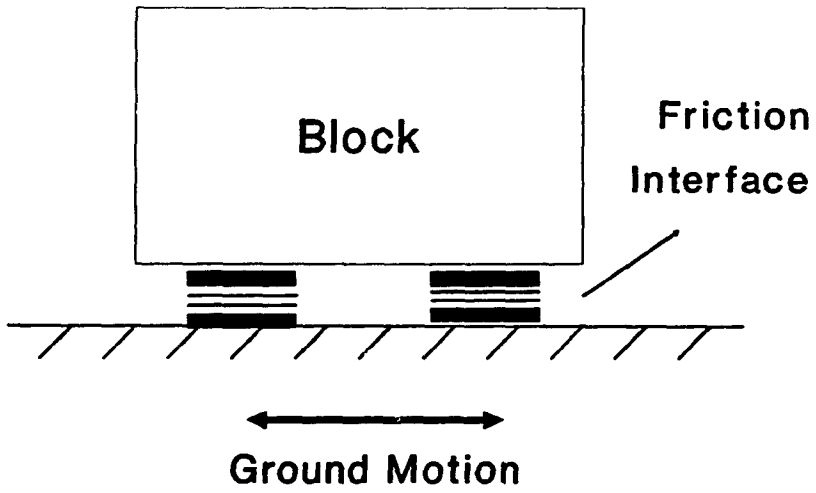

Fig.2 Sliding Rigid Block on Pure-Friction System

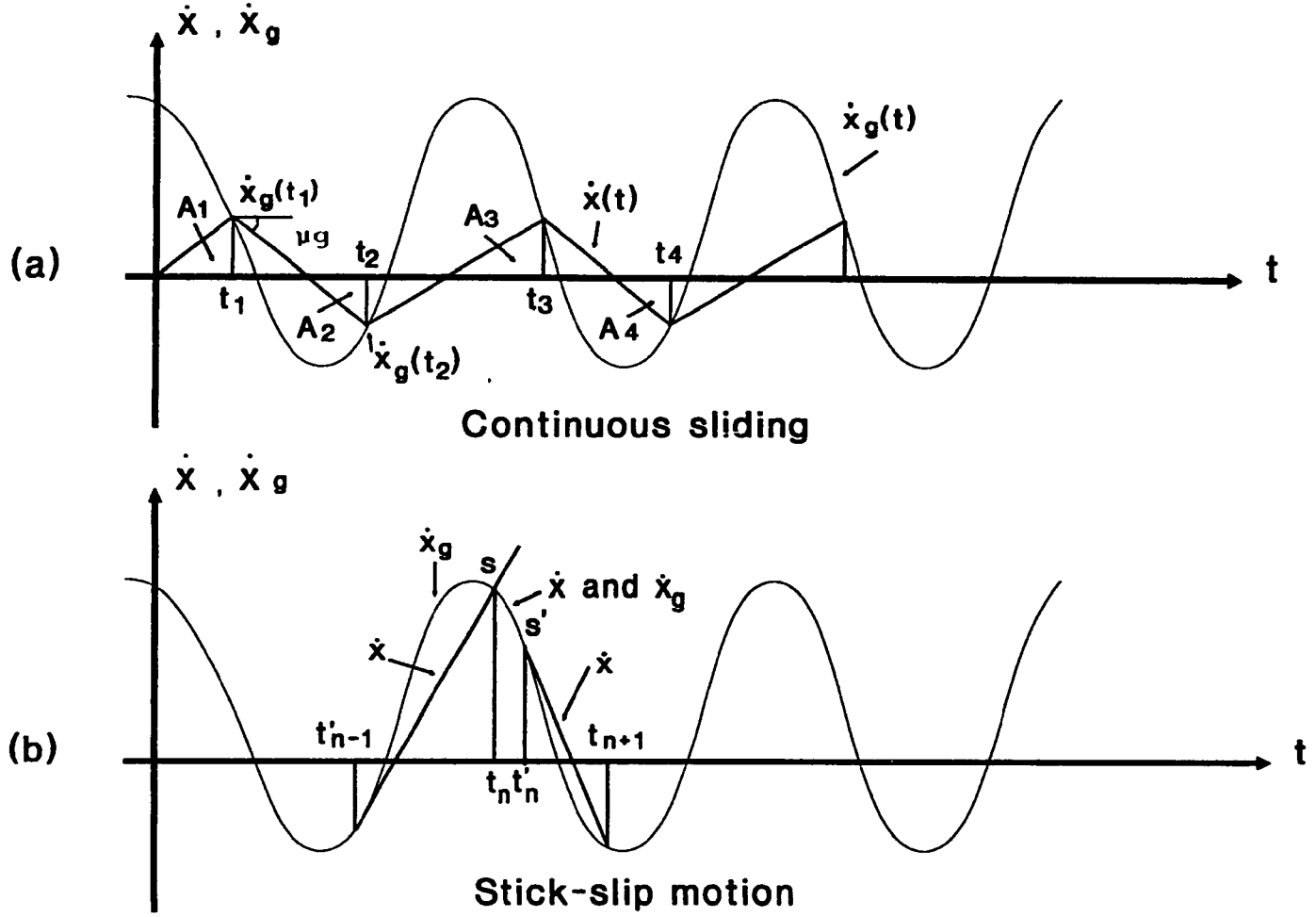

Fig.3 Ground Motion and Response

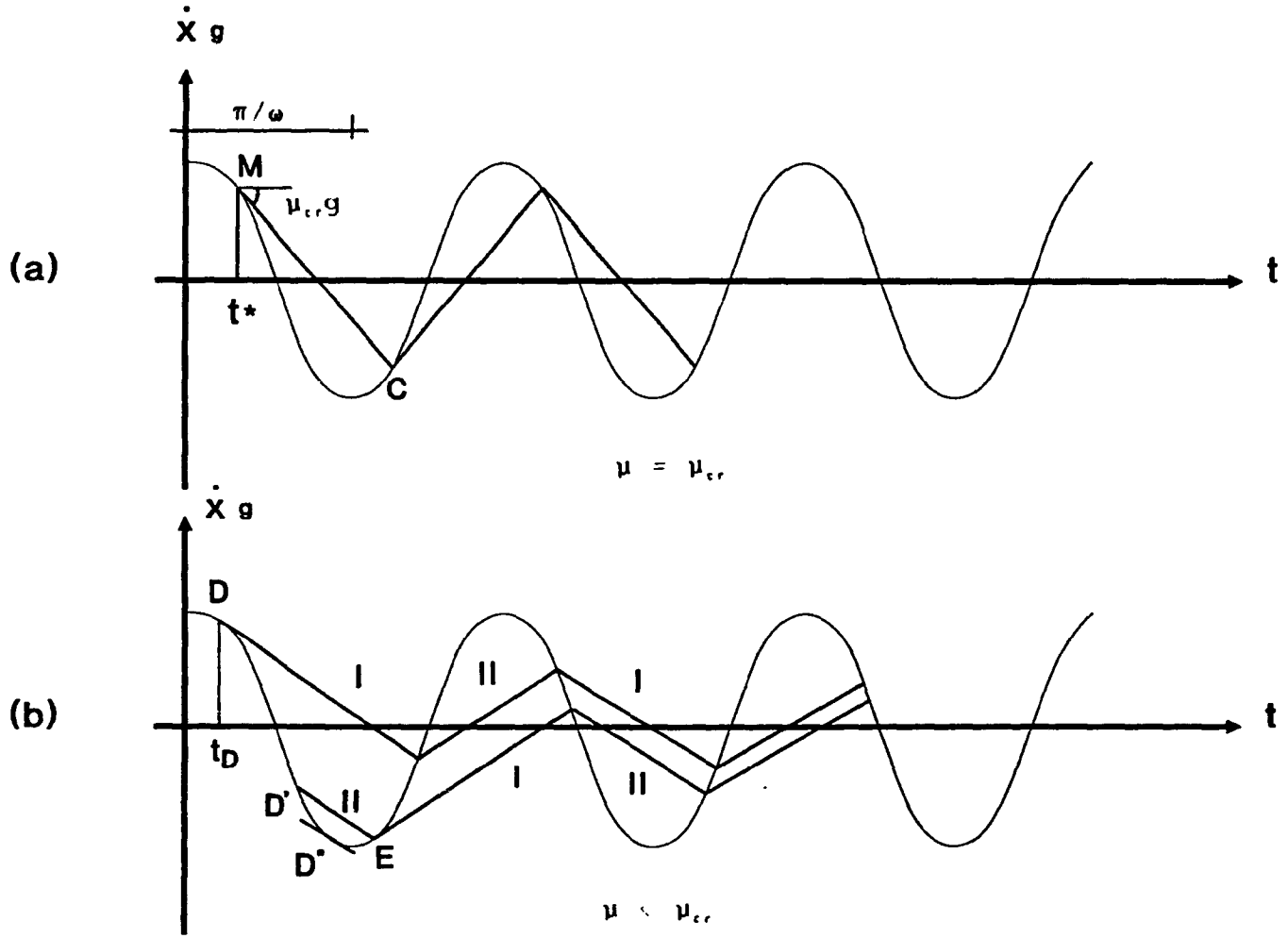

Fig.4 Critical Friction Coefficient and Response When $\mu < \mu_{cr}$

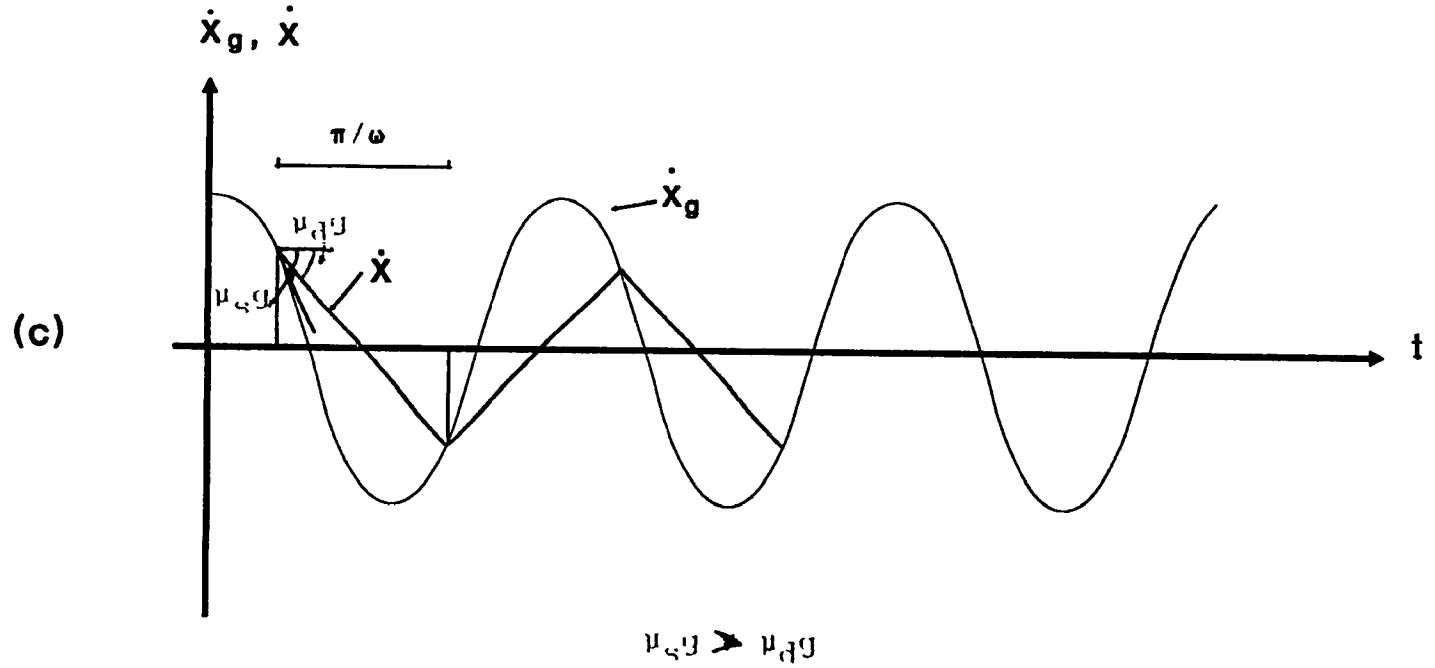

Fig.4 Critical Friction Coefficient and Response When $\mu < \mu_{cr}$

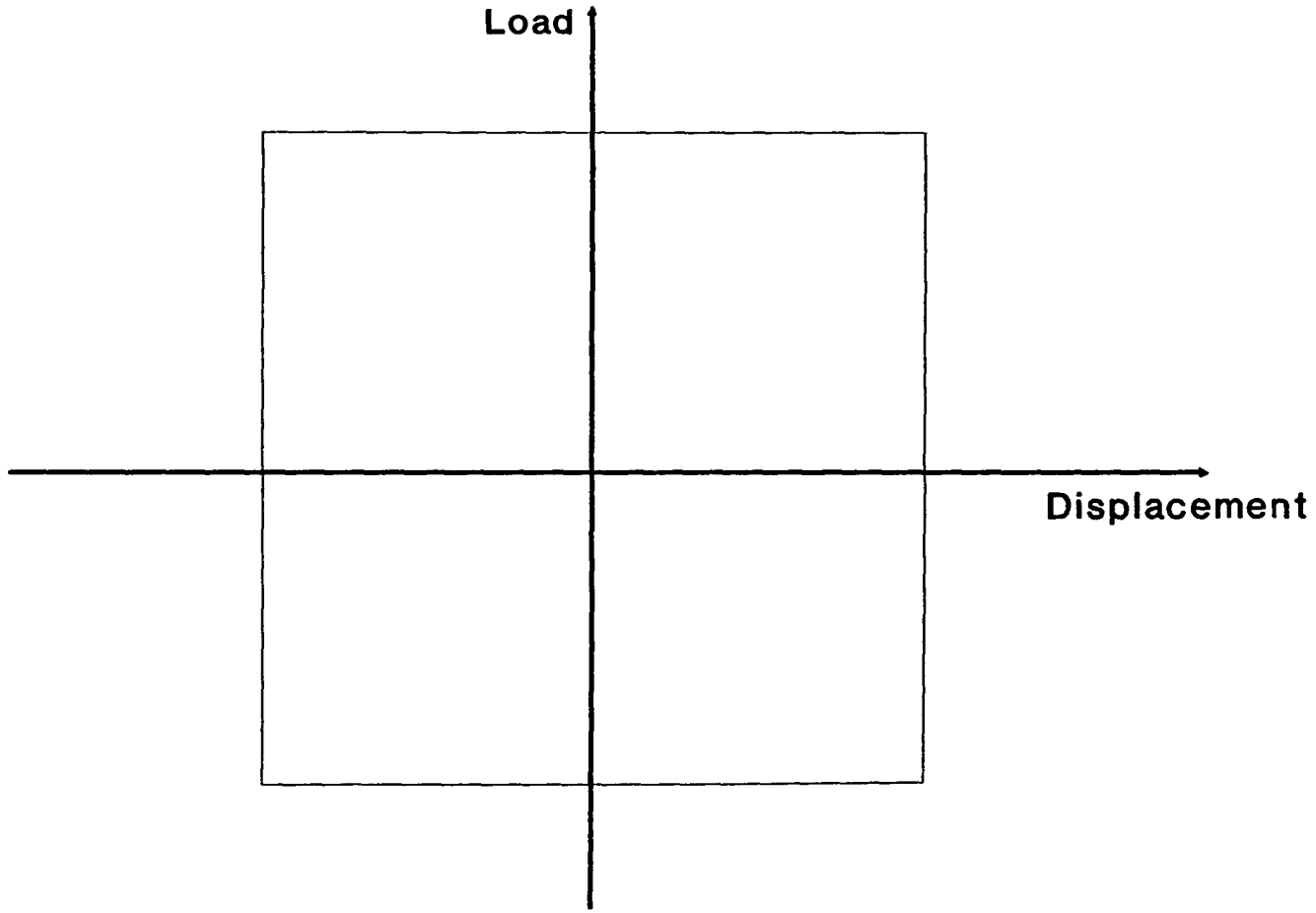

Fig. 5 Load-Displacement hysteresis loop (pure-friction system)

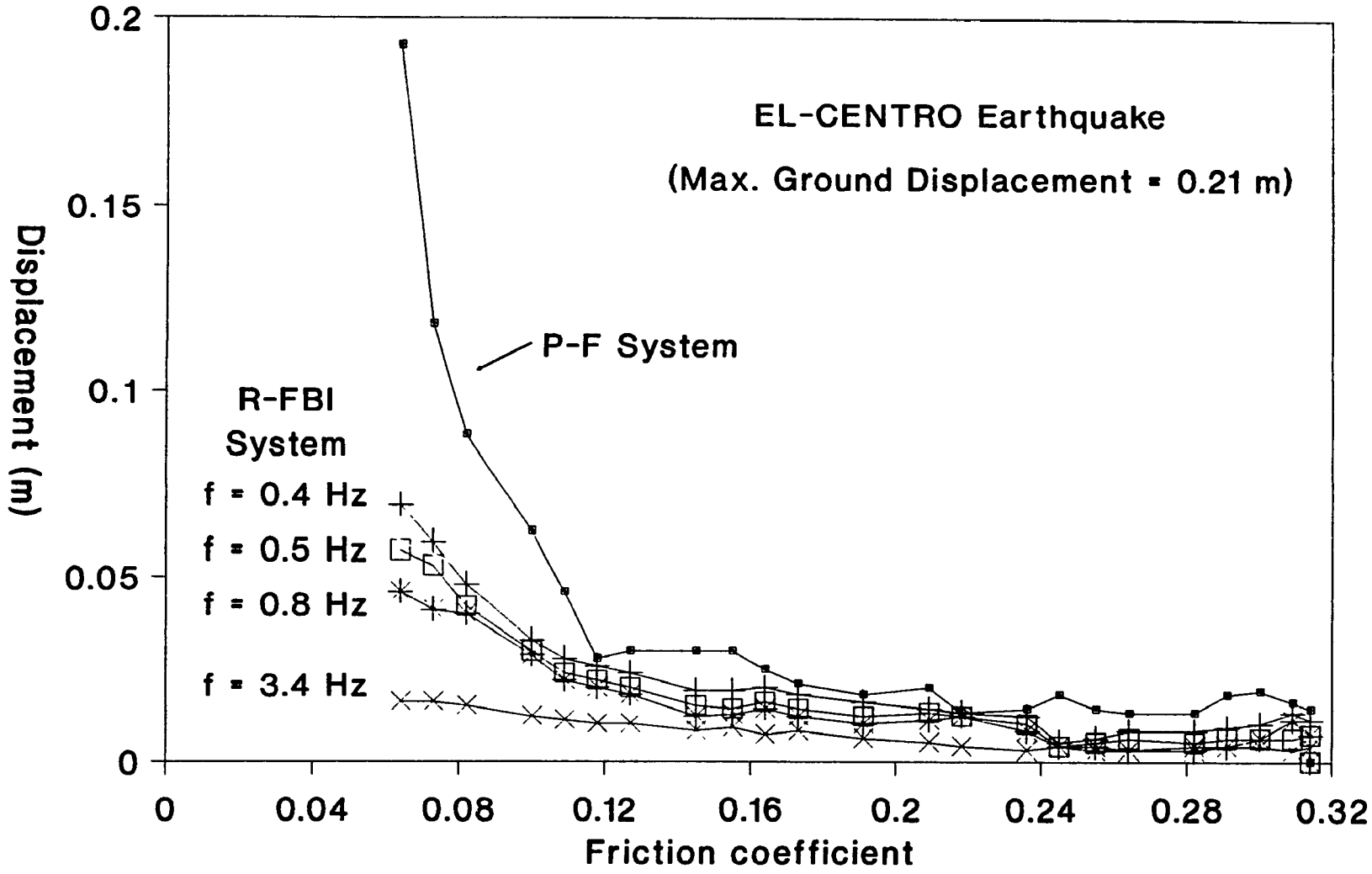

Fig.6 Horizontal Displacement Relative to the Ground for P-F and R-FBI Systems

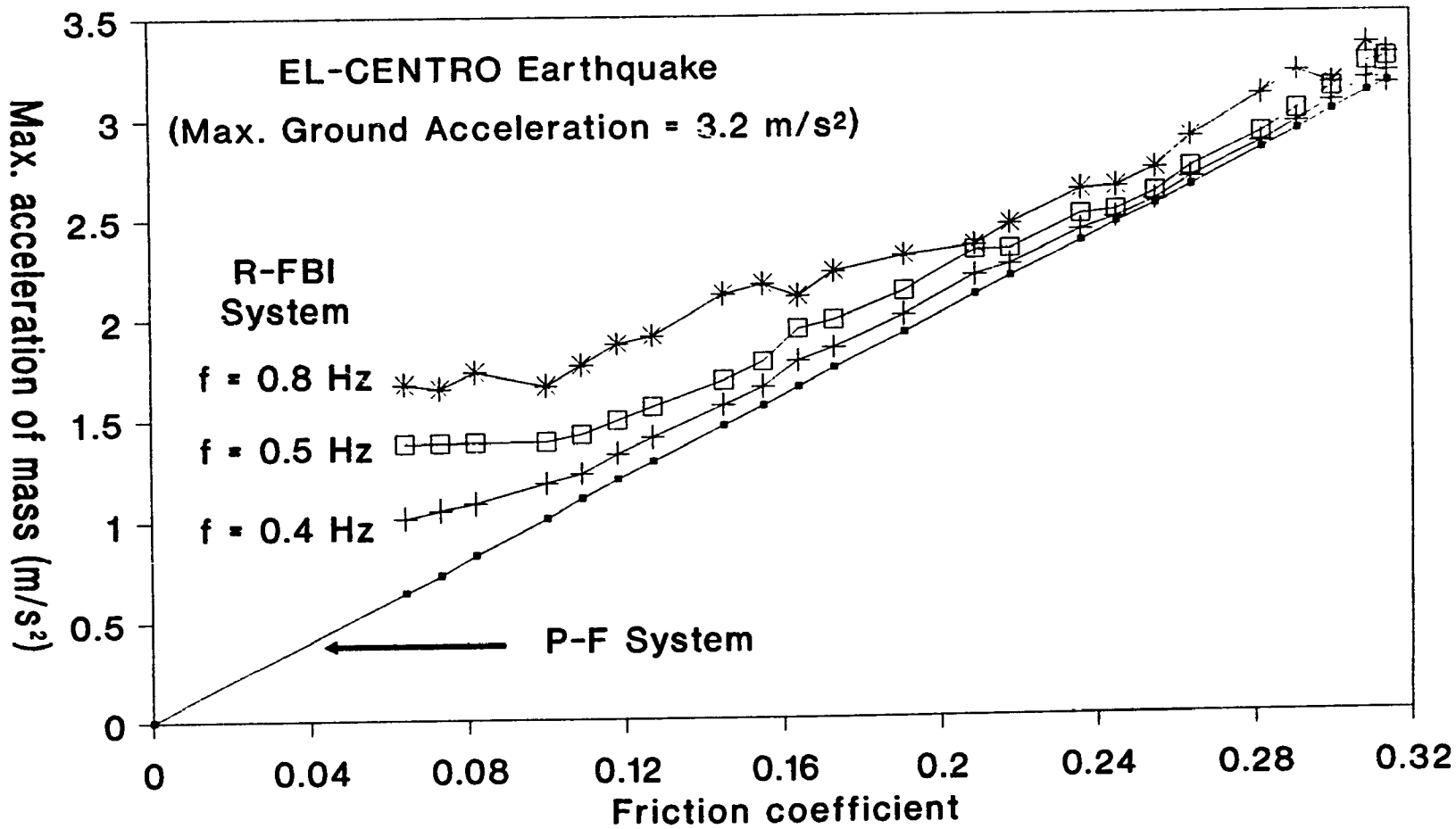

Fig.7 Horizontal Acceleration of the Block for P-F and R-FBI Systems

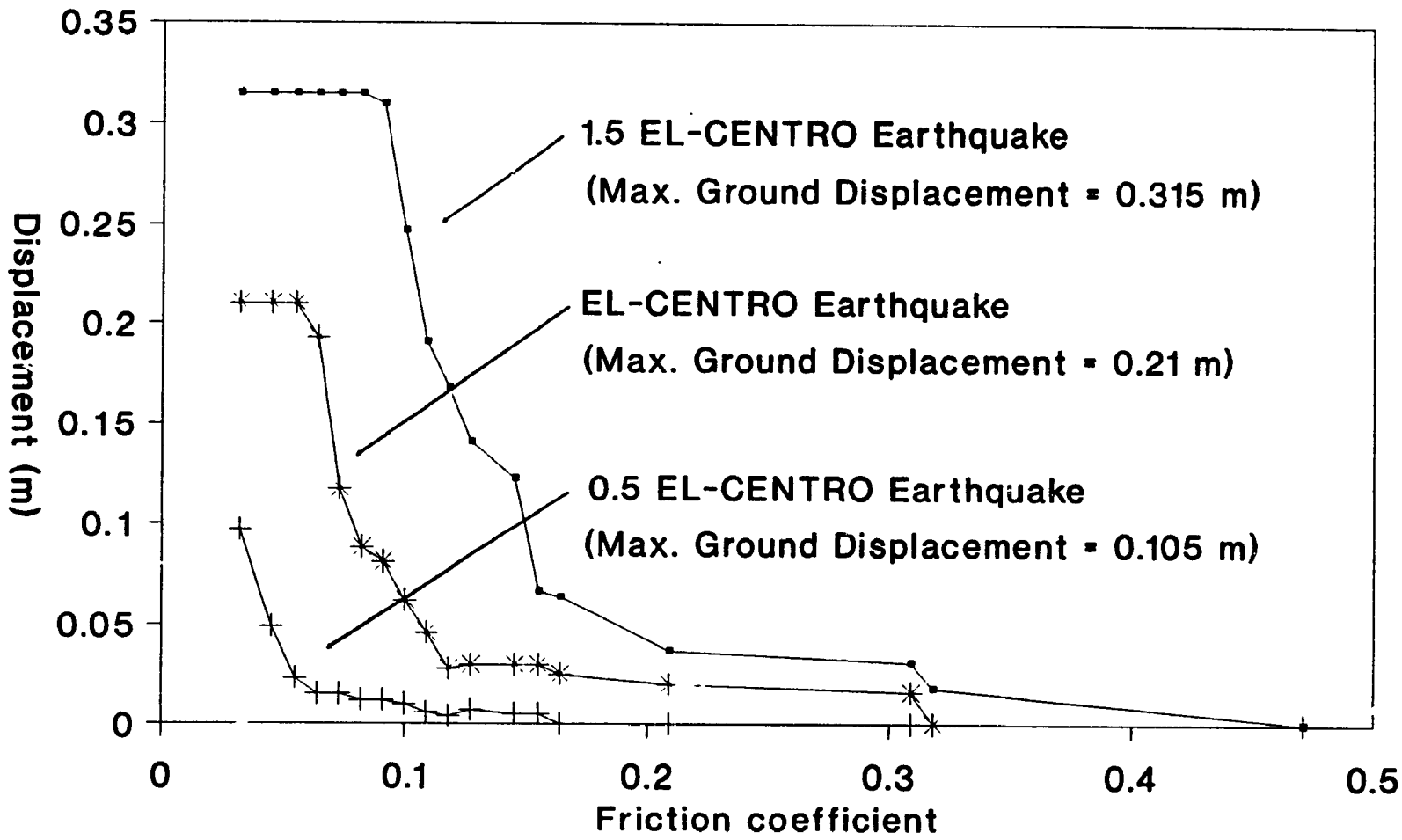

Fig.8 Displacement Responses for Different Intensities (Pure-friction System)

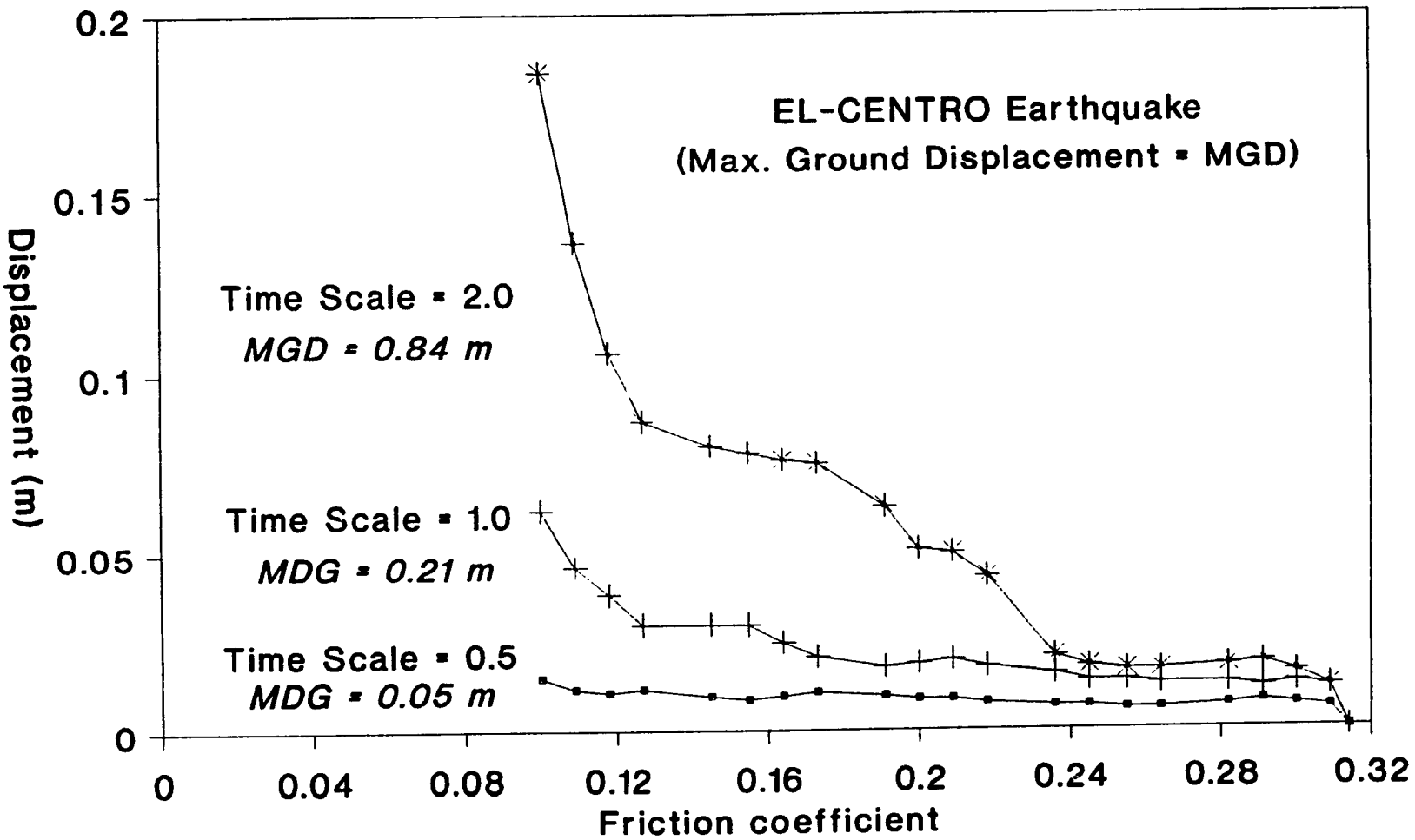

Fig.9 Displacement Responses for Different Frequency Contents (Pure-friction System)

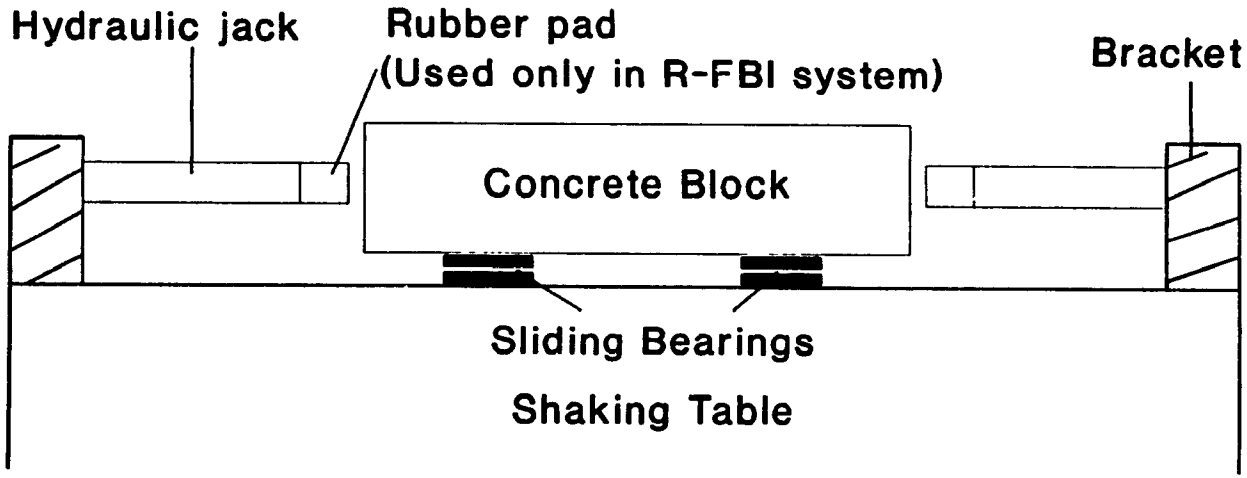

Fig.10 Testing Apparatus

Fig.11(a) Support Arrangement

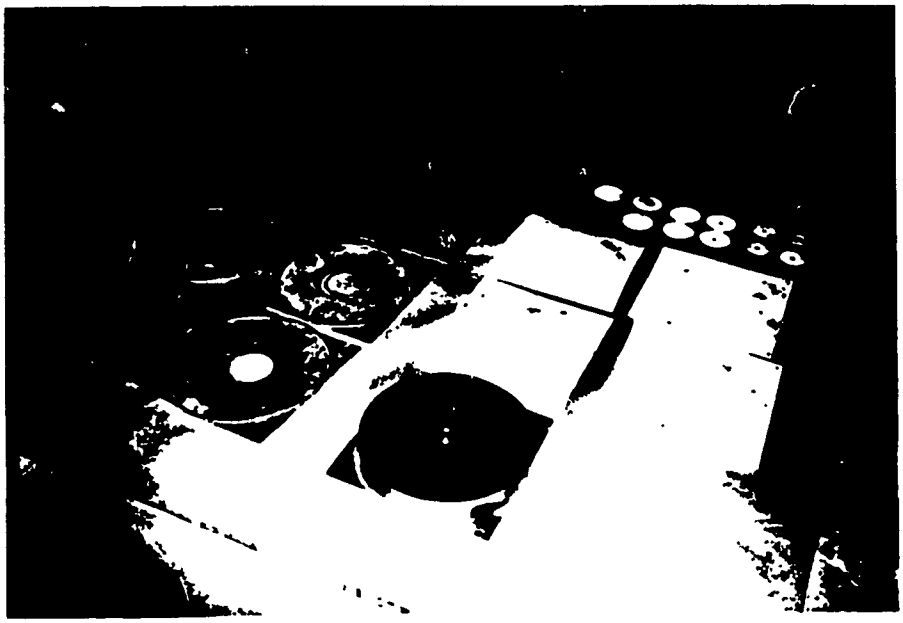

Fig.11(b) Materials and Specimens

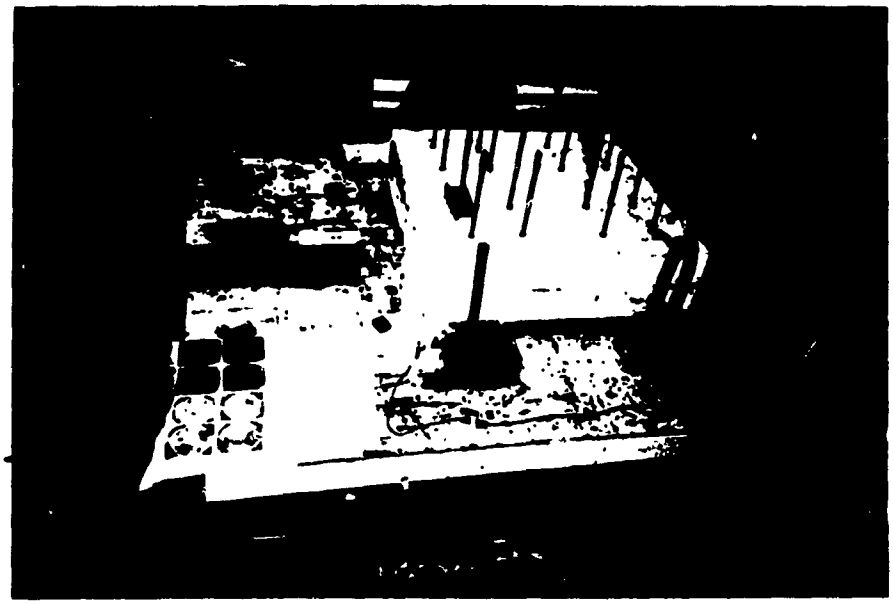

Fig.12(a) Testing Apparatus

Fig.12(b) The Limit Device

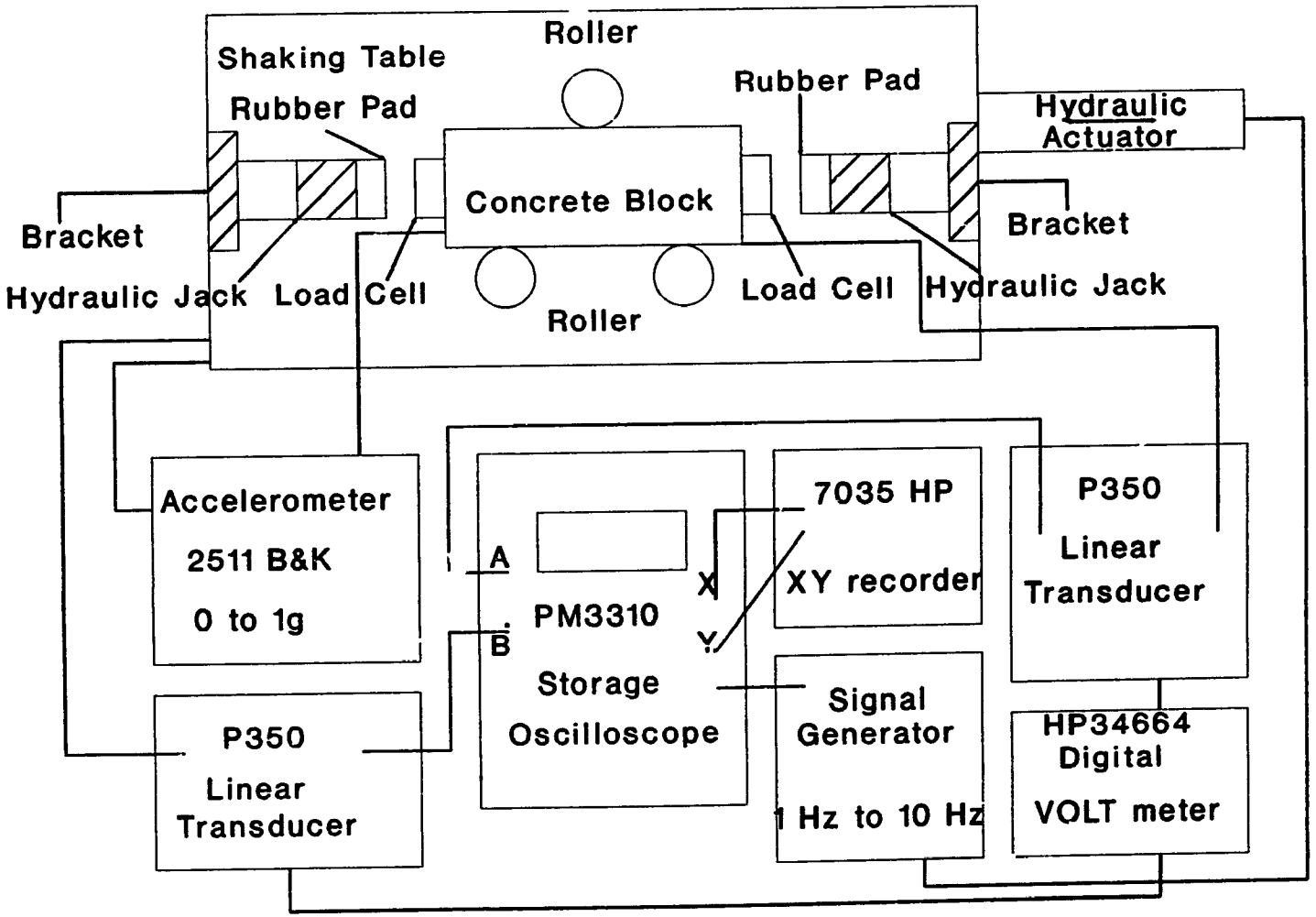

Fig.12(c) Testing Apparatus

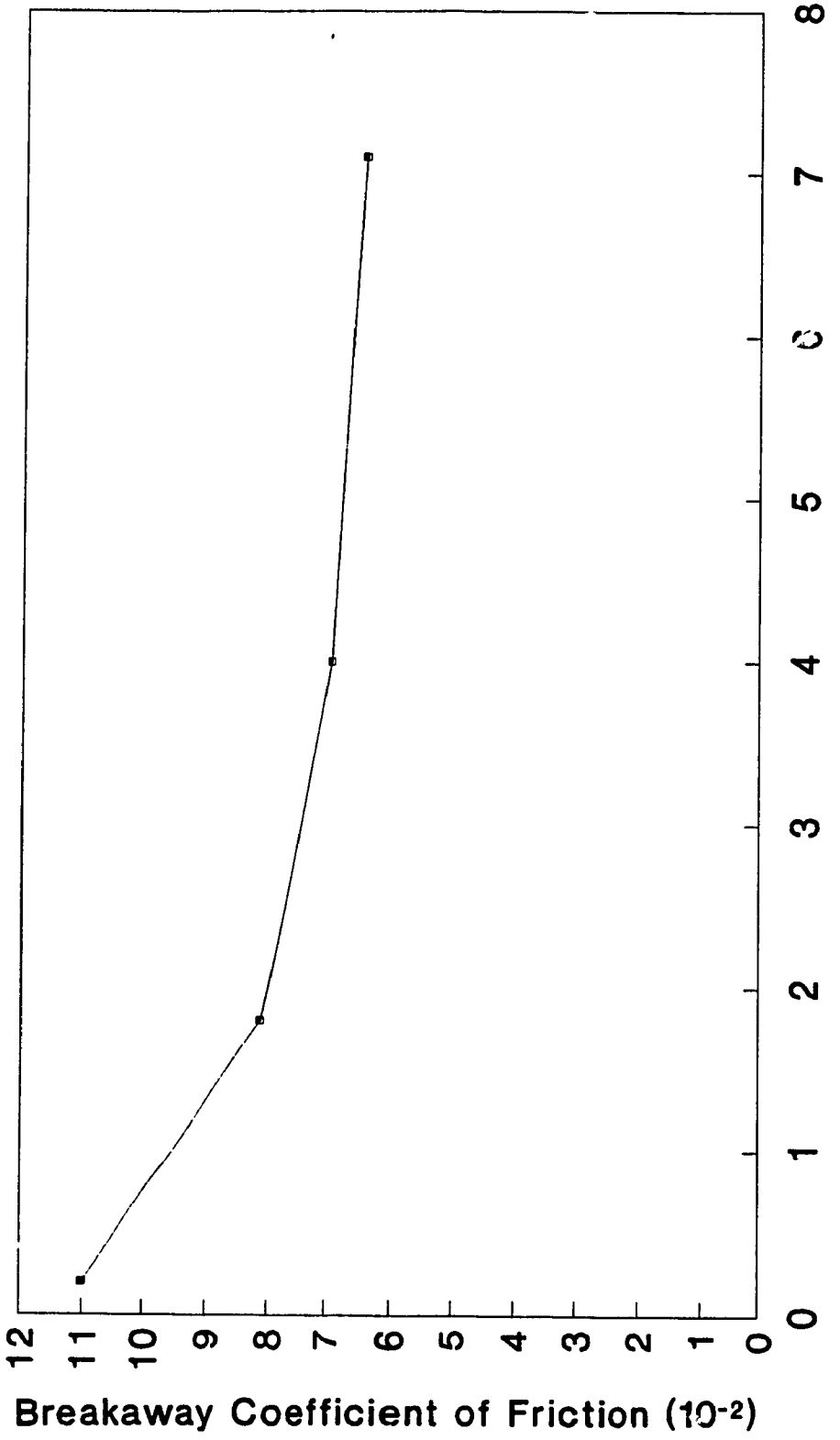

Fig.13 Effect of Pressure on Breakaway Coefficient of Friction

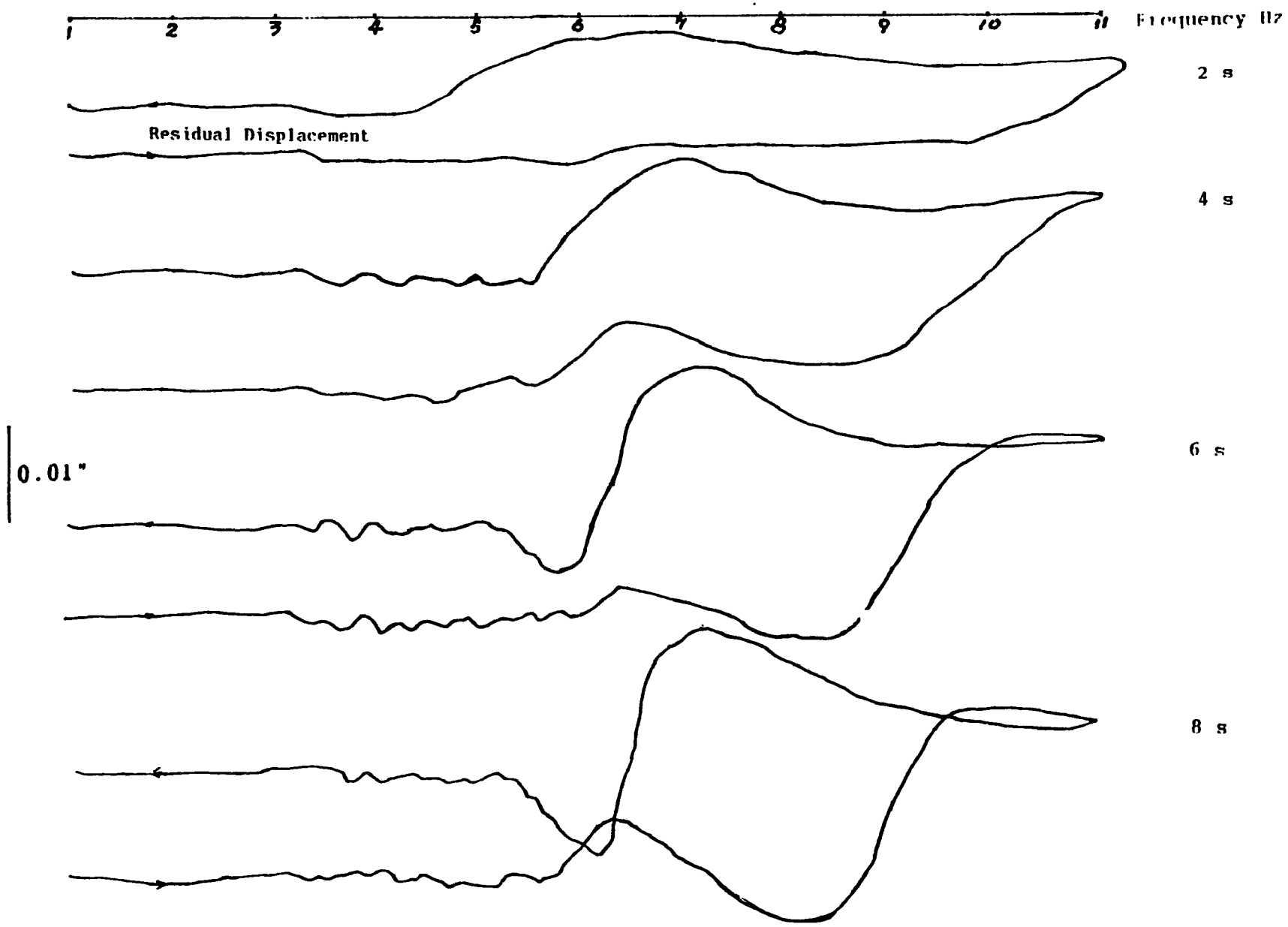

Fig.14 Effect of Sweep Time on Displacement
Polished Stainless Steel and Polished Steel

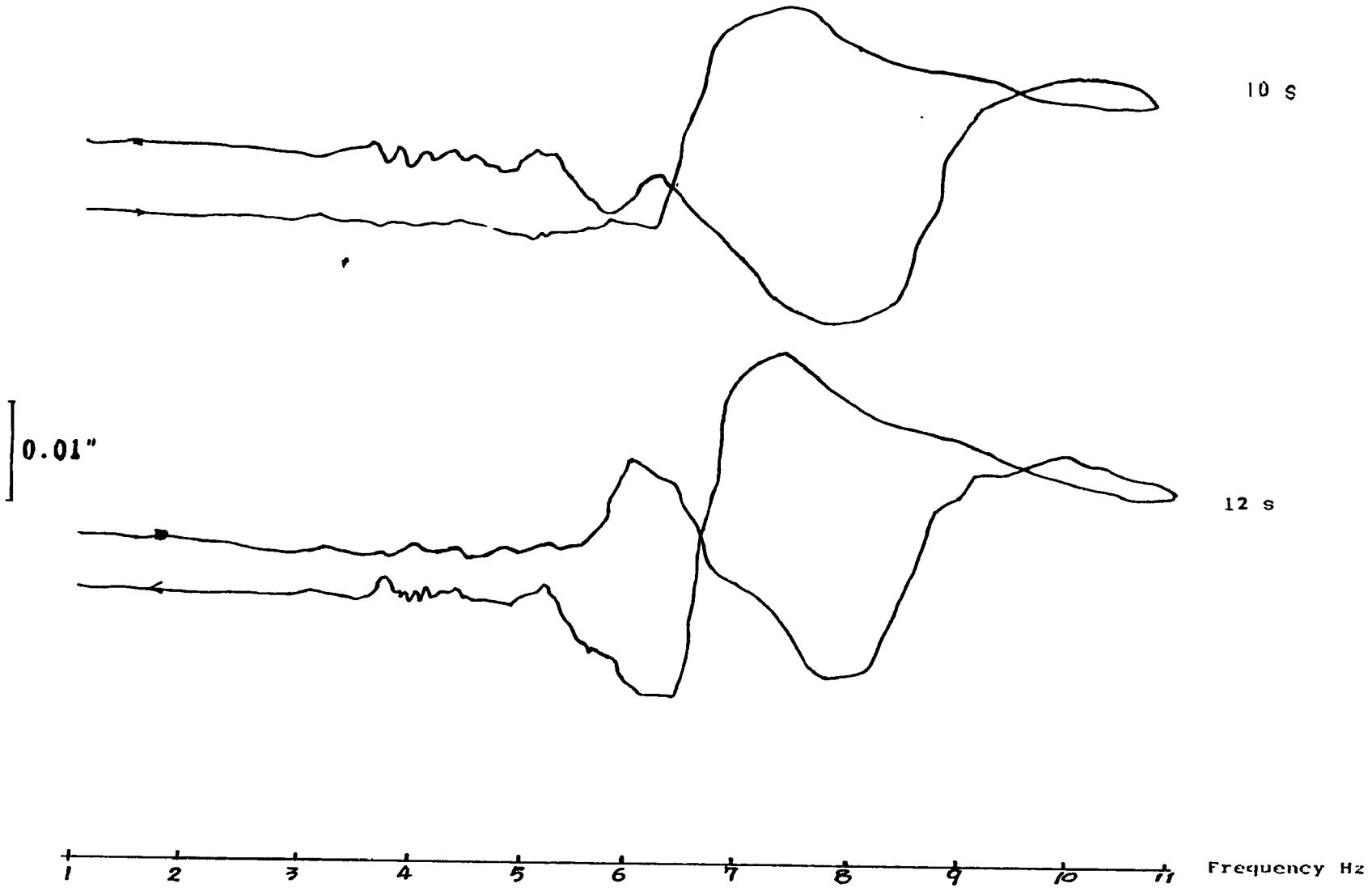

Fig.14 Effect of Sweep Time on Displacement Polished Stainless Steel and Polished Steel

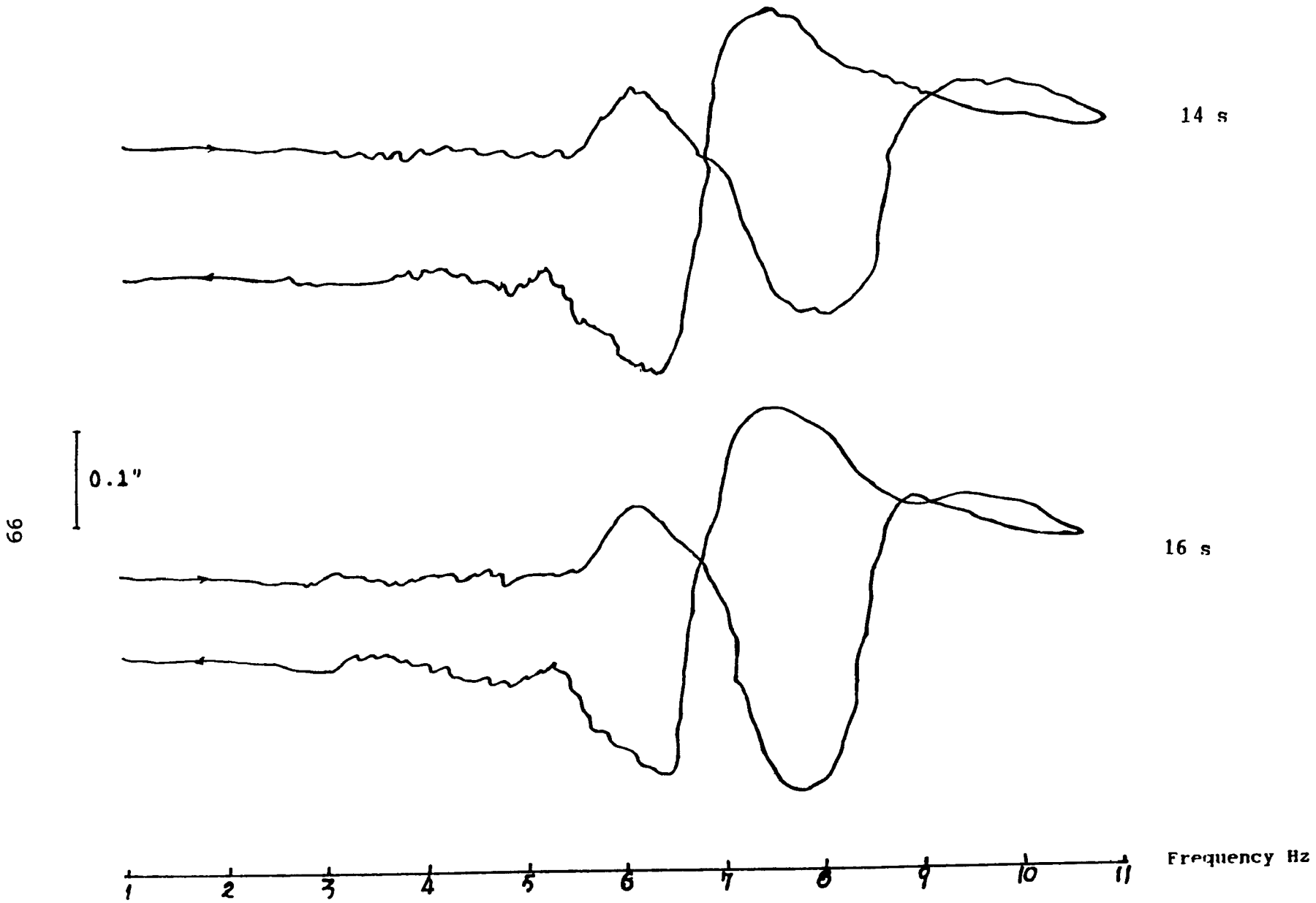

Fig.14 Effect of Sweep Time on Displacement
Polished Stainless Steel and Polished Steel

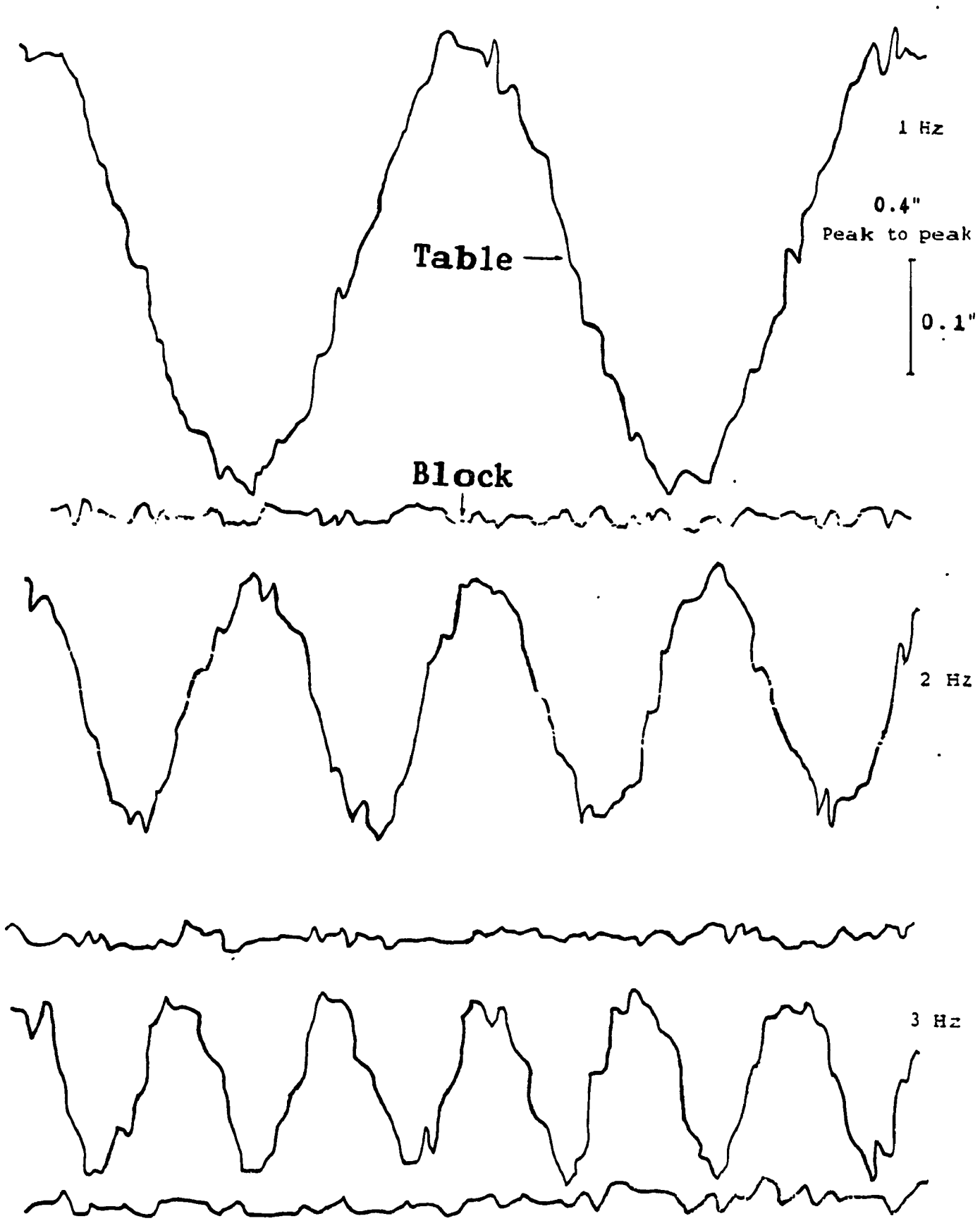

Fig.15 Displacement Time History
Polished Stainless Steel and Polished Steel

Continued

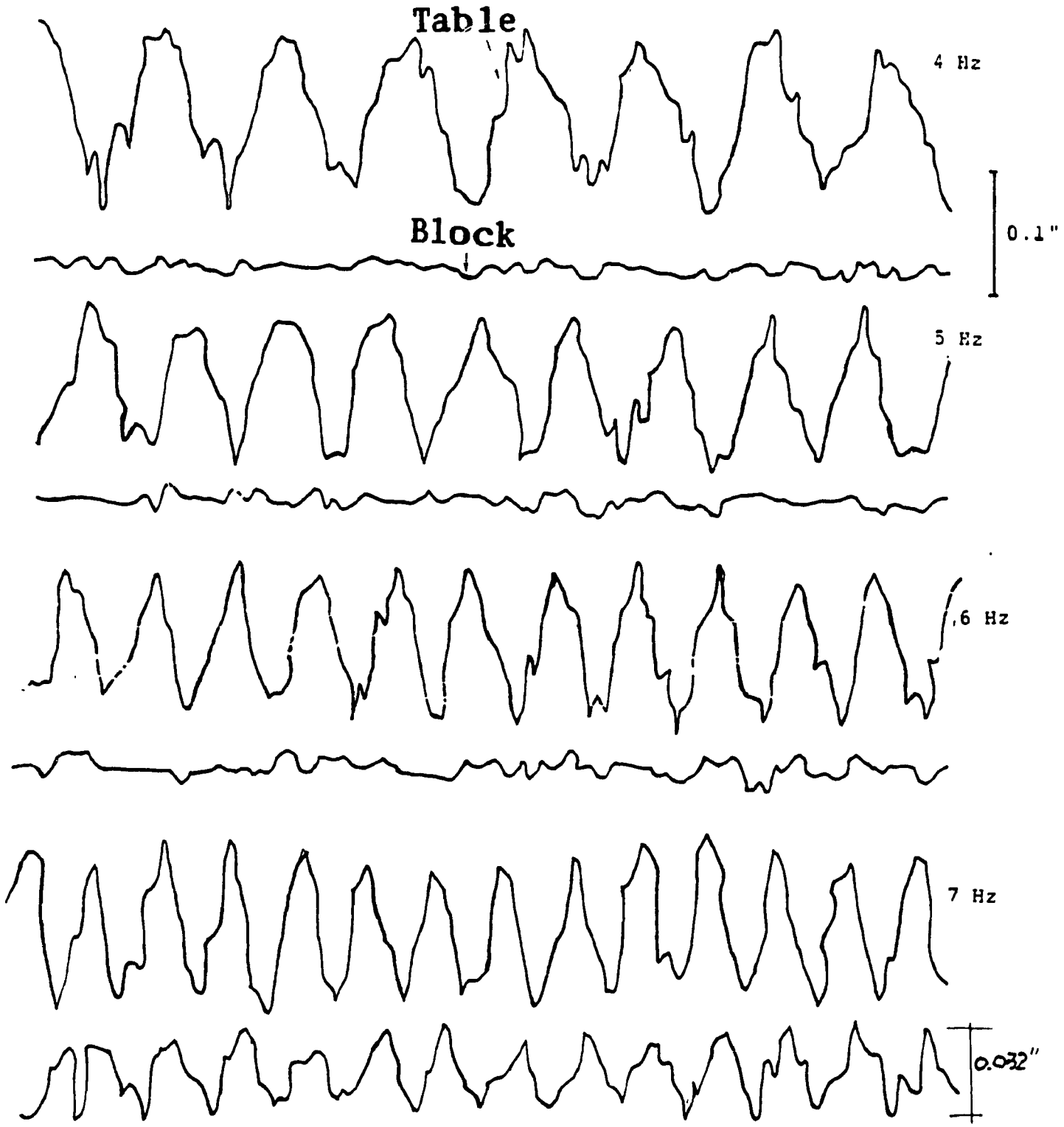

Fig.15 Displacement Time History Polished Stainless Steel and Polished Steel

Continued

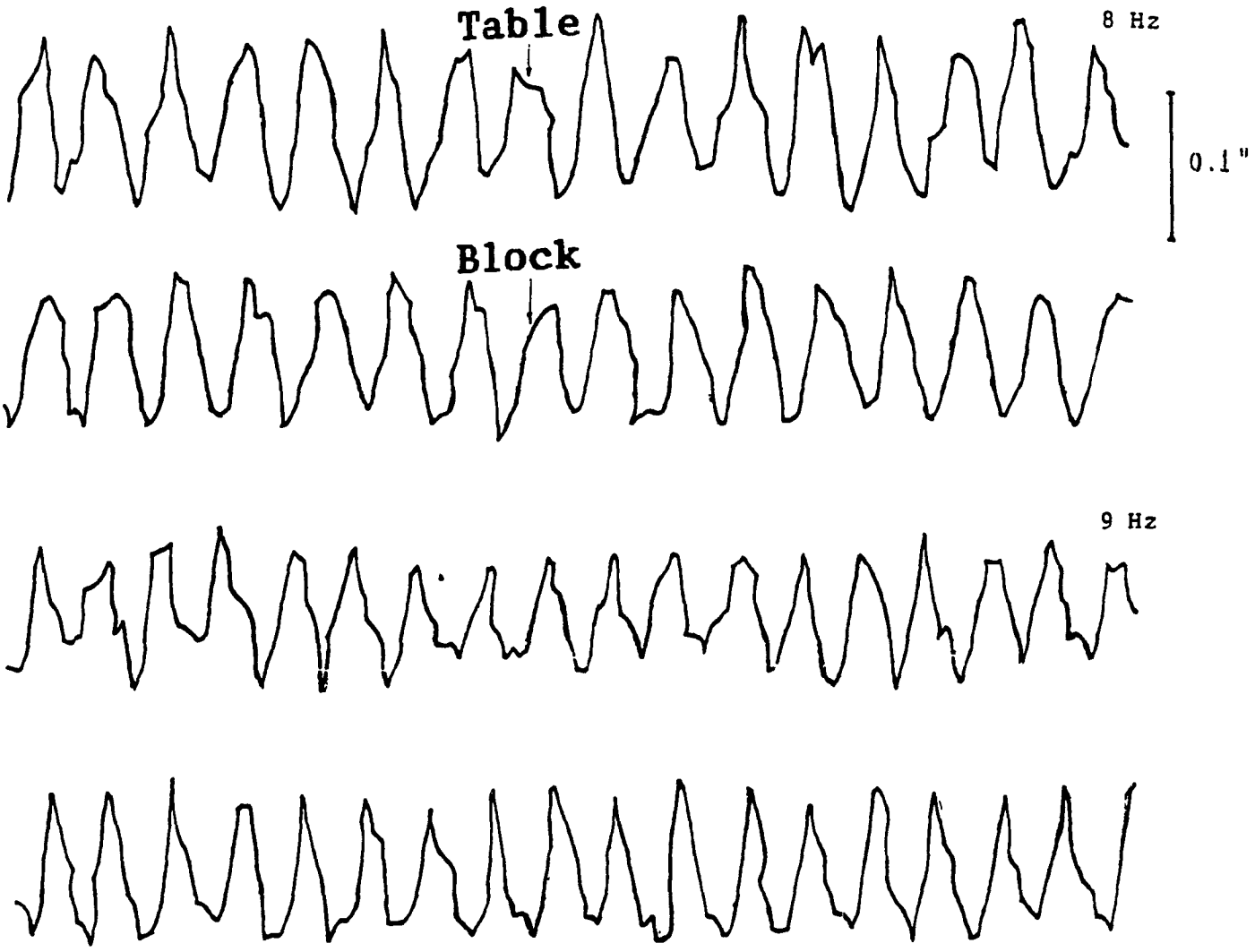

Fig.15 Displacement Time History
Polished Stainless Steel and Polished Steel

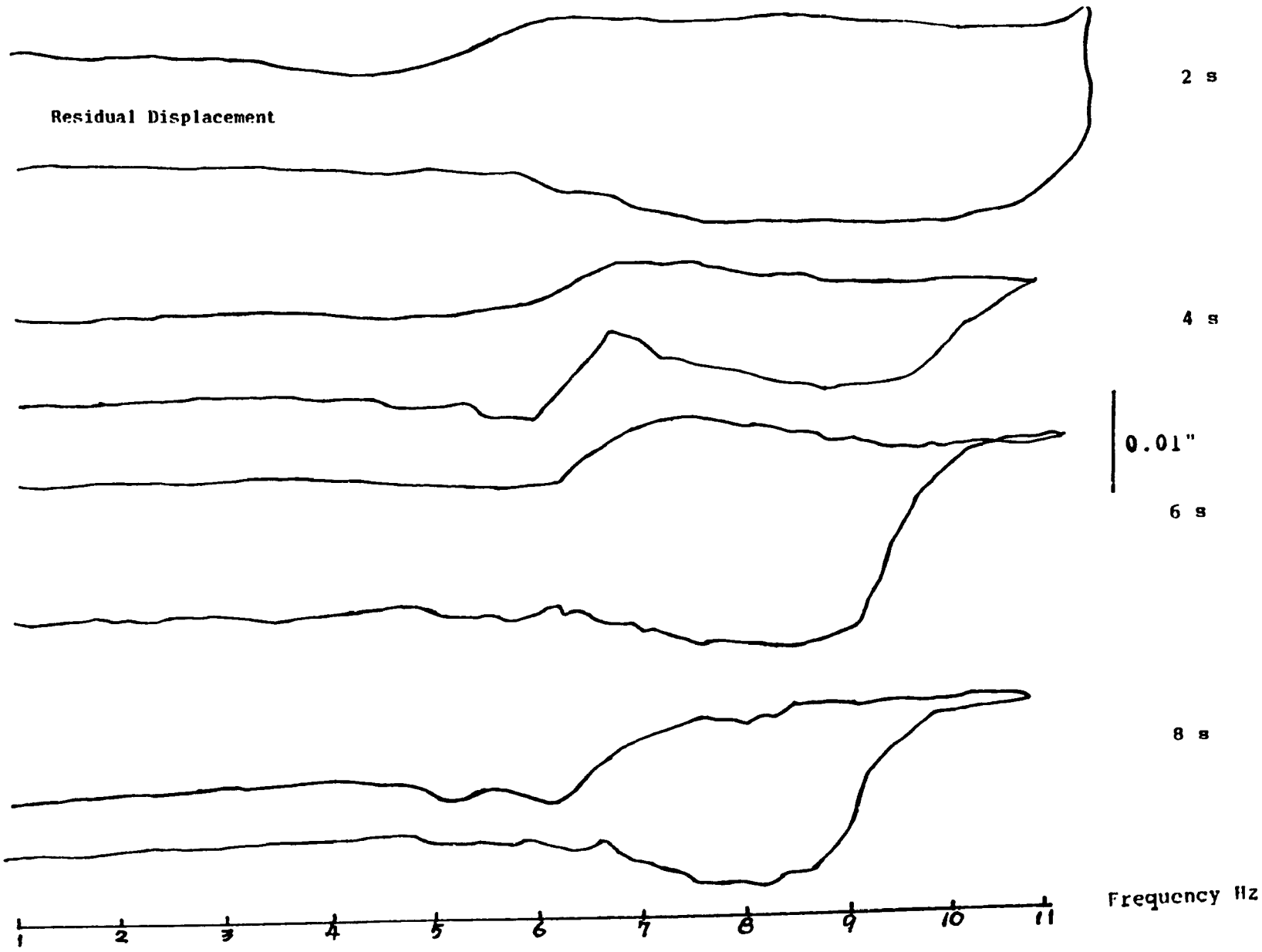

Fig.16 Effect of Sweep Time on Displacement Brass and Polished Steel

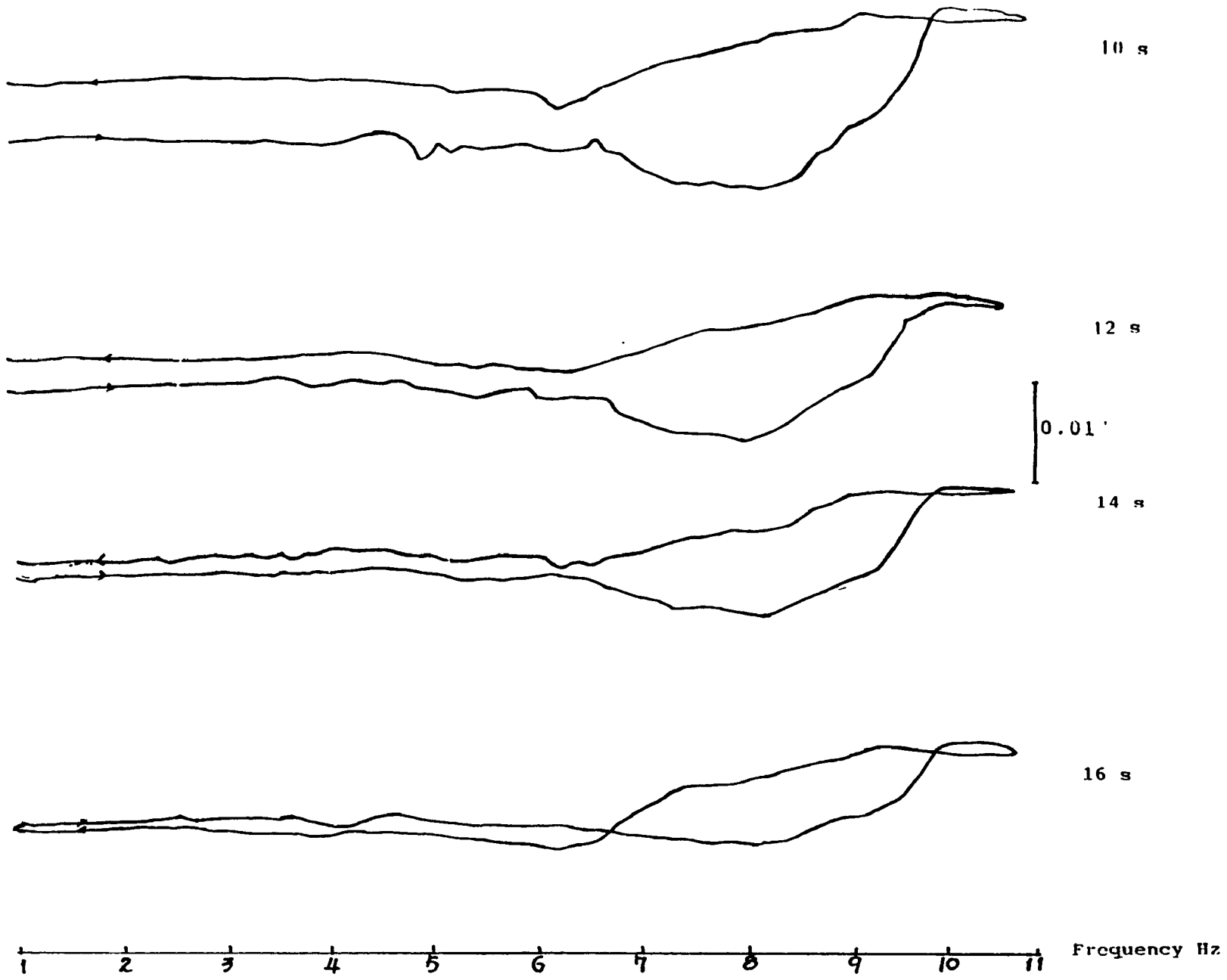

Fig.16 Effect of Sweep Time on Displacement Brass and Polished Steel

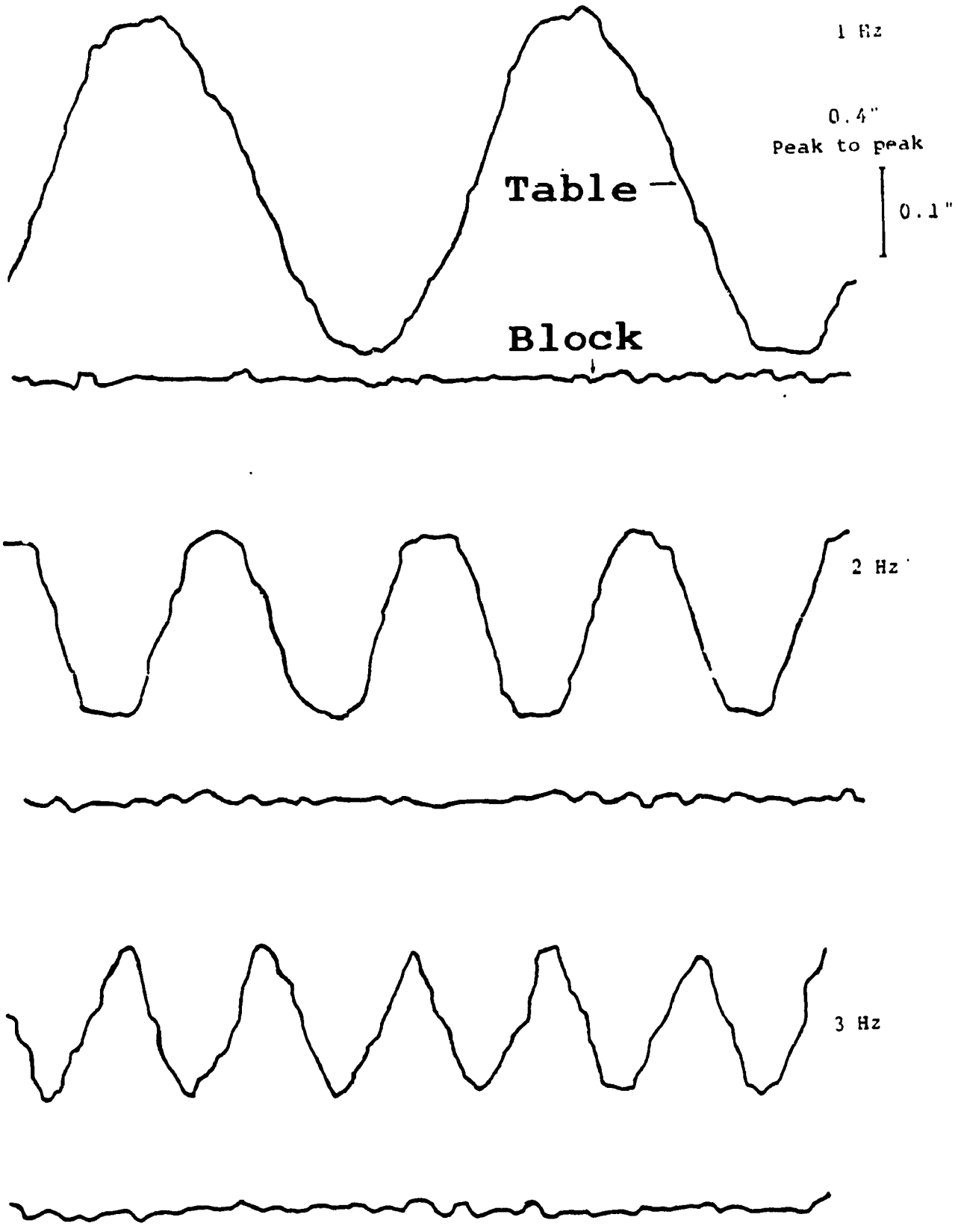

Fig.17 Displacement Time History
Brass and Polished Steel

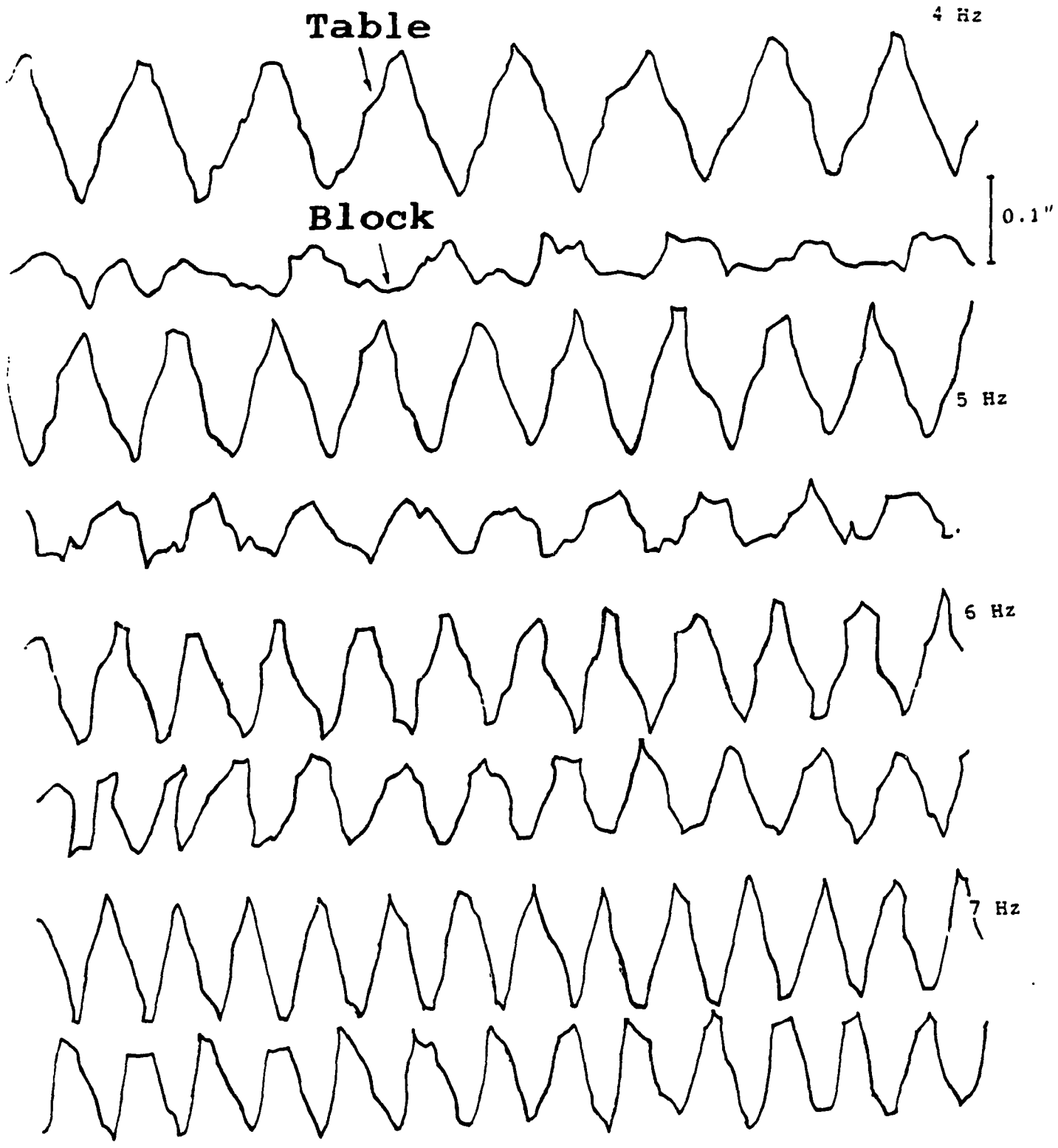

Fig.17 Displacement Time History Brass and Polished Steel

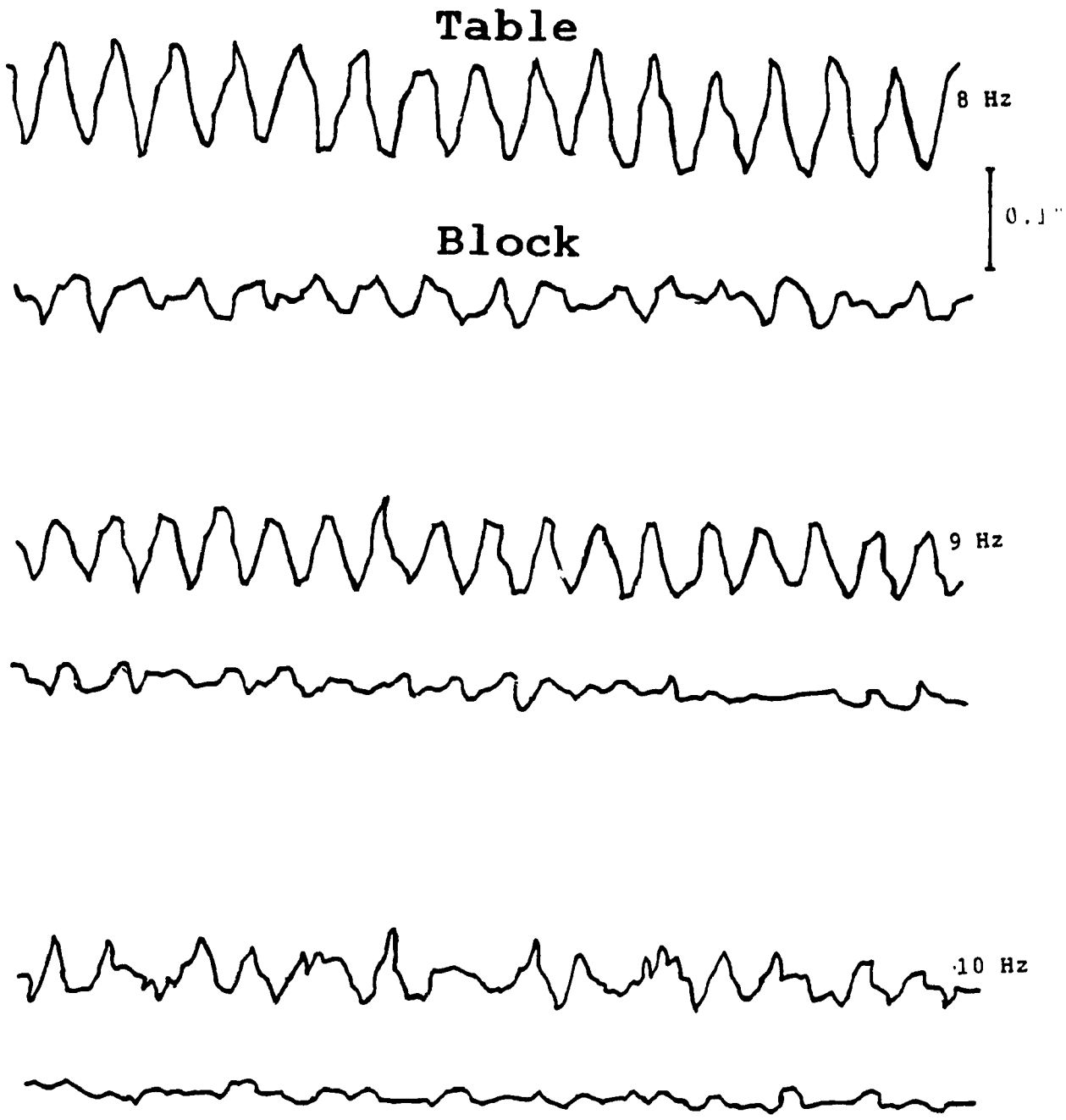

**Fig.17 Displacement Time History
Brass and Polished Steel**

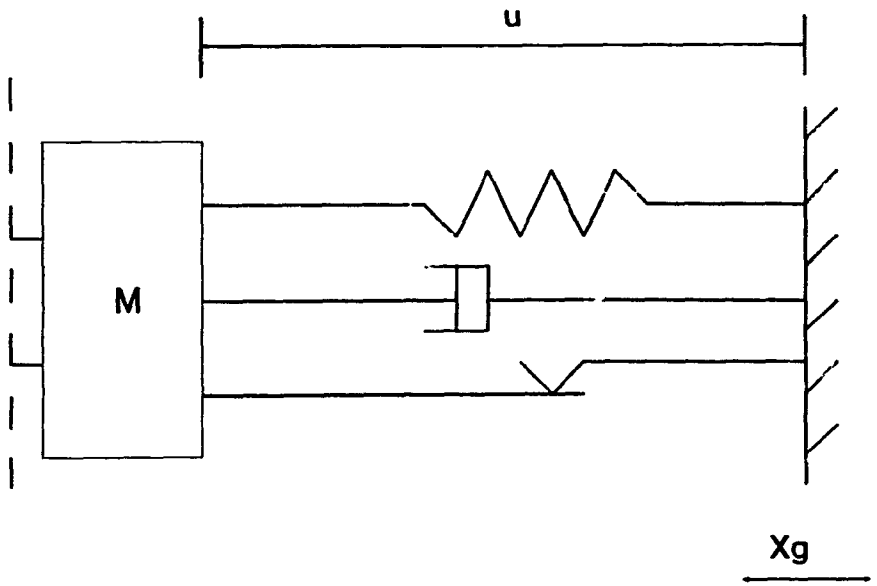

Note: Xg = ground motion u = relative motion

Fig.18 Schematic Diagram of R-FBI System

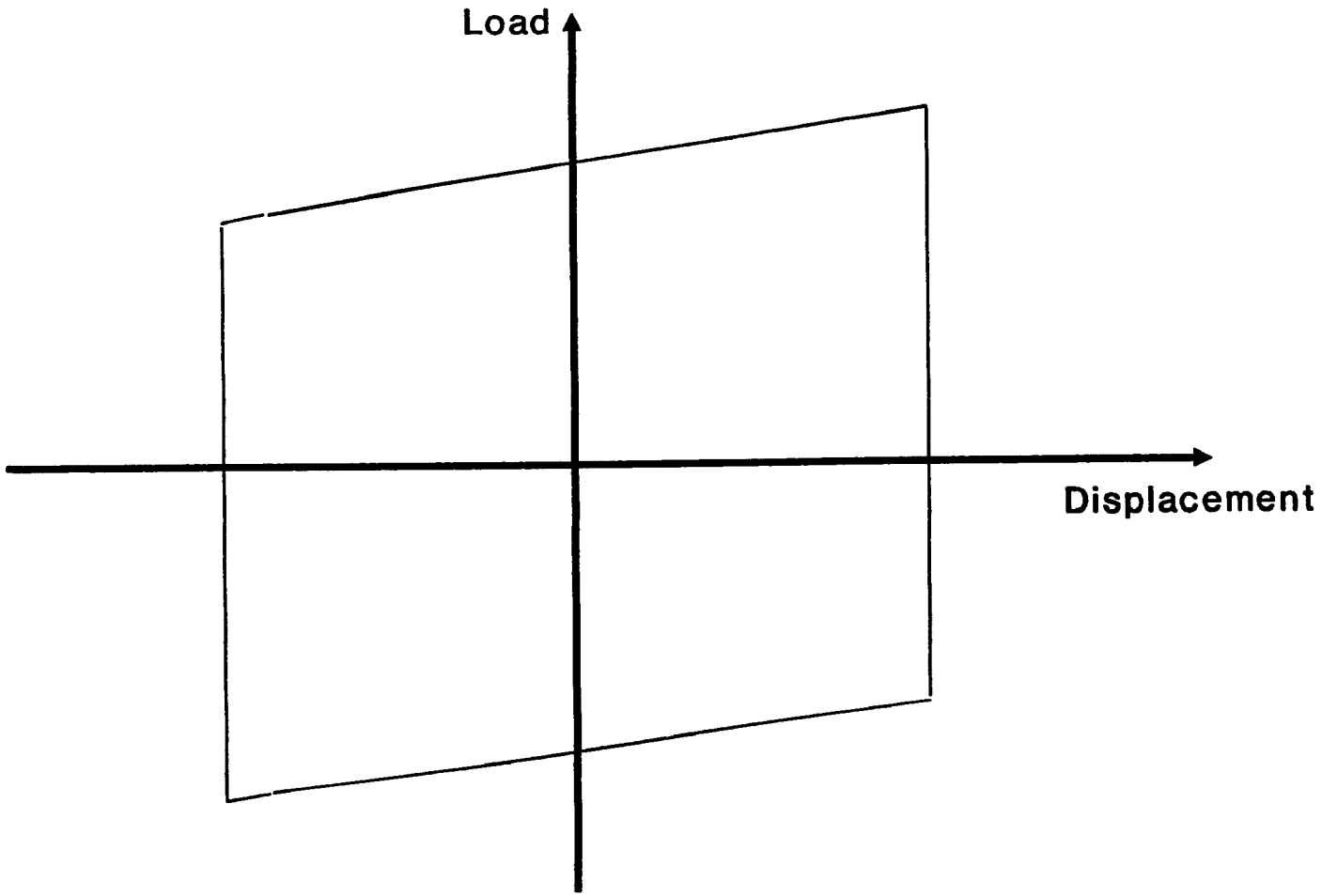

Fig.19 Load-Displacement Hysteresis Loop (R-FBI system)

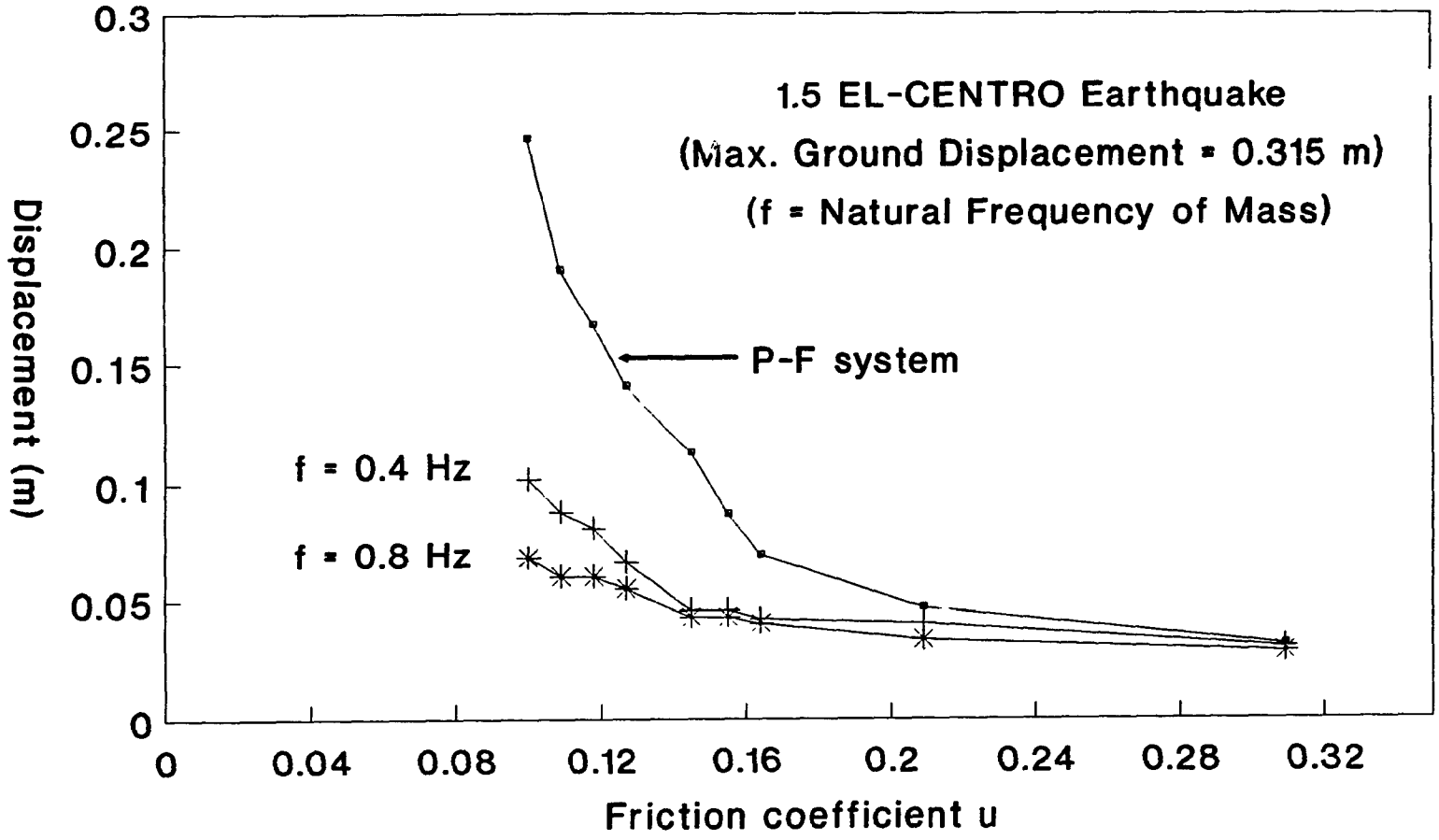

Fig.20 Horizontal Relative Displacement Responses

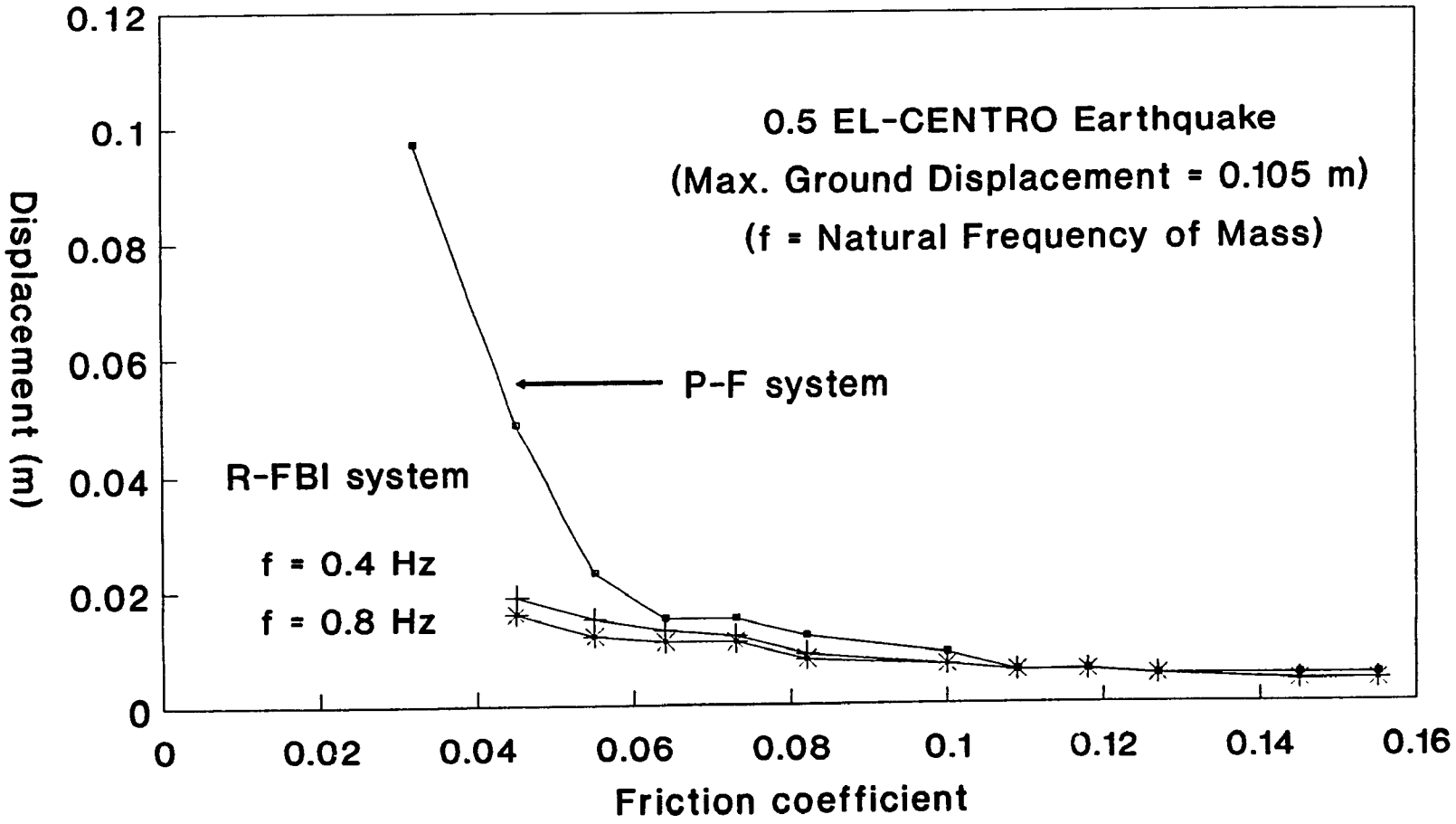

Fig.21 Horizontal Relative Displacement Responses

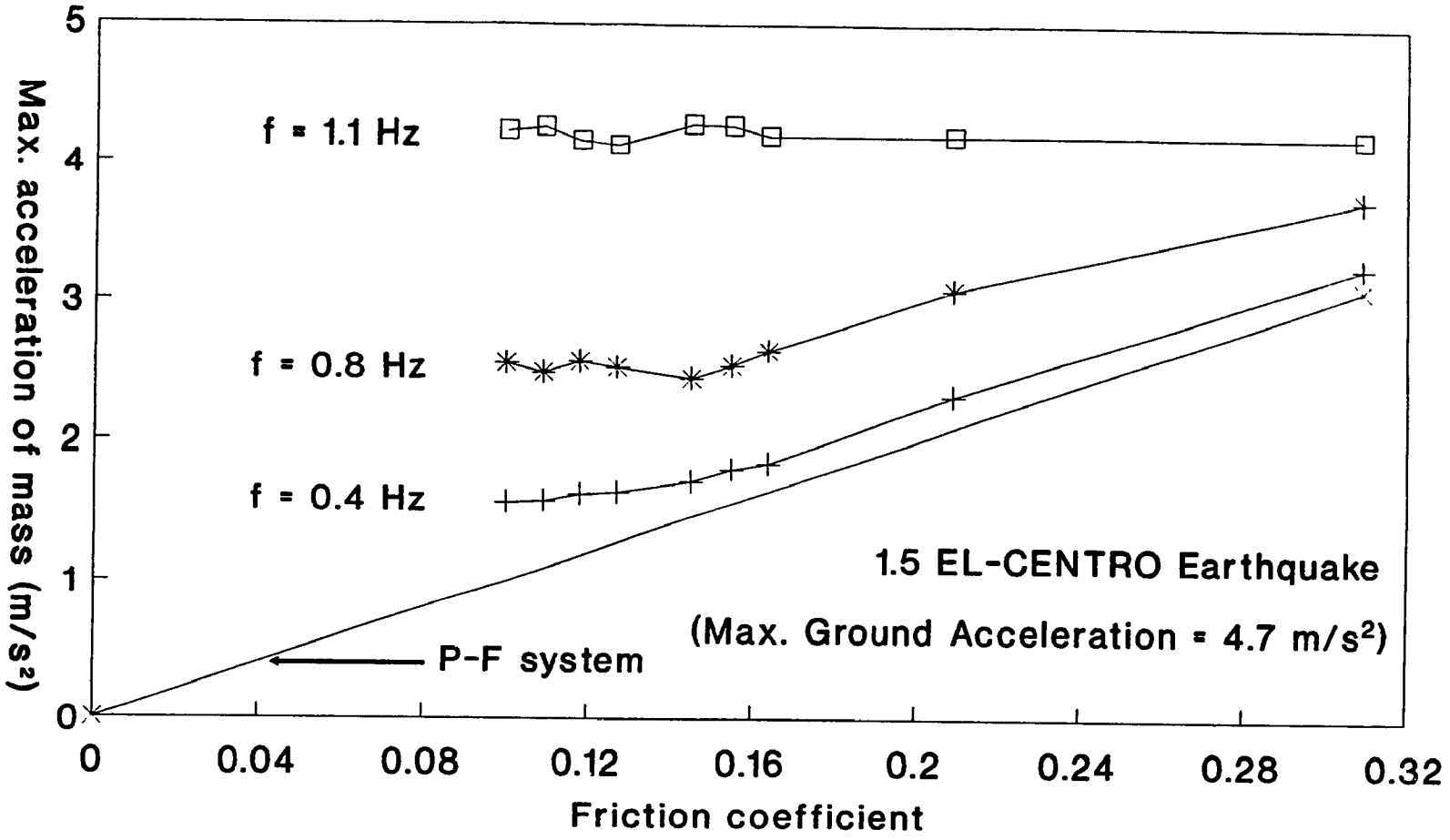

Fig.22 Horizontal Acceleration of the Block for R-FBI System

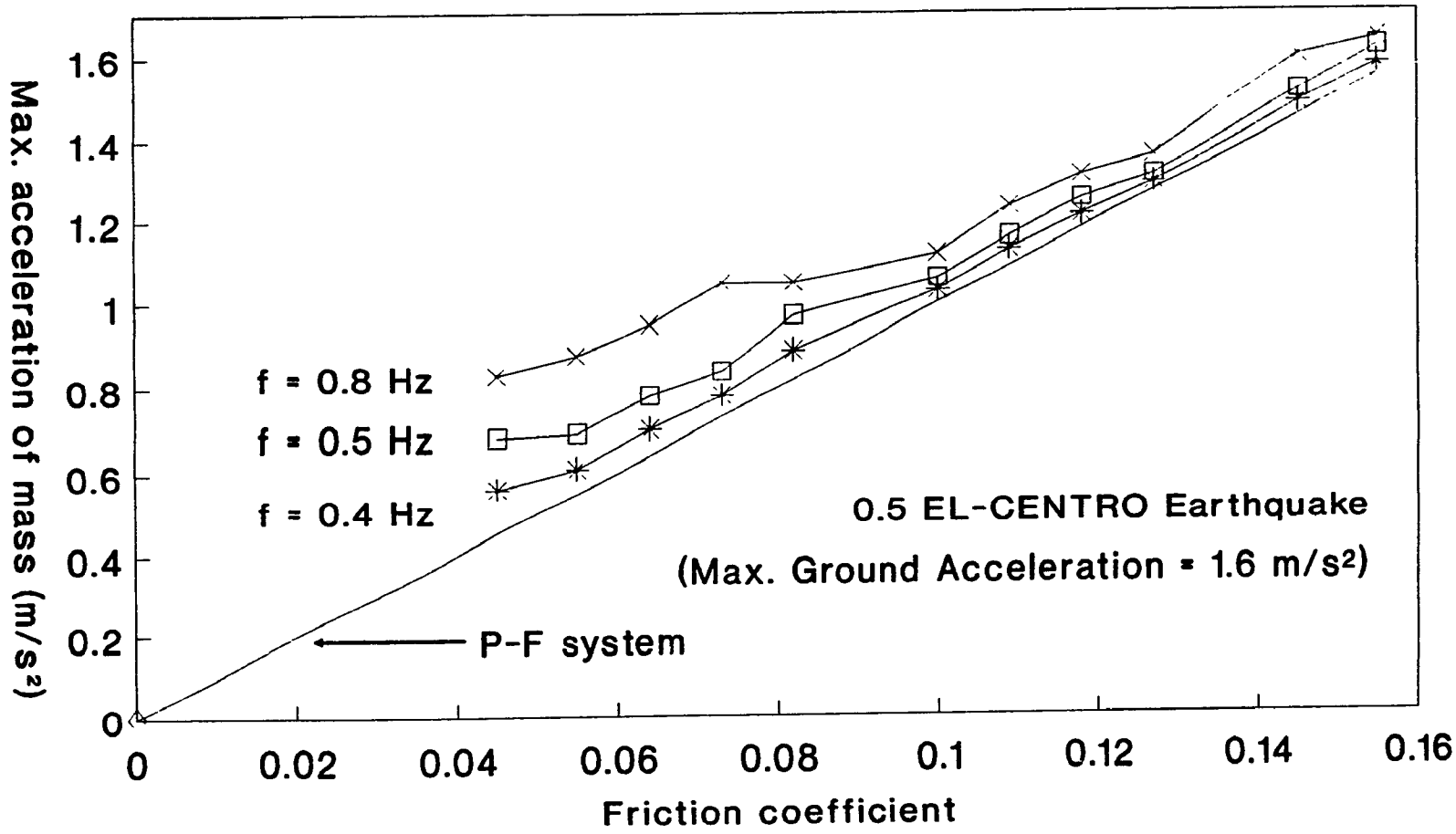

Fig.23 Horizontal Acceleration of the Block for R-FBI System

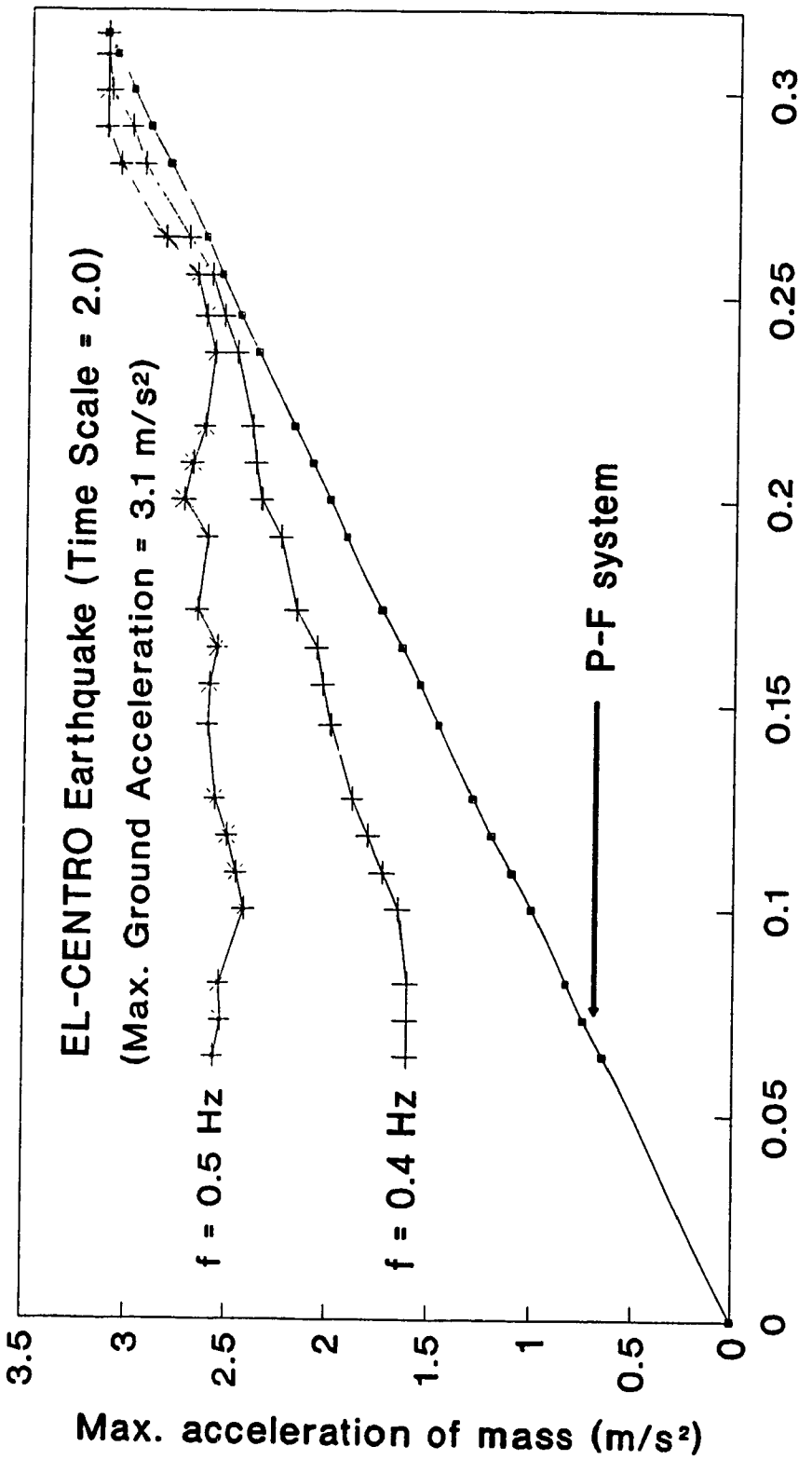

Fig.24 Horizontal Acceleration Responses

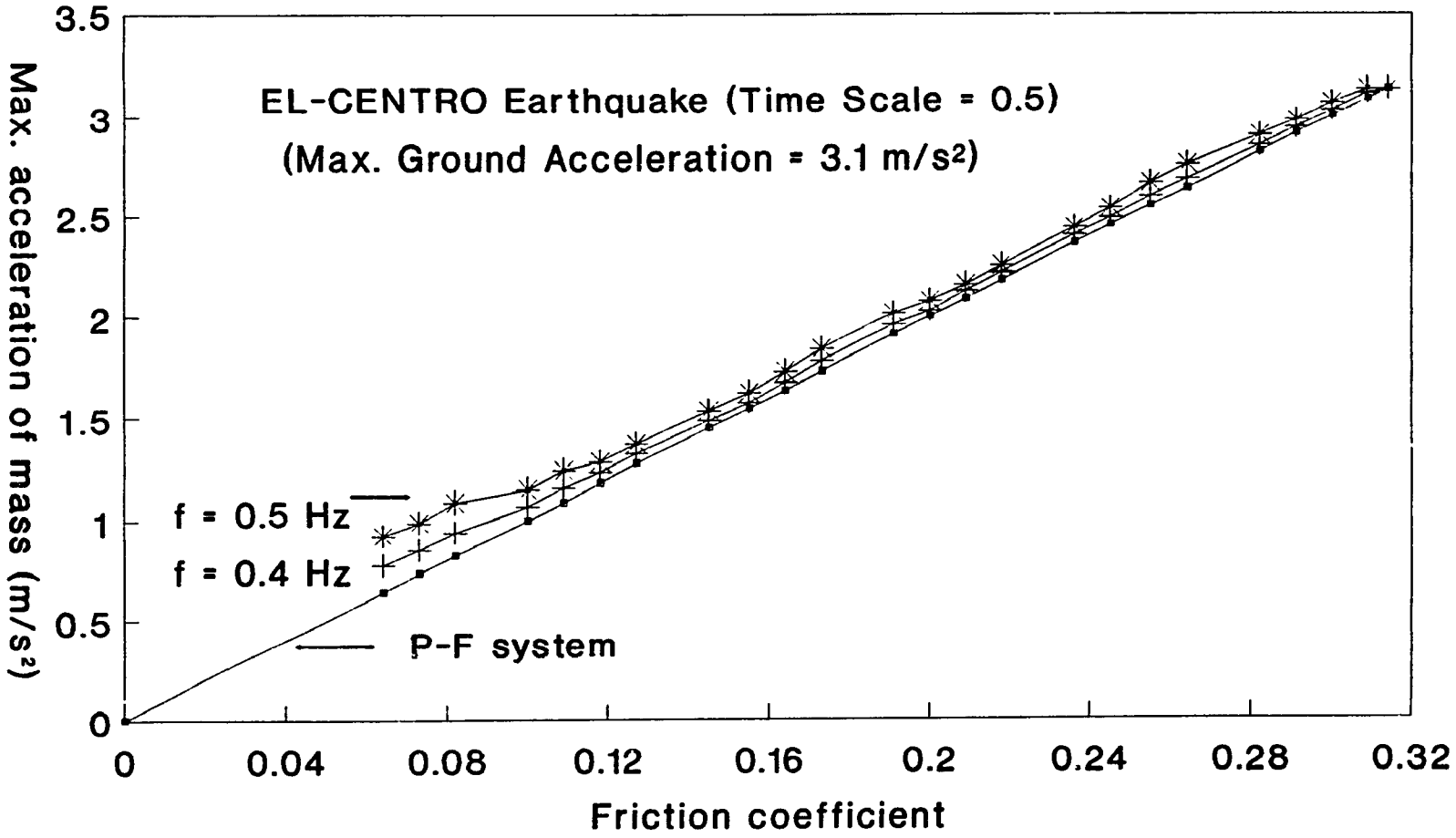

Fig.25 Horizontal Acceleration Responses

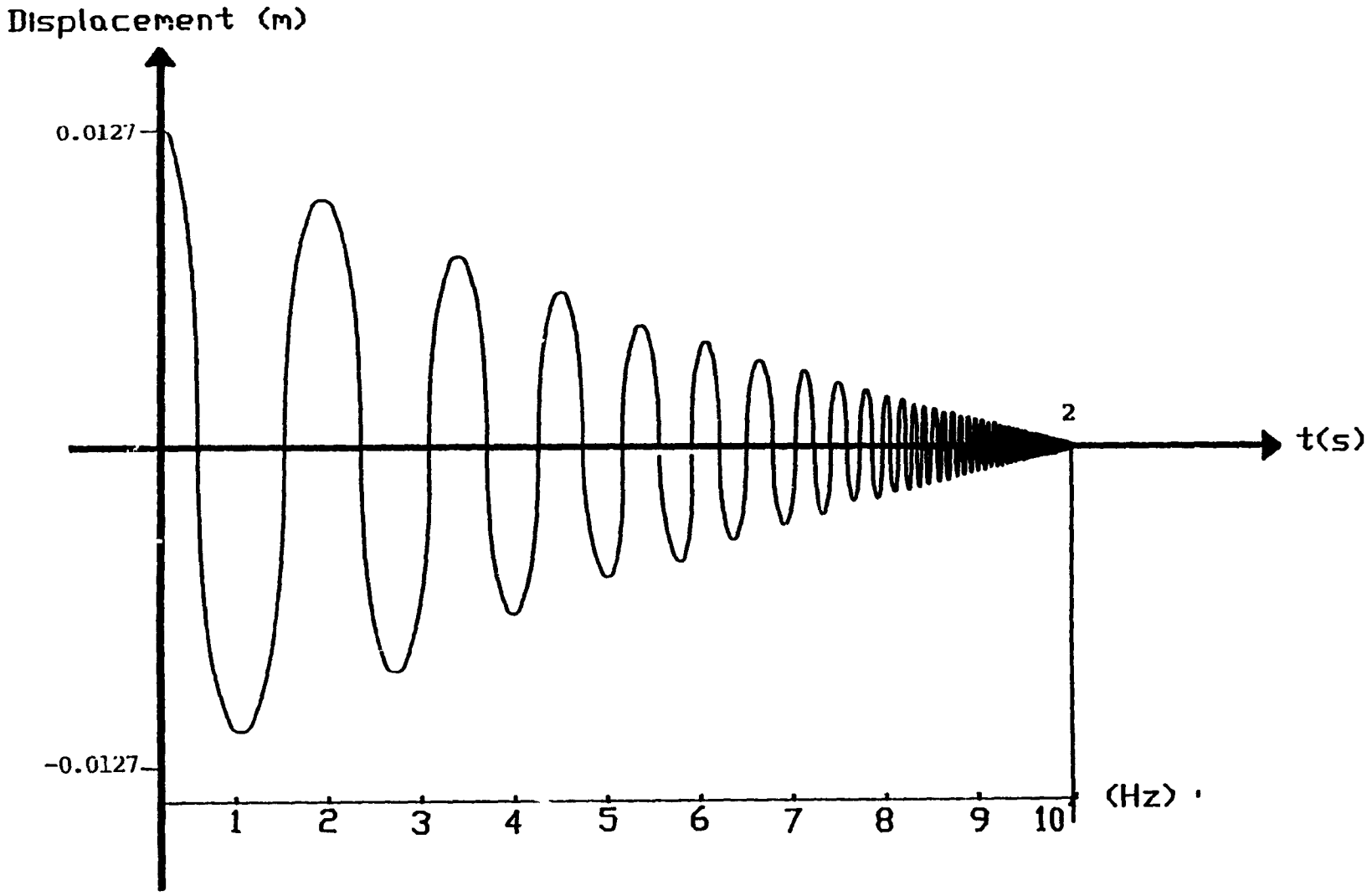

Fig.26 Cosine-curve Signal Input

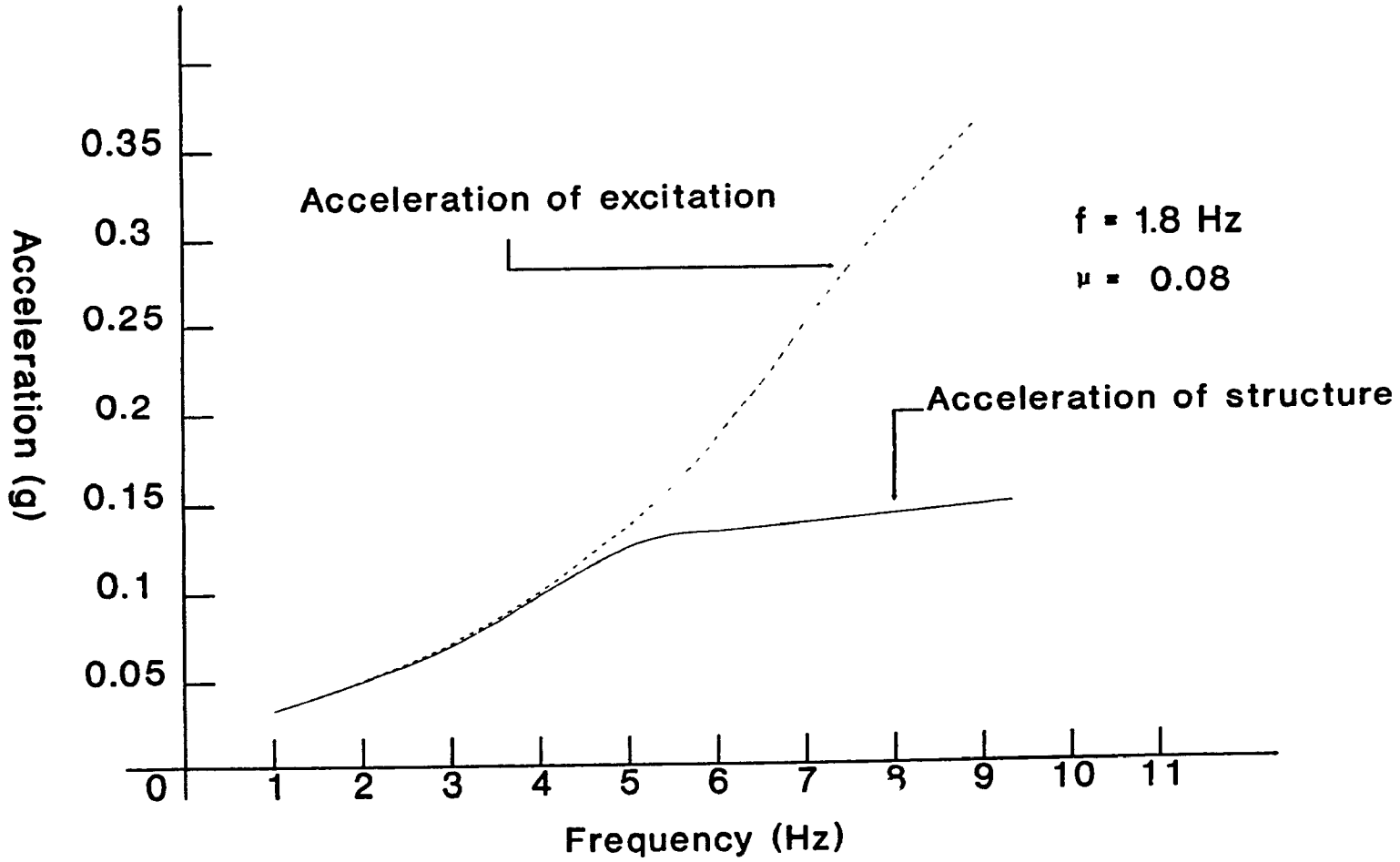

Fig.27 Horizontal Acceleration Response

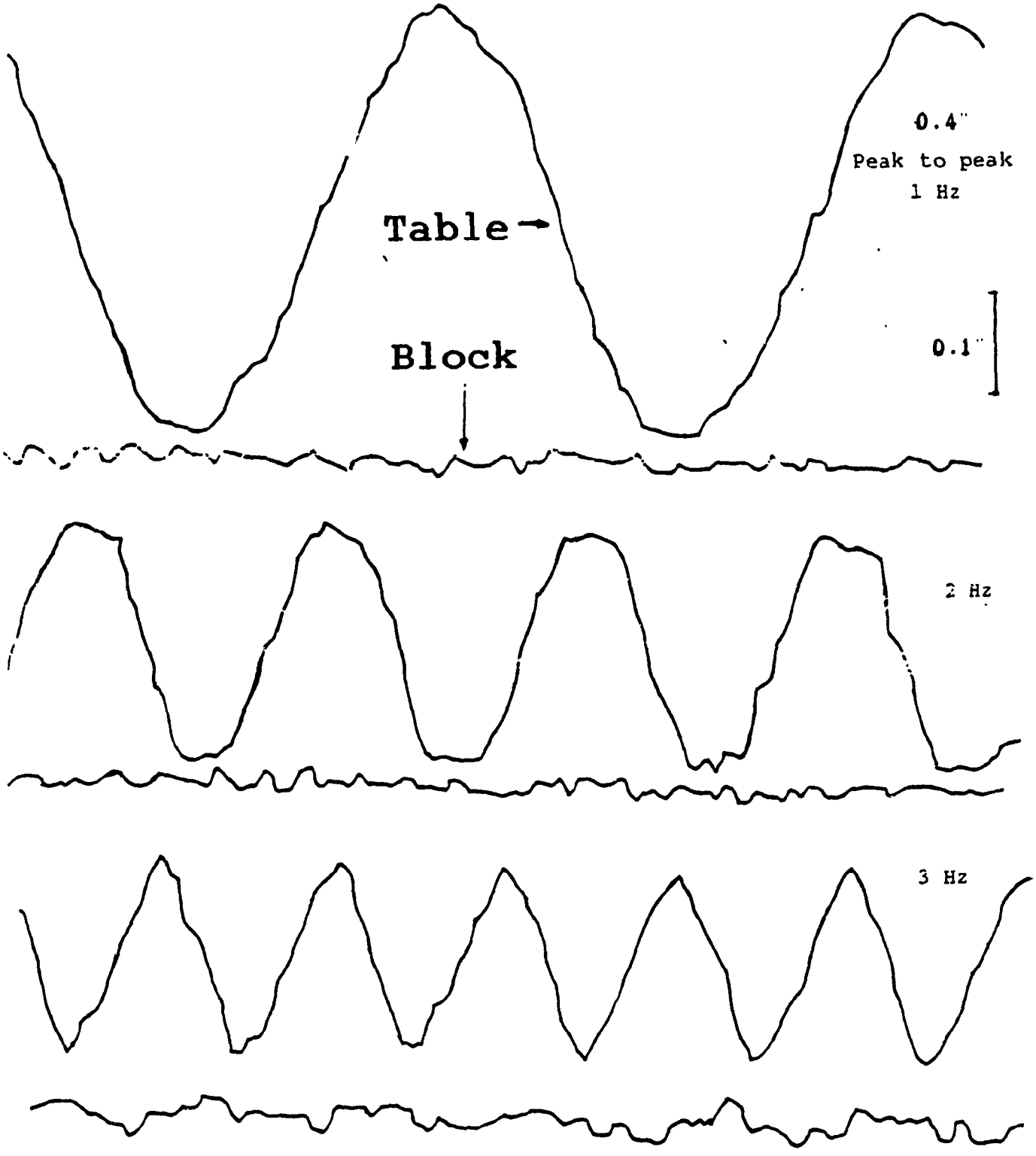

Fig.28 Displacement Time History
Teflon and Polished Stainless Steel
Natural Frequency = 1.8 Hz

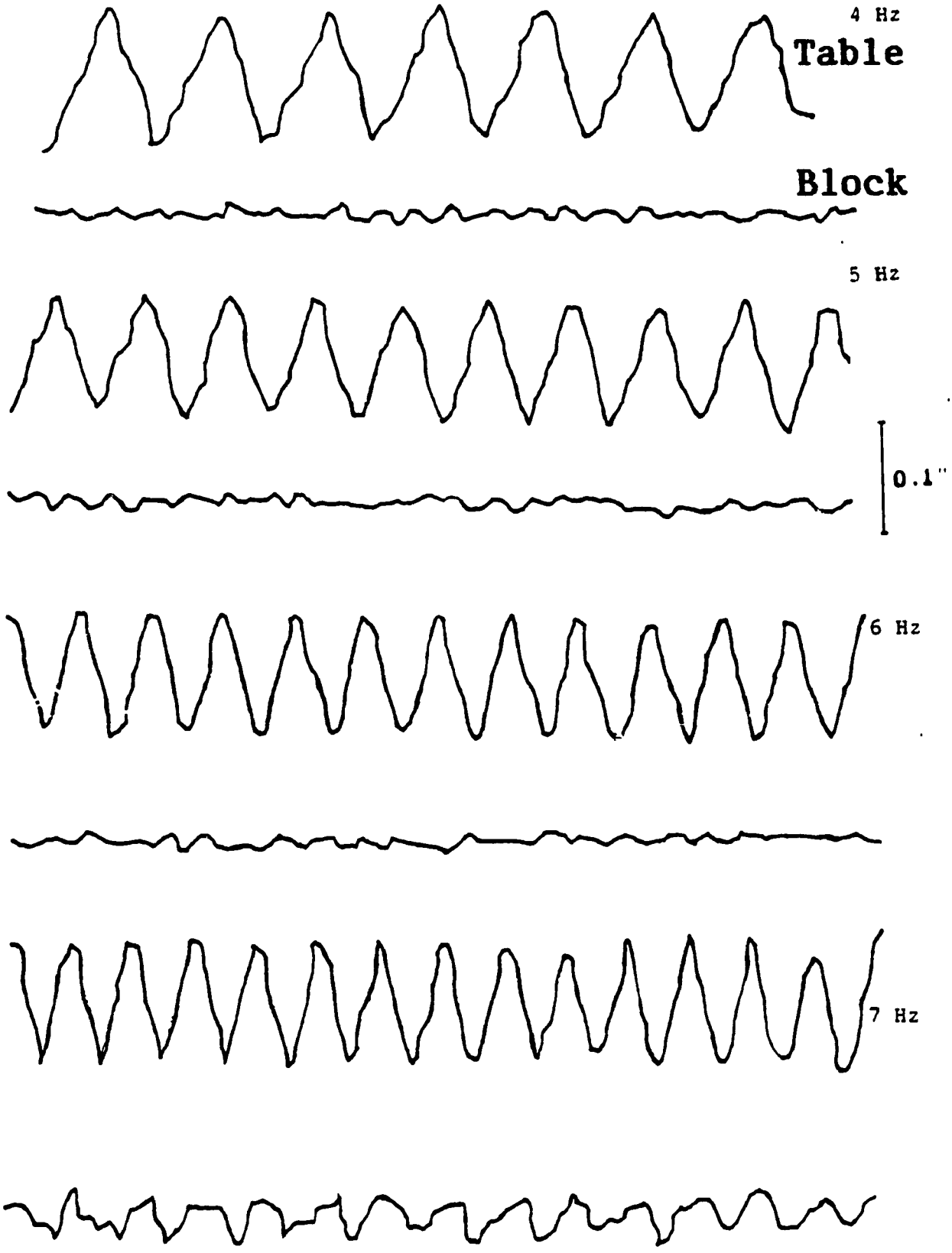

Fig.28 Displacement Time History
Teflon and Polished Stainless Steel
Natural Frequency = 1.8 Hz

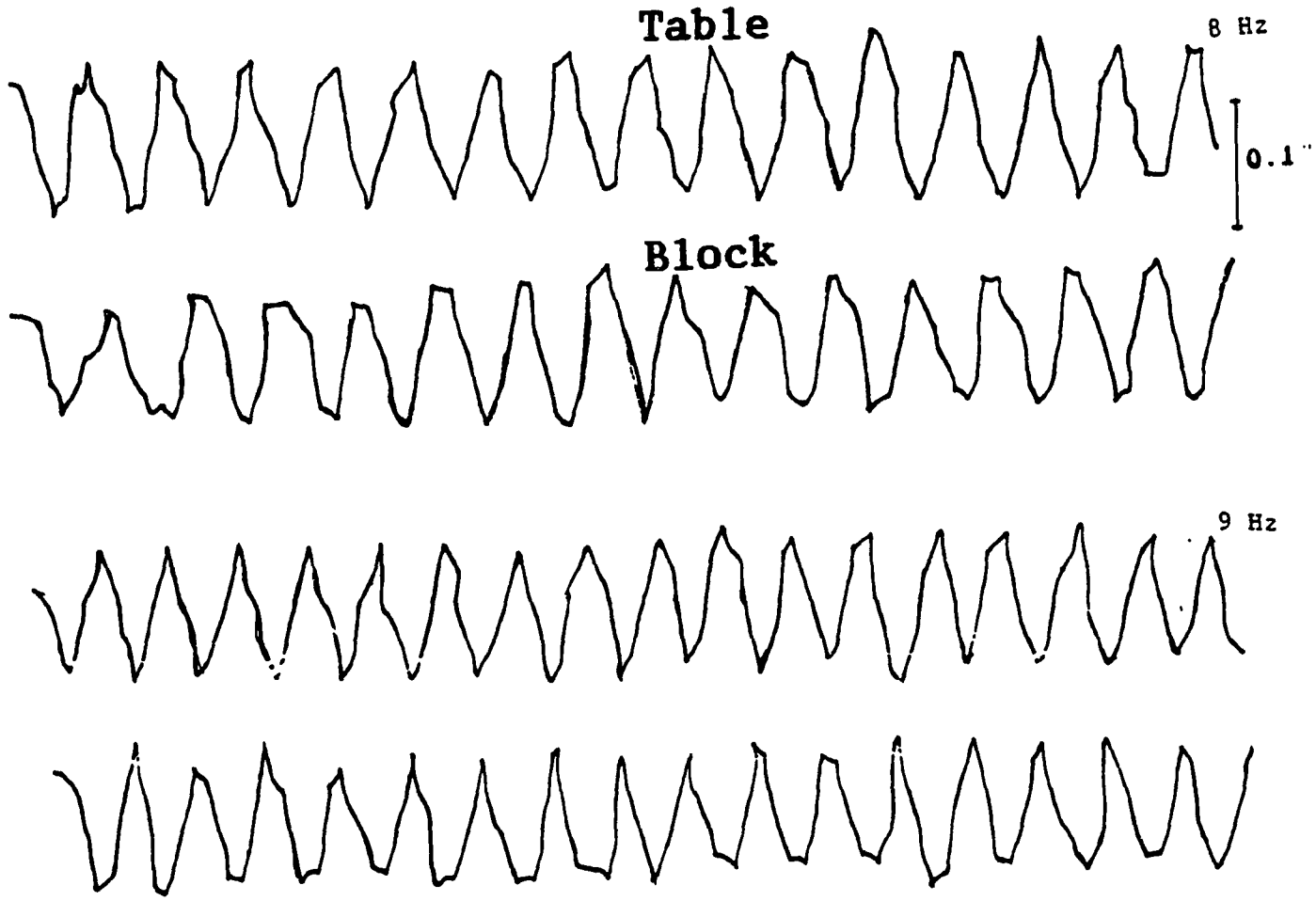

Fig.28 Displacement Time History
Teflon and Polished Stainless Steel
Natural Frequency = 1.8 Hz

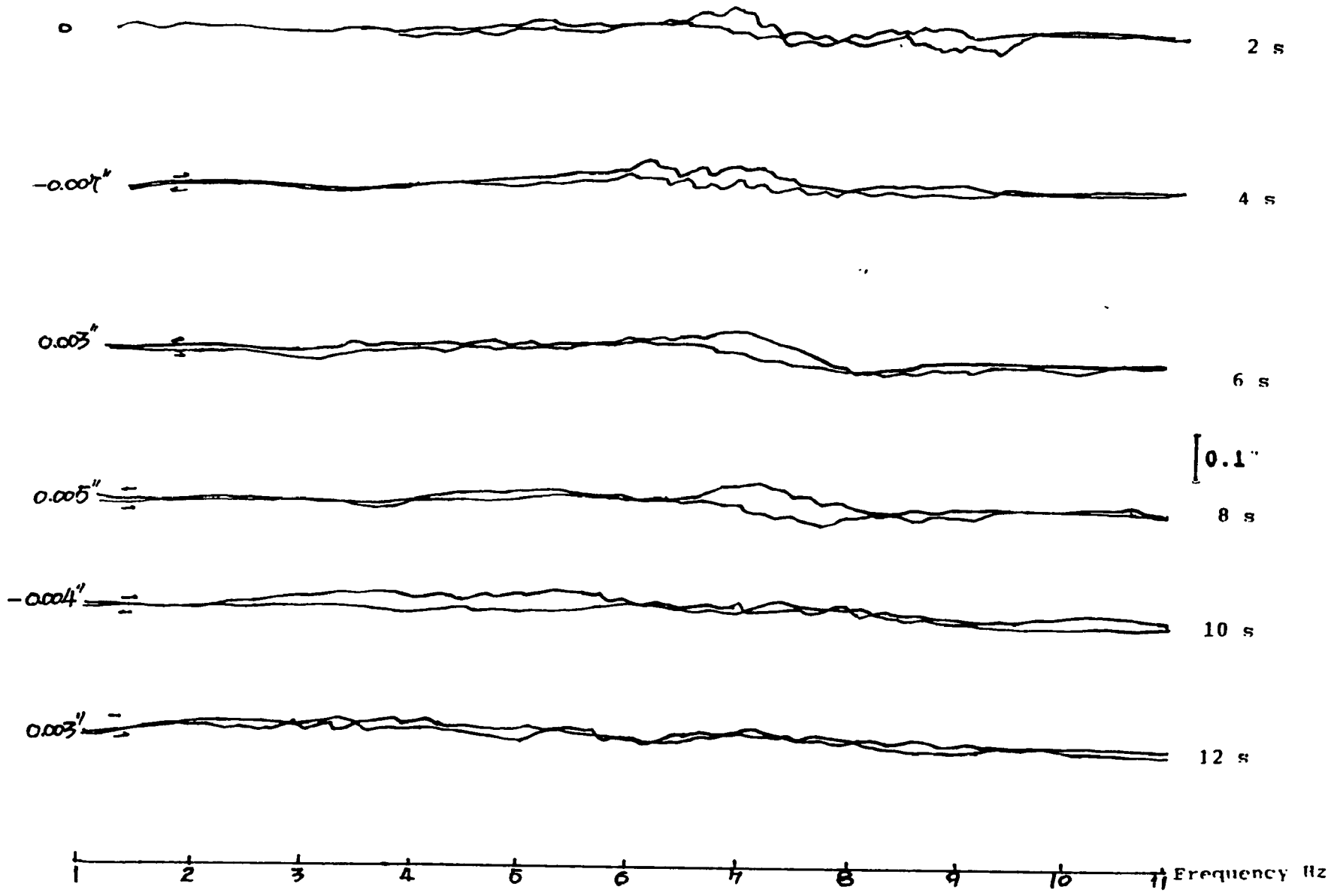

Fig.29 Effect of Sweep Time on Displacement
Teflon and Polished Stainless Steel
Natural Frequency = 1.8 Hz

Continued

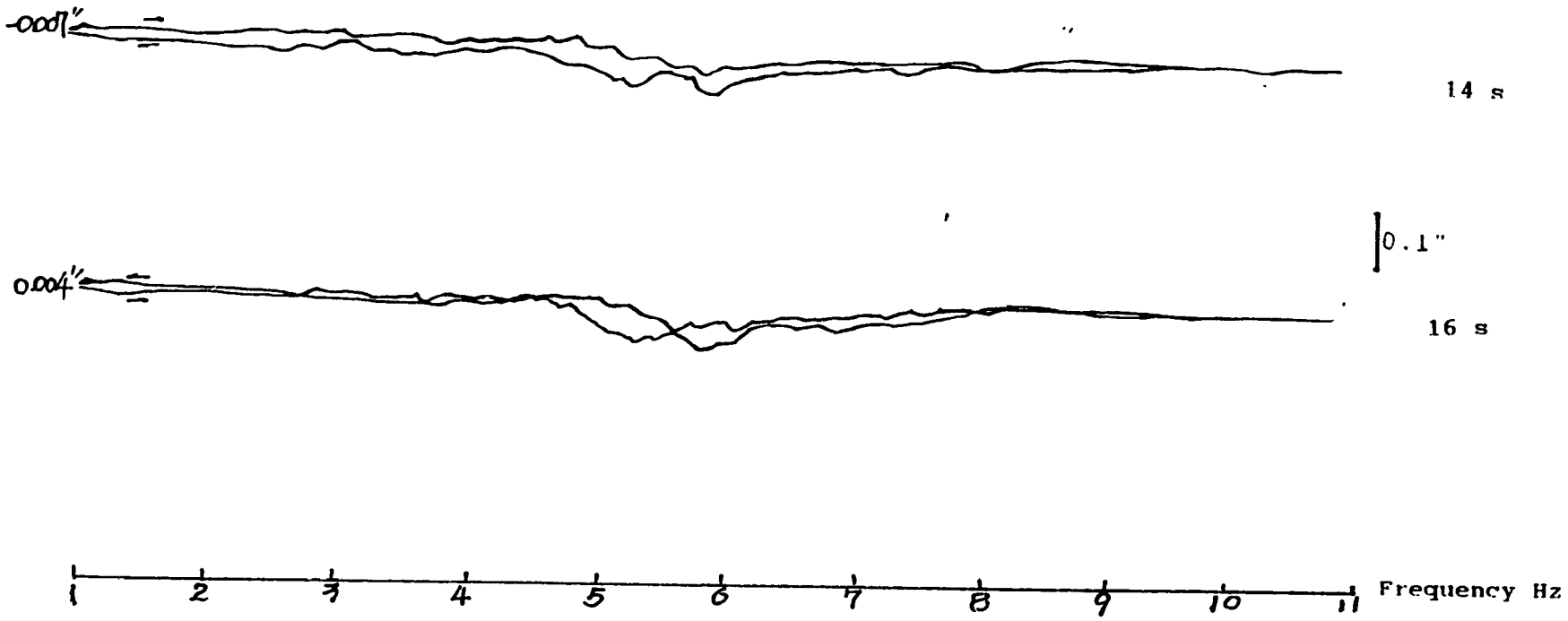

Fig.29 Effect of Sweep Time on Displacement Teflon and Polished Stainless Steel Natural Frequency = 1.8 Hz

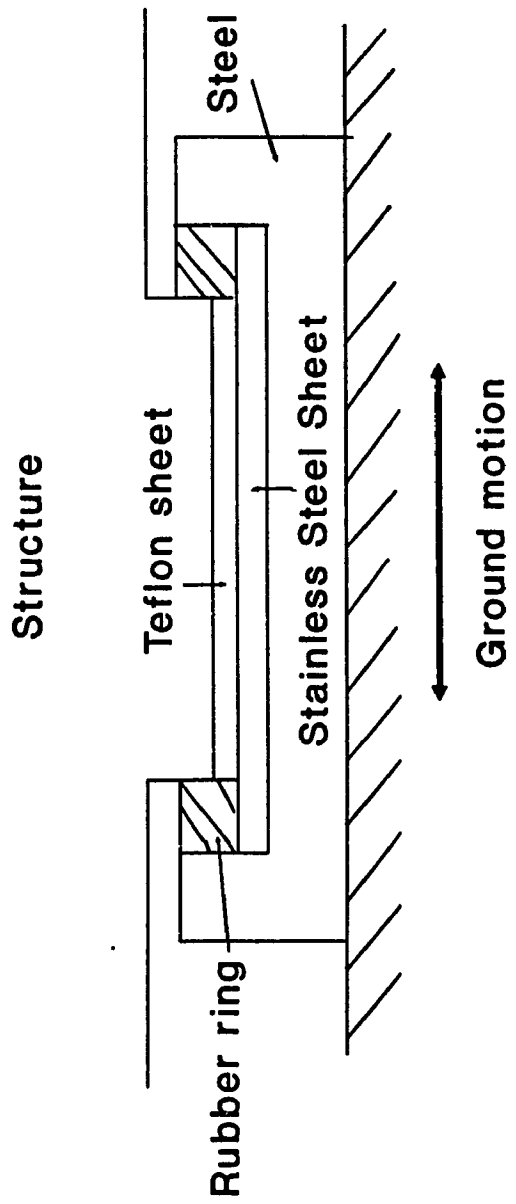

Fig.30 Modified R-FBI System

TABLES

Table 1 Static Coefficients of Friction

Sliding surface	S.C.F	Sliding surface	S.C.F
Mild steel and brass	0.318	Polished steel and P.S.S	0.122
Teflon(180x180mm) and P.S.S	0.110	Teflon(D=60mm) and P.S.S	0.081
Teflon(D=40mm) and P.S.S	0.069	Teflon(D=30mm) and P.S.S	0.064

Note:

(1) S.C.F = Static coefficient of friction

(2) P.S.S = Polished stainless steel

(3) D = Diameter

(4) μ for leaded brass and stainless steel = 0.2

Table 2 Time History of R-FBI system

Time (s)	0.05	0.10	0.15	0.20	0.25	0.30	0.35	0.40	0.45	0.50
F_f (N)	410	0.66	-412	1.22	948	2.44	-935	3.27	1573	4.58
F_s (N)	0	0	0	0	0	0	0	0	0	0
Time (s)	0.55	0.60	0.65	0.70	0.75	0.80	0.85	0.90	0.95	1.00
F_f (N)	-1528	5.13	1600	1600	-1600	-1600	1600	1600	-1600	-1600
F_s (N)	0	0	25	184	-75	-570	-287	874	1266	139
Time (s)	1.05	1.10	1.15	1.20	1.25	1.30	1.35	1.40	1.45	1.50
F_f (N)	1600	1600	-1600	-1600	1600	1600	-1600	-1600	1600	1600
F_s (N)	-437	368	622	-452	-800	516	1177	-119	-741	835
Time (s)	1.54	1.60	1.65	1.70	1.75	1.80	1.84	1.90	1.95	
F_f (N)	-1600	-1600	-1600	1600	-1600	-1600	-1600	1600	-1600	
F_s (N)	1732	3	-1143	314	1232	-327	-1328	287	1288	

Note:

F_f = Friction force, F_s = Spring force

Spring constant = 2.6×10^5 N/m, Coefficient of friction = 0.08

Frequency sweeps from 1 Hz to 10 Hz in 2 seconds.

Natural frequency = 1.8 Hz